

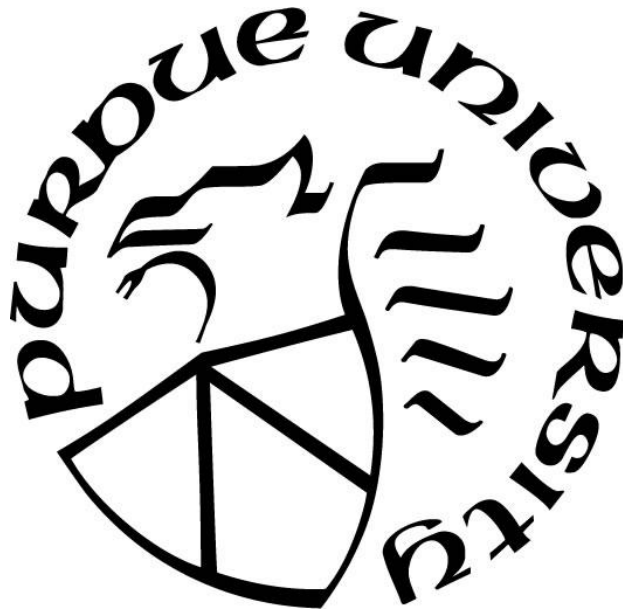
**COMPUTATIONAL MODELING OF TRANSFORMING GROWTH
FACTOR- β 2 RECEPTOR COMPLEX ASSEMBLY**

by
Michelle Ingle

A Thesis

*Submitted to the Faculty of Purdue University
In Partial Fulfillment of the Requirements for the degree of*

Master of Science



Agricultural and Biological Engineering

West Lafayette, Indiana

December 2019

THE PURDUE UNIVERSITY GRADUATE SCHOOL
STATEMENT OF COMMITTEE APPROVAL

Dr. David M. Umulis, Chair

Department of Agricultural and Biological Engineering

Dr. Nathan S. Mosier

Department of Agricultural and Biological Engineering

Dr. Kevin V. Solomon

Department of Agricultural and Biological Engineering

Approved by:

Dr. Nathan S. Mosier

This thesis is dedicated to my family and friends. Thank you for your love and support.

ACKNOWLEDGMENTS

I would like to thank my advisor and committee chair, Dr. David M. Umulis for his support and guidance in completing this thesis. In addition, I would like to thank Dr. Nathan S. Mosier and Dr. Kevin V. Solomon for serving on my committee and providing beneficial suggestions and comments. This thesis would not be possible without their helpful inputs and constructive criticisms.

I am very grateful for my lab-mates Sanniv Ganguly, Lukasz Burzawa, Juan Andres Carvajal, Linlin Li, Tze-Ching Wu, Xu Wang, Matthew Thompson, and Bobby Madamanchi for their collaboration and help. I especially want to thank Dr. Bobby Madamanchi for his valuable mentorship and patience in equipping me with the tools and resources needed to complete this thesis.

A special thanks goes to the Purdue Military Research Initiative for giving me the opportunity to pursue a higher education while in the military.

I thank Dr. Andrew P. Hinck at the University of Pittsburgh, for providing invaluable feedback and knowledge. I would also like to extend my sincere thanks to my friends and colleagues for their support and encouragement.

Finally, I want to thank my family who has always been a source of inspiration and strength. *Soli Deo gloria.*

TABLE OF CONTENTS

LIST OF TABLES	6
LIST OF FIGURES.....	8
ABSTRACT.....	11
1. INTRODUCTION.....	13
2. BACKGROUND.....	14
2.1 TGF- β Superfamily	14
2.2 TGF- β Receptor Complex Assembly Pathway.....	15
2.3 Betaglycan	17
2.4 Results of TGF- β Signaling Dysregulation	18
2.5 Mathematical Modeling Importance.....	19
3. COMPUTATIONAL MODEL OF BETAGLYCAN-MEDIATED TGF- β 2 RECEPTOR COMPLEX ASSEMBLY PATHWAY.....	22
3.1 Abstract.....	22
3.2 Introduction.....	22
3.3 Results	28
3.4 Discussion.....	44
3.5 Methods.....	46
3.6 Supplementary Figures.....	47
3.7 Supplementary Materials.....	51
4. CONCLUSIONS AND FUTURE DIRECTIONS.....	70
APPENDIX.....	73
REFERENCES	127

LIST OF TABLES

Supplemental Table 1: Available SPR data for No Receptor Recruitment model of TGF- β 1 ligand. The “A”, “B”, and “C” labels in the chart point to the specific source or test the data was obtained from per row. Bolded rates in reaction 1 are the values used in the final model.	56
Supplemental Table 2: Available SPR data for No Receptor Recruitment model of TGF- β 2 ligand. The “A”, “B”, and “C” labels in the chart point to the specific source the data was obtained from per row. The bolded rates in reaction 1 are the values used in the final model. ...	57
Supplemental Table 3: Available SPR data for No Receptor Recruitment model of TGF- β 3 ligand. The “A”, “B”, and “C” labels in the chart point to the specific source the data was obtained from per row. Bolded rates in reaction 1 are the values used in the final model.	58
Supplemental Table 4: Available SPR data for Single-stage Receptor Recruitment model of TGF- β 1 ligand. The “A”, “B”, and “C” labels in the chart point to the specific source or test the data was obtained from per row. The rows highlighted in red show the reactions changed when adding the T β RII Recruitment of T β RI of T β RI by T β RII. Bolded rates in reaction 4 are the values used in the final model.....	61
Supplemental Table 5: Available SPR data for Single-stage Receptor Recruitment model of TGF- β 2 ligand. The “A”, “B”, and “C” labels in the chart point to the specific source the data was obtained from per row. The rows highlighted in red show the reactions changed when adding the experimentally determined recruitment of T β RI by T β RII. The bolded rates in reaction 4 are the values used in the final model.	62
Supplemental Table 6: Available SPR data for Single-stage Receptor Recruitment model of TGF- β 3 ligand. The “A”, “B”, and “C” labels in the chart point to the specific source the data was obtained from per row. The rows highlighted in red show the reactions changed when adding the experimentally determined recruitment of T β RI by T β RII. The bolded rates in reaction 4 are the values used in the final model.	63
Supplemental Table 7: Available SPR data for Two-stage Receptor Recruitment model of TGF- β 1 ligand. The “A”, “B”, and “C” labels in the chart point to the specific source or test the data was obtained from per row. The rows highlighted in red show the reactions changed when adding the experimentally determined recruitment of T β RI by T β RII. The rows highlighted in blue show the reactions affected when adding the theorized recruitment of T β RII by T β RI.	65
Supplemental Table 8: Available SPR data for Two-stage Receptor Recruitment model of TGF- β 2 ligand. The “A”, “B”, and “C” labels in the chart point to the specific source the data was obtained from per row. The rows highlighted in red show the reactions changed when adding the experimentally determined recruitment of T β RI by T β RII. The rows highlighted in blue show the reactions affected when adding the theorized recruitment of T β RII by T β RI.....	66
Supplemental Table 9: Available SPR data for Two-stage Receptor Recruitment model of TGF- β 3 ligand. The “A”, “B”, and “C” labels in the chart point to the specific source the data was obtained from per row. The rows highlighted in red show the reactions changed when adding the	

experimentally determined recruitment of T β RI by T β RII. The rows highlighted in blue show the reactions affected when adding the theorized recruitment of T β RII by T β RI..... 67

LIST OF FIGURES

Figure 1: Schematic and biology of TGF- β receptor signaling complex formation. (A) All three TGF- β ligands (TGF- β 1/2/3) signal through a tetrameric signaling complex composed of two Type II receptors (blue bean) and two Type I receptors (purple bean) and its formation can be aided by a membrane bound coreceptor, betaglycan (green bean). Receptor complex assembly is formed through reversible reactions (double-sided arrows). The colored arrows indicate where cooperative receptor recruitment was found and/or tested. The Single-stage Receptor Recruitment (SRR) model accounts for the recruitment of T β RI by T β RII (red arrows) and the Two-stage Receptor Recruitment (TRR) model builds off the SRR model by further incorporating the recruitment of T β RII by T β RI (blue arrows). (B) Cooperative receptor recruitment is a biological interaction where the presence of one receptor increases the affinity of another receptor, usually a weak affinity receptor. (C) In the TGF- β 2 system, betaglycan with two domains (orphan, BG-O, and zona-pellucida, BG-ZP, domains) is predicted to enhance TGF- β 2 signaling by increasing the affinity of the T β RII (blue receptor). Betaglycan dissociates and T β RI (purple receptor) binds, creating half of the tetrameric signaling complex. 26

Figure 2: Results of simulated models vs published data and parameter selection when no BG is present. (A) Changing the value of the default receptor concentration, 160 nM, and the default absolute rates (blue line) while having a uniform dissociation constant (on-rate/off-rate ratio), does not improve the RMSE value for the NRR and SRR models. (B) The degree of recruitment (red to blue lines) with the best-fit for the hypothesized receptor recruitment of T β RII by T β RI was approximately 5-fold. (C) With the predetermined SEF value of 50 and receptor concentration of 160 nM across all models, the “best-fit” simulations (solid lines) are able to obtain results similar to experimental data (dotted lines) (Cheifetz et al., 1990). 32

Figure 3: Poor performance in three models when BG is added. (A) The parameter sets with an SEF of 50 and a receptor concentration of 160 nM (colored dots) for each TGF- β 2 model are displayed together. A tradeoff between tetramer production and BG enhanced signal is present across all of the models. (B) The signaling enhancement of the three ligand isoforms by BG across the three models was greater in the TGF- β 2 (blue line) system than TGF- β 1/ β 3 (green and red lines) systems. The data was normalized to the amount of signal produced in each model with no BG present, therefore, the black dotted horizontal line represents no increase in signal by adding BG. (C) The absolute signaling concentrations (dashed lines) for the three ligand systems (same coloring as Figure 3C) across the three models are shown. The NRR model produced almost no TGF- β 2 signal and the TRR model produced two times more TGF- β 2 signal than the SRR model. (D) When BG was added (x-axis), the TRR model at 75% recovery, was the best at recapitulating TGF- β 2 signal to levels comparable to TGF- β 3 signal (blue dashed line). Higher concentrations of BG inhibit TGF- β 2 signal as seen by the bell shape curves on the graph. (E) TGF- β 2 species composition of the signaling species and TGF- β 2/BG/T β RII/T β RI across each model. The TRR model produced more tetramer (bright pink) than the NRR and SRR models, and the major species in all models is TGF- β 2/BG/T β RII/T β RI (light red). 35

Figure 4: TGF- β 2/BG/T β RII/T β RI inconsistency solved by small increase in BG-ZP dissociation to ligand-complex. TRR model outperforms other models in recapitulating betaglycan behavior. (A) A depiction of the inconsistency previously found where TGF- β 2/BG/T β RII/T β RI complex

(circled in red) was the most prevalent species out of all the species created. This abundance was hypothesized to inhibit the formation of signaling species. (B) When TGF- β 2/BG/T β RII/T β RI species is not required to be transient and contributes to signal, there is no biphasic effect across a wide range of ligand concentrations (x-axis) and BG concentrations (colored lines), 0.001 to 5 nM and 0 to 4980 nM, respectively. (C) A species composition analysis at peak signal, with a receptor concentration of 160 nM, and a SEF of 50, shows minimal increases in BG-ZP dissociation reduces the abundance of TGF- β 2/BG/T β RII/T β RI species in the SRR and TRR models. NRR model requires a larger increase in BG-ZP dissociation compared to SRR and TRR models. The BG-ZP dissociation fold increase selected for each model was when increasing the BG-ZP dissociation did not impacted the signaling results with the parameter ranges tested. This behavior is reached whenever 90% of the maximum signal is achieved. (D) TGF- β 2 signal in the TRR model (orange line) can recover greater than 95% of TGF- β 3 signal (blue dashed line) while the TGF- β 2 signal in the SRR model (green line) can recover roughly 75% of TGF- β 3 signal. 39

Figure 5: Distinguishing between models and BG-mediated TGF- β 2 signal hypotheses. (A) Across a broad range of parameter sets, almost any increase in the dissociation of BG-ZP (orange points) outperforms the original parameter sets with no increase in BG-ZP dissociation (black points). (B) When requiring the TGF- β 2/BG/T β RII/T β RI species to be transient, the RMSE analysis captures how the models measure up to no BG and BG system requirements in all three ligand systems. The NRR model was incorporated again to show effectiveness of adding cooperative receptor recruitment into the TGF- β receptor signaling complex formation in the presence and absence of BG. Each model shows BG's inhibitory effect on TGF- β 's signal by the concave shape of the graphs. Across a wide range of BG concentrations (x-axis) the TRR model recapitulates no BG and BG behavior the best in all three ligand systems until BG inhibits TGF- β signal causing the RMSE to increase. (C) A testable distinction between the SRR and TRR models was found in the BG to receptor ratio required to achieve the biphasic effect on TGF- β 2 signal by BG. Across a wide range of ligand concentrations, 0.001-5 nM, the SRR model (red points) needs 4.7-4.9 time more BG to induce the biphasic effect than the TRR model (blue points). (D) Zoomed in diagram of the receptor complex assembly that highlights the final conclusions. The red and blue arrows represent the types of cooperative receptor recruitment that is hypothesized to be present and the green arrow indicates an increase in the dissociation of TGF- β 2/BG/T β RII/T β RI improves model performance under certain conditions. 42

Supplemental Figure 1: There are minimal effects in decreasing the absolute rates of each ligand system independently across a range of receptor levels (100-340 nM). (A) In both the NRR and SRR models, when the fold decrease in TGF- β 1 rates are held constant (red to blue lines) and TGF- β 2 and TGF- β 3 absolute rates are varied (bars present at each dot) there is minimal change in the RMSE value. (B) When the fold decrease in TGF- β 2 rates are held constant (red to blue lines) and TGF- β 1 and TGF- β 3 absolute rates are varied (bars present at each dot) there is minimal change in the RMSE value. (C) When the fold decrease in TGF- β 3 rates are held constant (red to blue lines) and TGF- β 1 and TGF- β 2 absolute rates are varied (bars present at each dot) there is minimal change in the RMSE value. 47

Supplemental Figure 2: Minimal impact in the RMSE value when decreasing the absolute rates (red, blue, green, and purple lines) across multiple values for T β RI's recruitment of T β RII. Each graph represents one value for the degree of recruitment T β RI has on T β RII across a range of receptor levels (x-axis). Due to the computational screen set up, the median values of degree

recruitment have more absolute rates tested than the end values. Degree recruitment of 0.001 and 700 has only one absolute rate (1-fold decrease) shown. Degree of recruitment 0.007 and 137 have two absolute rate values (1 and 5-fold decrease) shown. Degree of recruitment 0.038 and 27 have three absolute rate values (1, 5, and 27-fold decrease) shown. Degree of recruitment 0.2 and 5 have four absolute rate values (1, 5, 27, 137-fold decrease) shown. 48

Supplemental Figure 3: Across a broad range of values for the degree of recruitment T β RI has on T β RII (colored lines), a 5-fold degree recruitment produced the lowest RMSE at a receptor level of 160 nM. 49

Supplemental Figure 4: With no BG present, an SEF equal to 50, and specific absolute rates chosen, altering the concentrations of T β RI (red to blue lines) and T β RII (x-axis) independently, minimally affect the RMSE analysis (y-axis)..... 50

ABSTRACT

Transforming growth factor (TGF)- β 1, TGF- β 2, and TGF- β 3 are secreted signaling proteins that play an essential role in tissue development, immune response, and physiological homeostasis. TGF- β ligands signal through a tetrameric complex made up of two type I receptors (T β RI) and two type II receptors (T β RII). Dysregulation of TGF- β signaling has been linked to uncontrolled cell proliferation and cancer metastasis. An accurate understanding of TGF- β 's receptor complex assembly pathway may allow for pharmacological intervention and/or preservation of proper TGF- β signaling.

Amongst the ligand types, TGF- β 1 and TGF- β 3 are efficient signalers, presumably by strong binding to both type I and II receptors. However, TGF- β 2 has a very weak affinity for T β RII and requires an additional membrane-bound protein called betaglycan (BG) to achieve similar levels of downstream signaling. While computational modeling has been performed on the signaling pathway of the TGF- β system, to date no computational modeling has aimed to decipher BG's role in the potentiation of TGF- β 2 signal. To determine the role of BG in selectively facilitating signaling by TGF- β 2, we developed computational models with different assumptions based on the levels of cooperativity between receptor subtypes and types of BG behavior (No Receptor Recruitment model, Single-stage Receptor Recruitment model, and Two-stage Receptor Recruitment model).

With each of the receptor recruitment models we hypothesized that BG uses two domains to successfully enhance TGF- β 2 signaling. This model was first proposed in Villarreal et al., 2016 and is further investigated in this work using a two-step computational approach. First, a root mean square error (RMSE) calculation was performed between our computational models with no BG present and published experimental signaling data in cell lines with no BG present. Lower RMSE values indicate the simulated data is more representative of experimental signaling behavior when no BG is present. The second round of model validation was performed by adding BG into the simulations and comparing its behavior to experimentally determined and hypothesized behaviors of BG.

In summary, the simulations indicate there may be more cooperative receptor recruitment present in the system than stated in literature. Furthermore, it appears that BG binding to TGF- β 2 ligand through two domains provides an effective transfer mechanism that can be tuned to

control differential signaling between TGF- β ligand subtypes. Experiments were then suggested in order to support or refute one of the models offered in this thesis. For the purpose of uncovering how BG enhances TGF- β 2 signaling, the computational work performed in this thesis highlights the areas where researchers should focus their experimental efforts and provides a baseline model for further computational work in the TGF- β system.

1. INTRODUCTION

TGF- β signaling has known roles in cell proliferation, apoptosis, integrin expression, extracellular matrix component expression, cell differentiation of various organs, and plays a complex role in immune system regulation (Letterio and Roberts, 1998; Moses, 1992; Serra et al., 1997; Siegel et al., 2003; Tucker et al., 1984). Altered TGF- β signaling has been shown to play a role in promoting uncontrolled cell proliferation, cancer metastasis and/or disruption of immune tolerance (Fabregat et al., 2014; Massagué, 2000). TGF- β signaling is implicated in numerous types of cancers and therefore is an attractive therapeutic target to treat multiple oncogenic states, however the promise of therapeutic intervention relies on an improved understanding of the TGF- β receptor complex assembly pathway.

Direct analysis of how the tetrameric signaling unit forms is limited with biological methods due to the inability to isolate intermediate macromolecules and analyze their binding kinetics in real time. Mathematical modeling in biology allows for iterative testing of system hypotheses to see if the implications of the models are consistent with observed experimental data (Wilkinson, 2012). The research presented in this thesis uses the flexibility in mathematical modeling to investigate a proposed mechanism for BG-mediated TGF- β 2 signaling and suggest biological experiments for model validation or invalidation.

In brief, the work presented herein includes the necessary background information on the TGF- β system under question as well as a brief background on the mathematical tools used to study TGF- β signaling (Chapter 2). Next, a manuscript is proposed based on the results of this research (Chapter 3). The description of these results includes supplementary figures and materials, as well as a link to access the codes of the models developed which are available on GitHub. Hard copies of the codes are available in the appendix section of this work. Finally, a summary is presented that includes a discussion of the conclusions from the deterministic modeling and suggests further work that should be accomplished with mathematical modeling and biological experimentation (Chapter 4).

2. BACKGROUND

This chapter briefly examines the key biological and mathematical concepts required for general audiences to understand the conclusions drawn from the computational modeling performed on the TGF- β 2 receptor complex assembly pathway. This includes: (i) introducing prior knowledge on the protein superfamily TGF- β 2 falls under; (ii) introducing what is known about the receptor complex assembly pathway in the TGF- β subgroup; (iii) the importance of betaglycan in TGF- β 2 signaling; (iv) why studying this growth factor is important; (v) reasoning for computational methods used and describing computational work performed thus far on the TGF- β receptor complex assembly pathway.

2.1 TGF- β Superfamily

The founding member of the TGF- β superfamily was a disulfide-linked homodimer discovered in virally transformed cells in 1981 (Roberts et al., 1981). It had a “transforming” effect on the cells by stimulating anchorage-independent growth in soft agar. Since then, the TGF- β superfamily has grown to consist of over 30 structurally related proteins which are known to be involved in the regulation of tissue development, integrity, and repair (Hyytiäinen et al., 2004; Kingsley, 1994; Massagué, 2000).

These proteins can be divided into several subgroups with associated tasks. TGF- β 's and bone morphogenetic proteins (BMPs) regulate embryonic patterning, while growth and differentiation factors (GDFs) regulate cartilage and skeletal development, and lastly, activins/inhibins regulate pituitary hormone release and play a role in other developmental processes during embryogenesis (Hinck, 2012; Casari et al., 2014). During the late 1980's when the regulatory tasks of the TGF- β superfamily were being investigated, three different isoforms, polypeptides with sequence homology, of the founding TGF- β members were discovered only in vertebrates and were named TGF- β 1, TGF- β 2, and TGF- β 3 (Mason et al., 1985).

Even though TGF- β 1, TGF- β 2, and TGF- β 3 were found to have 70-80% sequence homology, knockout studies showed they have separate functions in embryogenesis. TGF- β 1 deficient mice died shortly after birth from an autoimmune inflammatory disease (Kulkarni et al.,

1993; Martin et al., 1995; Shull et al., 1992). TGF- β 2 knock-out mice had defects in cardiac, lung, and spinal cord development and did not live much past birth (Bartram et al., 2001; Sanford et al., 1997). The deletion of TGF- β 3 in mice developed cleft palates and pulmonary defects (Kaartinen et al., 1995; Proetzel et al., 1995). Two possible mechanisms are popularized to explain the varying phenotypic outcomes observed in knockout mice. The first mechanism proposes a tissue-specific expression of the TGF- β isoforms and the second mechanism proposes each isoform possess some unique biological activity and is not tissue-specific (Yang and Kaartinen, 2007). Another important functional difference between the three isoforms is the differential affinities for the TGF- β ligands to the TGF- β receptors and the variability in the use of coreceptors.

2.2 TGF- β Receptor Complex Assembly Pathway

TGF- β 's signal transduction pathway activates when a ligand bound type II receptor binds to one type I receptor and continues to build towards full signaling capacity when a heterotetrameric complex of one ligand, two type II (T β RII), and two type I (T β RI) receptors is formed on the cell membrane (Figure 1A). These complexes pass the signal from the extracellular environment to the intracellular environment by a cascade of phosphorylated Smad proteins that enter the nucleus and regulate targeted gene expression. The heterotetrameric signaling complex induces four-fold greater nuclear pSmad accumulation than other heterodimer complexes (Huang et al., 2011). The method of TGF- β signaling is well established, but the steps in receptor Complex assembly pathway on the cell membrane are not as well-known.

There are two general relationships present in the TGF- β superfamily between the receptor and ligand, (1) ligand-independent and (2) ligand-dependent receptor complex assembly. Ligand-independent receptor complex assembly occurs when there are preformed complexes (PFC's) of the receptor or receptor subpopulations on the cell membrane in the absence of the ligand. These preformed receptors or subpopulations mediate complex assembly or initiate signaling when the ligand is present. In ligand-dependent receptor complex assembly, the receptor complex assembly pathway does not start until the ligand is introduced to the cell. Cell experiments have found small amounts of T β RI and T β RII receptor homodimers and heterodimers present in the rough endoplasmic reticulum (ER) of cells in the absence of TGF- β

ligand (Gilboa et al., 1998). Although this seems to favor the ligand-independent assembly there are opposing experiments that heavily support the ligand-dependent assembly for the TGF- β members in the TGF- β superfamily.

To create preformed receptor dimers, the cytoplasmic domains and ectodomains of the receptors interact to stabilize the complex (Gilboa et al., 1998; Huang et al., 2011). The predicted interaction of ectodomains between the receptors would partially occupy or spatially disrupt the ligand binding site. Therefore, preformed complexes would decrease the favorability of ligand binding. Another reason supporting the ligand-dependent assembly is the extremely low to non-existent concentration of the heterodimer found in the cell when the ligand is absent. The heterodimer interaction is what initiates the signaling cascade, and there is substantial enhancement of this species in the rough ER when the ligand is present (Huang et al., 2011; Wells et al., 1999).

Structural analysis on the domain interactions between the ligand and receptors also support a ligand-dependent assembly. With the structure of the heterotetrameric signaling complex elucidated, the receptor homodimers (T β RII/T β RII or T β RI/T β RI) found in the cell ER of previous experiments would hinder the receptor complex assembly pathway. The full tetrameric ligand-receptor complex for the three TGF- β isoforms does not show a direct homomeric receptor-receptor interaction but only a direct heteromeric interaction (T β RII/ T β RI) (Villarreal et al., 2016). The lack of homomeric interaction in the final heterotetrameric receptor, means the homomeric preformed receptors would need to dissociate with each other before binding to the ligand. Although a ligand-independent system has not been disproven for TGF- β , the majority of experimental evidence supports a ligand-dependent system. The next important question in the receptor complex assembly pathway is how the receptor forms once the ligand is present.

Once the ligand is present, there are generally two different mechanisms for how the signaling receptors form, “sequentially” or “cooperative”. A sequential binding mode is when a receptor of higher affinity binds to the ligand and then recruits a receptor of lower affinity (Attisano et al., 1996). A cooperative binding mode is characterized by both receptor types being expressed with relatively equal affinities, the ligand then binds to either T β RI or T β RII and receptor cross-linking occurs to form the receptor complex (Liu et al., 1995). TGF- β is

hypothesized to be a sequential process due to the thermodynamics and cell experimentation results.

Statistical thermodynamics predict a step wise process because the simultaneous binding of the ligand to two receptor chains requires a very rare trimolecular reaction kinetic (Nickel et al., 2009). In all three ligands, there are multiple surface plasmon resonance experiments that show a much higher affinity for the ligand to bind to T β RII then for the ligand to bind to T β RI. This follows a sequential process as the high affinity type II receptor binds to the ligand and recruits the low affinity type I receptor (Huang et al., 2014; Radaev et al., 2010; Villarreal et al., 2016). Cell experimentation found that the composite binding epitope between the TGF- β 3/T β RII complex forms a functional binding site for T β RI (Huang et al., 2014). This epitope indicates a step-wise or sequential, addition of receptors which also supports a ligand-dependent receptor complex assembly pathway.

The discovery of this binding epitope alongside other studies have shown that a ligand bound T β RII increases the affinity of T β RI by greater than 300-fold in all three isoforms (Radaev et al., 2010). This biological interaction is termed receptor recruitment or receptor cooperativity (Figure 1B). Surface plasmon resonance studies have identified the recruitment of T β RI by a ligand bound T β RII but have not investigated the possibility of the recruitment of T β RII by a ligand bound T β RI.

As mentioned previously, the three isoforms of TGF- β express different binding affinities relative to their receptors. In 1990, TGF- β 1 was found to be 20-fold more potent than TGF- β 2 in the presence of both receptor types (Cheifetz et al., 1990). The difference in their effective signal was due to the relative affinity of each ligand to the Type II receptor. TGF- β 1 and β 3 binding affinity was 200-fold greater than TGF- β 2's binding affinity to T β RII (De Crescenzo et al., 2006). Later on, it was shown that TGF- β 2 required a membrane bound co-receptor known as betaglycan (BG) to produce comparable signaling to TGF- β 1 and β 3 (Huang et al., 2014; Radaev et al., 2010; Villarreal et al., 2016).

2.3 Betaglycan

A unique biomolecular interaction incorporating coreceptor BG is essential in the formation of functionally relevant TGF- β 2 signaling interface (Groppe et al., 2008; López-

Casillas et al., 1993; Massagué, 2008; Villarreal et al., 2016). Although, BG can bind to all isoforms of TGF- β , TGF- β 2 ligand is singled out as exhibiting an extreme requirement for BG to produce a comparable signaling to TGF- β 1/3 (Heldin and Moustakas, 2016; Villarreal et al., 2016). Ironically, co-receptor BG is expressed in many cell types in amounts superior to type I and II protein receptors (Villarreal et al., 2016). Without BG present, development of fetal mice does not continue past embryogenesis due to heart and liver defects (Wiater et al., 2006). The absence of BG during development has been shown to disrupt mesenchyme formation in the heart and branching morphogenesis in the lung (Brown et al., 1999). Additionally, either the overexpression or downregulation of BG appears to play an important role in the progression of cancer, influencing cell proliferation, motility, invasiveness and tumorigenicity (Iolascon et al., 2000; Jelinek et al., 2003; Klein et al., 2001). With previous studies establishing the essentiality of proper BG expression, it has been difficult to elucidate how BG potentiates TGF- β 2 signaling with biological experimentation alone. One recent model proposed by Villarreal et al., 2016, describes a stepwise cooperative binding mechanism where the two protein domains of BG bind to the ligand, thereby increasing the affinity of T β RII to the ligand. T β RII then recruits T β RI which displaces one domain of BG from the ligand-receptor compound forming a quaternary BG species, TGF- β 2/BG/T β RII/T β RI (Figure 1C). This species is thought to be unstable, leading to a rapid dissociation of the second domain of BG. Once the second domain of BG is dissociated, another T β RI and T β RII monomer binds to form the heterotetramer for maximum signaling capacity. At this point, it becomes not only important to test the model put forward by Villarreal et al., 2016, but to test the potential dynamic behaviors and leading assumptions that may arise from this proposed model.

2.4 Results of TGF- β Signaling Dysregulation

In addition to regulation of cell proliferation, immune response, integrin expression, and extracellular matrix component expression, TGF- β signaling in epithelial and endothelial cells regulate differentiation, apoptosis, and cytotaxis (Massagué, 2008). Due to its importance in these areas, dysregulation of TGF- β signaling has led to certain cancers and fibrosis through uncontrolled cell proliferation, cancer metastasis, and breaking of immune tolerance (Fabregat et al., 2014; Massagué, 2008).

One rare event that can disrupt the function of TGF- β signaling is through mutations in T β RII and Smad proteins. These mutations cause a structural deformation in the proteins that lead to inactivation of the signal transduction pathway (Massagué, 2000). Although mutations in T β RII and Smad proteins lead to the disruption in the tumor-suppressive function of TGF- β , it is more common for cancer cells to hijack TGF- β signaling to promote cell invasion, proliferation, and differentiation into invasive cell types (Massagué, 2000). Therefore, a key to preserving normal propagation of adequate TGF- β mediated signaling and developing effective cancer therapeutics, lies in an accurate understanding of intricate mechanistic details surrounding TGF- β receptor complex assembly. The work performed here aims to provide more insights into TGF- β signaling pathway by investigating the BG-mediated signal enhancement of TGF- β 2 through mathematical modeling.

2.5 Mathematical Modeling Importance

Mathematical modeling consists of three main steps: (i) the implementation of the model through the description of objects and defining their relationship with mathematical equations; (ii) use the model to validate or predict system behavior and (iii) evaluation of the model's implications to the reality of the biological system under study (Motta and Pappalardo, 2013).

Biological processes like the TGF- β 2 receptor complex assembly pathway are inherently complex and can seem counter intuitive if analyzed solely by observation. Biological phenomena's such as feedforward loops, nonlinear reaction kinetics, and random (stochastic) effects result in unpredictable biological behaviors that are troublesome to explain with laboratory experiments alone (Fischer et al., 2008; Motta and Pappalardo, 2013). The application of mathematical models to complex biological systems has allowed researchers to investigate how regulatory networks function together, predict how disruptions or dysregulation of these processes contribute to disease progression and development, and analyze perturbations in the system to generate hypotheses and suggest experiments for conclusion validation (Elowitz et al., 2002; Gardner et al., 2000; Karim et al., 2012; Schmierer et al., 2008; Umulis et al., 2010).

Computational models alone cannot prove or disprove biological hypotheses but are able to test the gaps of knowledge that laboratory experiments cannot. For example, surface plasmon resonance (SPR)-based biosensors are an excellent experimental tool to study biomolecular

interactions but cannot easily discriminate between specific and non-specific interactions with the sensor surface and have limited sensor area, leading to a diminished capacity for testing (Ahmed et al., 2010). SPR is also mass sensitive, so the sensitivity for binding kinetics of high molecular weight molecules is good but binding of low molecular weight compounds are more difficult (Ahmed et al., 2010). Direct analysis of how the tetrameric signaling unit forms is limited with biological methods due to the inability to isolate intermediate macromolecules and analyze their binding kinetics in real time. Therefore, a less restrictive process for analyzing the behavior of biochemical networks can be integrated in a deterministic and/or stochastic model (Abel et al., 2016). Theoretically, it allows hypotheses about the interactions between the intermediate macromolecules in TGF- β pathway to be tested freely.

Deterministic approaches use a set of ordinary differential equations to calculate expected behavior of a system under the law of mass action to observe the outcome for biological comparison and validation. Deterministic modeling has been applied to a wide range of biological systems, from the description of metabolism (Kremling et al., 2007), signaling pathways (Shinar et al., 2007) or gene regulation within cells (Tyson and Othmer, 1978), to probing the systematic effects in complex organisms (Gallenberger et al., 2012). Although, deterministic modeling has been a widely used tool in quantitative biology, it neglects noise or stochastic effects which are inherent to biological processes.

Stochastic approaches have been developed to capture the randomness (stochastic effects) that play a major role in signaling and regulation. Stochastic modeling used in this work uses the Gillespie algorithm to determine a discrete chemical master equation (CME) to numerically simulate the stochastic time evolution of a biochemical system (Hahl and Kremling, 2016; Gillespie 1976; Gillespie 2016).

To this date, there have been several mathematical models aimed at analyzing TGF- β signaling dynamics, leading to a better understanding of intracellular signaling components and roles of feedback loops in regulating TGF- β signaling responses (Cellière et al., 2011; Chung et al., 2009; Melke et al., 2006; Schmierer et al., 2008; Vilar et al., 2006; Wegner et al., 2012; Zi et al., 2011). Although there has been extensive modeling of TGF- β signaling dynamics, there have been no attempts to quantitatively analyze BG and its interaction with the TGF- β receptor complex assembly pathway. The computational modeling performed in this work aims to suggest experiments to support or refute a proposed model of TGF- β 2 receptor complex assembly

pathway under different perturbations of BG-mediated signal enhancement. This work seeks to build a useful model to benefit researchers in their investigations to further elucidate how BG enhances the TGF- β 2 signaling pathway and to provide baseline models for further computational experiments of the TGF- β family.

3. COMPUTATIONAL MODEL OF BETAGLYCAN-MEDIATED TGF- β 2 RECEPTOR COMPLEX ASSEMBLY PATHWAY

This chapter will be submitted for review.

3.1 Abstract

Transforming Growth Factor (TGF) TGF- β 1, TGF- β 2, and TGF- β 3 are secreted signaling proteins that play an essential role in tissue development, immune response, and physiological homeostasis. TGF- β ligands signal through a tetrameric complex made up of two type I receptors (T β RI) and two type II receptors (T β RII). Amongst the ligand types, TGF- β 1 and TGF- β 3 are efficient signalers, presumably by strong binding to both type I and II receptors (T β RI and T β RII, respectively). However, TGF- β 2 has a very weak affinity for T β RII and requires an additional membrane-bound protein called betaglycan (BG) to achieve similar levels of downstream signaling. To determine the role of betaglycan in selectively facilitating TGF- β 2 signaling, we developed computational models with different hypotheses based on the levels of cooperativity between receptor subtypes and types of betaglycan behavior. Using a combination of published kinetic rate data for known quantities and optimization to determine unknown quantities, we identified conditions for selective enhancement of TGF- β 2 signaling and provide support for additional receptor binding cooperativity that has been hypothesized but not tested in literature. In summary, it appears that betaglycan binding to TGF- β 2 ligand through two domains provides an effective transfer mechanism that can be tuned to control differential signaling between TGF- β ligand subtypes.

3.2 Introduction

Transforming Growth Factor- β (TGF- β) signaling in development and disease relies on three extracellular ligands, TGF- β 1, TGF- β 2, and TGF- β 3. TGF- β 's signal transduction pathway activates when one type II receptor and one type I receptor bind to initiate a cross-phosphorylation reaction that results in phosphorylation of an intracellular Smad molecule. While it is thought that receptor dimers are able to signal, the most efficient signaling comes

from a heterotetrameric complex between the ligand and two type II (T β RII) and two type I (T β RI). These complexes pass the signal from the extracellular environment to the intracellular environment by a cascade of phosphorylated Smad proteins that enter the nucleus and regulate targeted gene expression. The heterotetrameric signaling complex induces four-fold greater nuclear pSmad accumulation than other heterodimer complexes (Huang et al., 2011). Structural analysis, cell experimentation, and thermodynamics heavily support a ligand-dependent and step-wise oligomerization process (Nickel et al., 2009; Villarreal et al., 2016). Figure 1A reflects this knowledge and depicts the reaction pathways incorporated in our models for heterotetrameric complex assembly.

Published surface plasmon resonance data provide kinetic rates for many steps in the receptor assembly pathway. To establish a baseline model, we began with the assumption that later additions of T β RI and T β RII proceeded at the same rate as the original addition. Table S1 shows the rates for the model, including citation and a brief rationalization for their use. With the kinetic rates accounted for, we developed and tested three deterministic models to investigate a previously proposed mechanism by which BG selectively enhances TGF- β 2 signaling. The models were also used to identify the degree of receptor cooperativity needed in the receptor complex assembly pathway to produce data-consistent models.

For all three ligands, there are multiple surface plasmon resonance experiments that show a higher affinity of T β RII binding to the ligand compared to T β RI. This suggests a sequential process where the high-affinity type II receptor binds to the ligand first and then recruits the low-affinity type I receptor (Huang et al., 2014; Radaev et al., 2010; Villarreal et al., 2016). Cell experimentation supported this hypothesis by identifying a composite binding epitope between the TGF- β 3/T β RII complex that forms a functional binding site for T β RI (Huang et al., 2014). This data showed that the receptor assembly pathway is not only a sequential process but has cooperative receptor recruitment present through direct receptor-receptor contact in all three ligand types. A schematic of cooperative receptor recruitment is displayed by the blue and purple receptors in Figure 1B. The purple receptor would not normally bind to the ligand due to its weak binding affinity to the “free-floating” ligand in solution (top image in Figure 1B). However, the presence of a ligand bound blue receptor increases the binding favorability of the purple receptor to the ligand-complex through ligand localization affects and/or conformational changes to the ligand-complex. This interaction makes the binding of the purple receptor to the

ligand possible or increases the reactions occurrence (bottom image in Figure 1B). This cooperative receptor recruitment has been found in the TGF- β system where the blue and purple receptors are T β RII and T β RI, respectively (Groppe et al., 2008; Huang et al., 2014; Radaev et al., 2010; Villarreal et al., 2016). Therefore, the SRR model was developed and includes the experimentally proven recruitment of T β RI by T β RII, this is pictured by the red arrows in Figure 1A (Huang et al., 2014). Due to the stabilized epitope between T β RII and the ligand for increased binding of T β RI (SRR model) it is hypothesized there is a similar stabilizing epitope between the ligand and T β RI for increased binding of T β RII. Therefore, the TRR model was developed and includes the recruitment represented in the SRR model as well as a symmetric form of recruitment where a ligand-bound T β RI increases the affinity of T β RII to the ligand-complex. Similar symmetric and/or additive cooperative receptor recruitment interactions have been found in other receptor proteins such as RXR nuclear receptor, TCR, Proteinase-activated Receptor2 and TLR4 (Chen and Privalsky 1995; Martin-Blanco et al., 2018; Rallabhandi et al., 2008). The TRR model is visually represented by the red and blue arrows in Figure 1A. The recruitment of T β RII by T β RI has not been tested with biological methods due to the extremely low affinity of T β RI to the ligand and the resulting difficulty in obtaining the complex for measurement via surface plasmon resonance experiments. The computational approach used in this paper allowed us to test the validity of this symmetric receptor recruitment, the role of BG, and evaluate overall receptor oligomerization performance. In Figure 1A the black arrows are reactions that are the same between all tested models that differ in the degree of receptor cooperativity. The NRR model assumes no receptor recruitment is present and acts as a control to measure changes in signaling in the oligomerization pathway.

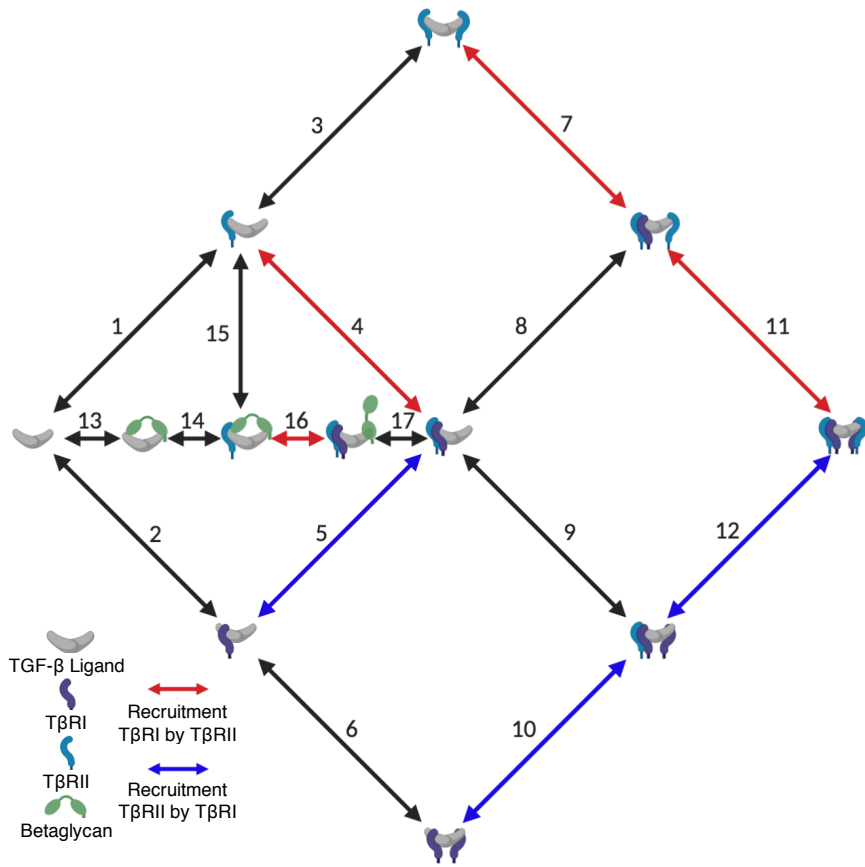
The next component added to our computational models and the one this paper mainly focuses on is the interaction of betaglycan (BG) with TGF- β 2. BG is a membrane-bound coreceptor that is vital in the TGF- β 2 system to produce effective signal transduction through the cell but is not required in the TGF- β 1 and TGF- β 3 systems. Without BG present in the TGF- β 2 system, mice die during embryogenesis due to heart and liver defects (Wiater et al., 2006). The absence of BG during development has been shown to disrupt mesenchyme formation in the heart and branching morphogenesis in the lung (Brown et al., 1999). Elucidating the mechanism by which BG enhances TGF- β 2 signaling will provide one more piece to the developmental picture.

The hypothesized BG-mediated TGF- β 2 signaling enhancement modeled in this paper was first proposed in Villarreal et al., 2016 and postulates that the two domains of BG interact with the ligand and receptors to create a more favorable pathway for receptor dimerization than if BG was not present (Figure 1C). In this "hand-off" mechanism, both of BG domains bind to the ligand (I) and increase the affinity of T β RII by localizing the ligand to the cell membrane and inducing a conformational change of the ligand-BG complex (II). The orphan domain of BG (BG-O) is then displaced from the ligand complex through the recruitment of T β RI (III). Then the zona pellucida domain of BG (BG-ZP) dissociates to form the heterodimer (TGF- β /T β RII/T β RI) and to allow the formation of the tetrameric signaling complex (IV). Not much is known about the TGF- β /BG/T β RII/T β RI species created in this proposed pathway. Experimental evidence supports the assumption that this species is transient due to the failure to capture TGF- β /BG/T β RII/T β RI in cross-linking experiments. Villarreal et al., 2016 proposed it may be a transient compound with a rapid dissociation of BG-ZP when bound in complex with T β RI, and therefore, is not a major contributor to the overall signal of the system. However, contrary to this view, it is technically challenging to capture quaternary intermediate species in general with current experimental tools and an absence of the intermediate species does not preclude formation of the complex in the dynamic signaling environment. With the available evidence taken into consideration our starting assumption is that this species is transient, and therefore, does not contribute to signal. The computational models created in this paper address these possibilities to weigh hypotheses on the role of BG and identify data-consistent mechanisms and assumptions needed to replicate in vitro BG behavior.

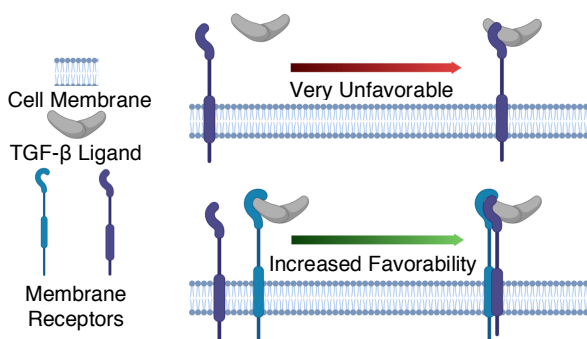
Models of BG behavior that are most consistent with observations have a number of evaluation criteria on BG behavior that include 1) enhancing TGF- β 2 signaling to levels comparable to TGF- β 1 and TGF- β 3, 2) increasing signal production in TGF- β 2 to a greater degree than TGF- β 1 and TGF- β 3, 3) inhibiting TGF- β signaling in a concentration dependent manner.

Figure 1: Schematic and biology of TGF- β receptor signaling complex formation. (A) All three TGF- β ligands (TGF- β 1/2/3) signal through a tetrameric signaling complex composed of two Type II receptors (blue bean) and two Type I receptors (purple bean) and its formation can be aided by a membrane bound coreceptor, betaglycan (green bean). Receptor complex assembly is formed through reversible reactions (double-sided arrows). The colored arrows indicate where cooperative receptor recruitment was found and/or tested. The Single-stage Receptor Recruitment (SRR) model accounts for the recruitment of T β RI by T β RII (red arrows) and the Two-stage Receptor Recruitment (TRR) model builds off the SRR model by further incorporating the recruitment of T β RII by T β RI (blue arrows). (B) Cooperative receptor recruitment is a biological interaction where the presence of one receptor increases the affinity of another receptor, usually a weak affinity receptor. (C) In the TGF- β 2 system, betaglycan with two domains (orphan, BG-O, and zona-pellucida, BG-ZP, domains) is predicted to enhance TGF- β 2 signaling by increasing the affinity of the T β RII (blue receptor). Betaglycan dissociates and T β RI (purple receptor) binds, creating half of the tetrameric signaling complex.

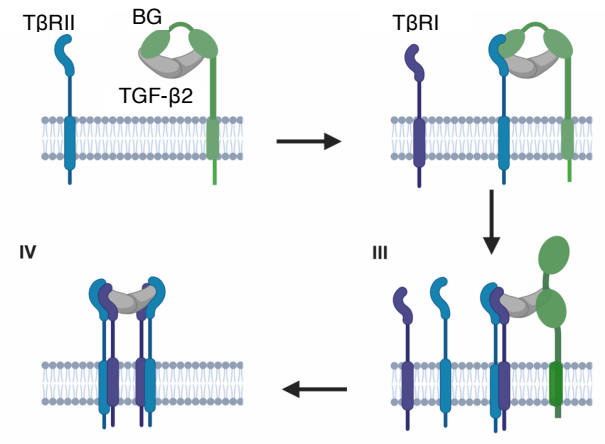
A. TGF- β Receptor Signaling Complex Formation



B. Cooperative Receptor Recruitment



C. Proposed Betaglycan Signal Enhancement



3.3 Results

To establish minimal requirements for our BG and receptor signaling simulation, we relied on a combination of quantitative and qualitative BG observations for model evaluation. The evaluation criteria are based on observations from specific experimental results previously published to discriminate BG function. The evaluation criteria for our betaglycan models are listed below.

Evaluation Criteria:

- BG increases signal production in TGF- β 2 to a greater degree than TGF- β 1/3 (Villarreal et al., 2016).
- BG recovers TGF- β 2 signaling to levels comparable to TGF- β 1/ β 3 ligands (Cheifetz et al., 1990; Villarreal et al., 2016).
- BG can inhibit TGF- β signaling in a concentration dependent manner (Eickelberg et al., 2002; Karim et al., 2012; Serpe et al., 2008).

There is strong theoretical and experimental evidence that the third statement in our evaluation criteria is a reasonable BG behavior to expect--BG inhibits TGF- β signaling in a concentration dependent manner. The most notable evidence for supporting this statement comes from experimental work published in 2002 which demonstrated BG acts as an antagonist to TGF- β signaling in certain cell lines (Eickelberg et al., 2002). Theoretically, A coreceptor that sequesters ligand from the extracellular environment to present it to the receptor for binding, has the ability to act as a competitive inhibitor at high concentrations. This biphasic effect was also demonstrated in 2012 with the BMP coreceptor, CV-2 (Karim et al., 2012; Serpe et al., 2008). Furthermore, other coreceptors in the TGF- β family, with high sequence similarity to betaglycan, have been found to produce a biphasic effect in TGF- β signaling (Lastres et al., 1996; López-Casillas et al., 1991). Due to the strong theoretical and experimental evidence that BG acts as a competitive inhibitor in a concentration dependent manner, it was included in our evaluation criteria.

An important consideration for the computational models to accurately reflect a biological system is the incorporation of a surface enhancement factor (SEF). The SEF accounts for local increases in concentration and access of interacting receptors, thereby, enhancing second order reactions that occur on the cell membrane. Typically, there are two sequential resistances for a binding reaction to occur between two components-- the transport limited step

and the reaction limited step. The first, advantage to reactions that take place on a surface or cell membrane as opposed to one component in solution is that the reactions are essentially 2D once bound, removing a complete degree of freedom from 3D to 2D through a process often called a reduction of dimensionality. Even though transport may be slower relative to free solution, the reduced dimension provides greater probabilities of coming into contact with a binding partner. This can be modeled by an effective decrease in dissociation constants and this would apply equally to all surface-localized reactions. Therefore, reactions that take place between two membrane-bound macromolecules will have an increased favorability in comparison to a reaction where an extracellular signaling molecule has to find and favorably orient itself with a transmembrane protein (reactions 1, 2, & 13 in Figure 1A). Specific reasoning on quantifying the SEF value can be found in the supplemental material.

We first analyze the viability of the three receptor recruitment models (NRR, SRR, TRR) in all three TGF- β ligand systems. We use a two-step approach to evaluate the biological relevancy of each model and the proposed “hand-off” mechanism for BG-mediated TGF- β 2 signaling. First, we calculate a root mean square error between the computational models with no BG present to experimental signaling data in cell lines with no BG (Supplemental Material). Lower RMSE values indicate the simulated data is more representative of experimental signaling behavior when no BG is present. The second round of model validation was performed by adding BG into the simulations and comparing its behavior to the evaluation criteria of BG behaviors mentioned in literature and listed in the introduction (Cheifetz et al., 1990; Eickelberg et al., 2002; Villarreal et al., 2016).

No betaglycan in simulations

The known and unknown parameters, starting conditions that affect the model output, in the no BG simulations were similar across all three ligand types (β 1/2/3) and across two of the receptor complex assembly models (NRR and SRR). The known parameters for the first simulations were ligand concentration and receptor concentration. The specific ligand concentrations selected, enabled comparison of simulated data to experimental data (Cheifetz et al., 1990). The starting receptor concentration selected, 160 nM, was the median receptor level found across a wide range of cell lines present in literature and converted to concentration (nM) with volume calculations found in the supplemental material (Supplemental Material).

Equimolar concentrations for T β RI and T β RRII were used in our simulations based on previous work on the TGF- β system operating with the same assumption (Chung et al., 2009). To ensure model consistency and integrity, a range of receptor concentrations, 100 to 250 nM, was tested to determine the effect of this parameter value on signal performance.

With the biophysical data available in literature, there is only one unknown parameter for each ligand type in the NRR and SRR models. The unknown parameter is the absolute rates of TGF- β 2 reaction 1 (including homologous reactions, see supplemental), and TGF- β 1 and TGF- β 3 reaction 2 (including homologous reactions, see supplemental). While the value of the dissociation constant for each reaction is known, the specific rates for the forward and reverse binding steps (absolute rates) are not known. To test the impact of these default values on the RMSE calculation, we performed a local sensitivity analysis on the forward and reverse binding steps by simultaneously increasing their values between 1 and 500-fold. The default rates were curated based on similar reactions with measured forward and reverse binding steps and were increased to relevant ranges found in literature. Simultaneously increasing the fold change in the forward and reverse binding steps preserved the experimentally measured dissociation constant and allowed us to determine the impact of changing the absolute rates on the RMSE calculations. As shown in Figure 2A, increasing the fold change value of the absolute rates to ranges that were observed in literature, did not improve model fit in either receptor recruitment model across a range of receptor concentrations. Furthermore, decreasing the absolute rate values to different degrees between the three ligand types did not lead to appreciable change in individual model fitness as measured by the RMSE calculations. For example, in the NRR model, decreasing TGF- β 1/3 reaction 2 et al. by 5-fold while decreasing TGF- β 2 reaction 1 et al. by 500-fold did not appreciably affect the RMSE analysis (Figure S1). Due to the minimal impact of changing the absolute rates for both models, the magnitude of the absolute rates chosen were the starting default values (blue line in Figure 2A). For both models, changing the default receptor value of 160 nM minimally affected the signaling pattern as shown in Figure 2A. The results of the local sensitivity analysis for receptor concentration supported the selection of our starting receptor concentration value.

The second simulation tested the accuracy of the TRR model when no BG is present. The known parameters for this simulation, ligand concentration and receptor concentration, were maintained from the first simulation. The unknown parameter conditions were the degree of

recruitment for the receptor recruitment added to reactions 5, 10, and 12 (reference Figure 1A), and the absolute rate values for these reactions. Similar to the first simulation, decreasing the values of the absolute rates while preserving the dissociation constants did not correspond to appreciable changes in RMSE values (Figure S2). Figure 2B shows the effect of increasing the degree of recruitment in the TRR model on the RMSE analysis. The bars at each point represent the minimal impact of changing absolute rates. The degree of recruitment to best fit the experimental data is roughly 5 (Figure 2B and S3). This value characterizes the degree of increased favorability that a ligand bound T β RI has on recruiting T β RII to the ligand-complex. With the default values used for our unknown parameters in all three receptor recruitment models, there was no appreciable change in the RMSE value when the equimolar assumption for T β RII and T β RI was relaxed (Figure S4) Therefore, a receptor concentration of 160 nM for T β RI and T β RII was maintained for further computations and should be assumed unless otherwise mentioned.

The parameter sets used for Figure 2C, represent a good solution for each model at a receptor concentration of 160 nM, SEF of 50, and default absolute rate values with similar magnitudes to the absolute rates already determined in SPR experiments. All three models can produce results that recapitulate TGF- β 2 signaling patterns with no betaglycan present, but relative to each other, the SRR and TRR models produce a better-fit to no BG experimental data. TGF- β 1 and TGF- β 3 were also modeled as a further validation of the working assumptions in each model. Although they are not the focus of our paper, they further validate our simulation set up by having similar signaling patterns in the SRR and TRR models as the kinetic rates for each reaction are very similar. As predicted, the NRR model underperforms in reproducing TGF- β 1 and TGF- β 3 behavior likely due to the lack of receptor recruitment that is present in the other models.

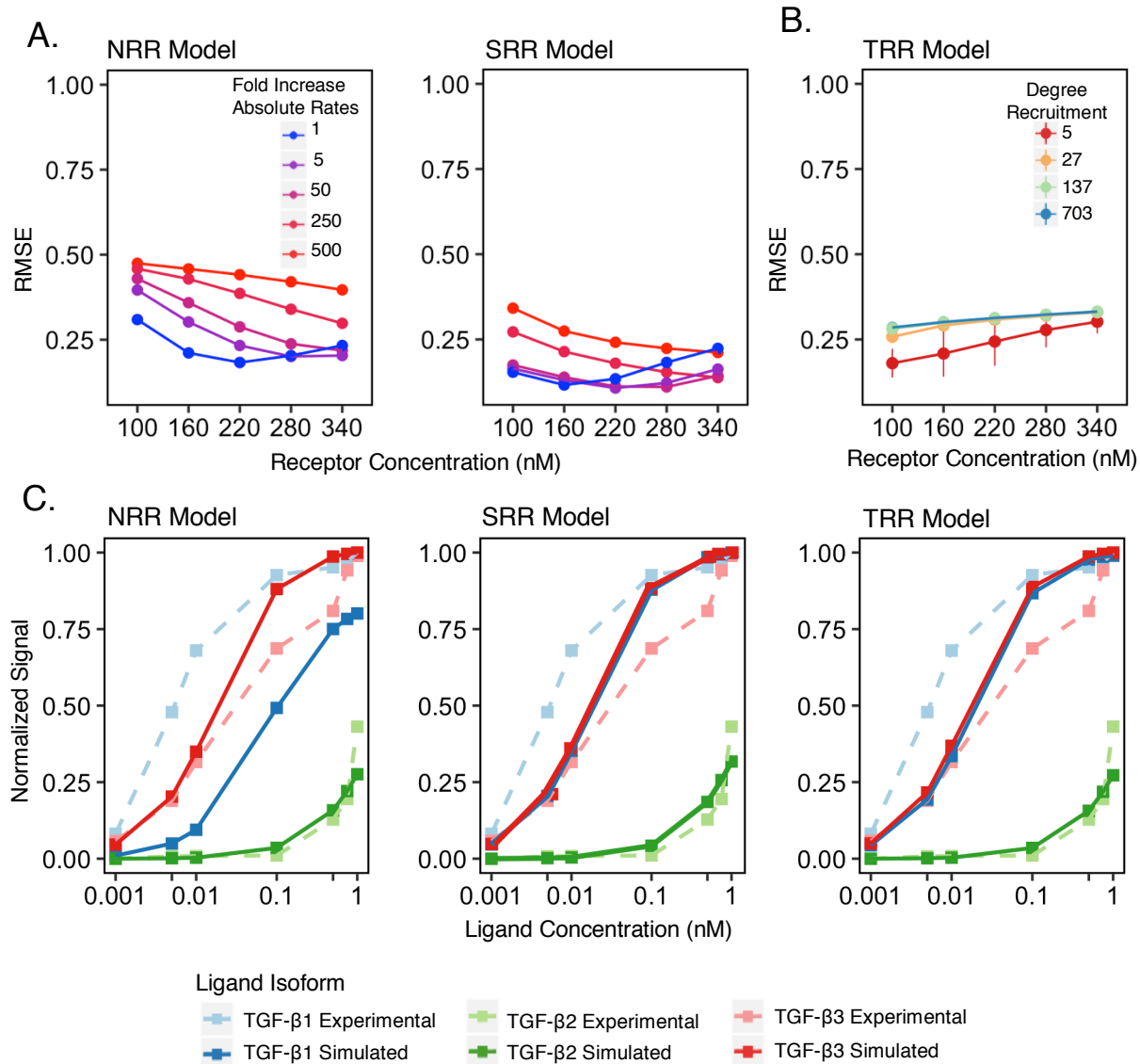


Figure 2: Results of simulated models vs published data and parameter selection when no BG is present. (A) Changing the value of the default receptor concentration, 160 nM, and the default absolute rates (blue line) while having a uniform dissociation constant (on-rate/off-rate ratio), does not improve the RMSE value for the NRR and SRR models. (B) The degree of recruitment (red to blue lines) with the best-fit for the hypothesized receptor recruitment of TβRII by TβRI was approximately 5-fold. (C) With the predetermined SEF value of 50 and receptor concentration of 160 nM across all models, the “best-fit” simulations (solid lines) are able to obtain results similar to experimental data (dotted lines) (Cheifetz et al., 1990).

The impact of betaglycan on receptor complex formation

For the second step of model validation, we added BG to the simulations. Figure 3A depicts how effective BG is in each model at enhancing the signal production of the TGF-β2

system in comparison to the percent of tetramer produced out of the signaling species and TGF- β 2/BG/T β RII/T β RI. The points represent every parameter set tested for the three models. A tradeoff is present between the amount of BG induced signal increase and the percent tetramer produced in all three models.

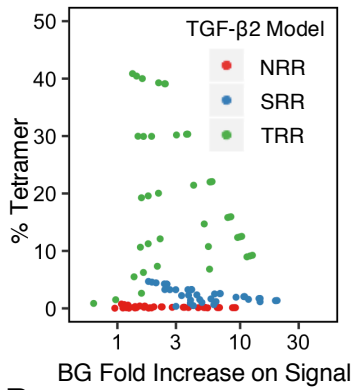
Figure 3B shows all three models meet the first and third evaluation criteria of BG behavior—there is a greater positive impact on TGF- β 2 signal (blue line) than TGF- β 1/3 (red/green lines) and BG inhibits signal in a concentration dependent manner. Each of the graphs are normalized to signaling levels with no BG present. Due to the normalizing technique the SRR model produces the best fold change out of the three models but produces less absolute signal (nM) than the TRR model (Figure 3C). Figure 3D shows how well each model meets the second and third evaluation criterium of BG behaviors-- BG produces TGF- β 2 signal that is comparable to TGF- β 3 signal and BG inhibits signal in a concentration dependent manner. The black dotted line represents no change in signal production when BG is added to the system. The blue dashed line is the peak signal that TGF- β 3 produces with no BG present in the system. As demonstrated by a BG concentration of 240 nM, all TGF- β 2 models experience a biphasic effect by BG where high concentrations repress TGF- β 2 signaling. BG's behavior in the TRR model performs the best by TGF- β 2 signal achieving roughly 75% of TGF- β 3 signaling. BG provides less than 20% recovery in the SRR model and almost zero percent recovery in the NRR model. A rescue closer to 100 % in TGF- β 2 signaling is preferred because experimental data shows that BG fully rescues TGF- β 2 signal to TGF- β 1 and TGF- β 3 signaling levels.

To investigate the causes of suboptimal TGF- β 2 signal rescue, we looked at all the individual species concentrations at steady state to obtain a better understanding of our models' behavior. Figure 3E is a breakdown of the signaling species and TGF- β /BG/T β RII/T β RI composition at steady state for each model. None of the models produce greater than 50% tetramer (bright pink) and all the models' major species is TGF- β /BG/T β RII/T β RI. This observance is at odds with the predicted behavior from our hypothesized model, that TGF- β /BG/T β RII/T β RI should be a transient species. This inconsistency may indicate that the transient species prediction is false, or the BG quaternary species is transient, but the inferred SPR kinetics are inaccurate for the dissociation of the TGF- β /BG/T β RII/T β RI species. Since the TGF- β /BG/T β RII/T β RI species could not be isolated, the inferred SPR measured rates for the dissociation of the BG quaternary species is the dissociation of the BG-ZP domain from a free

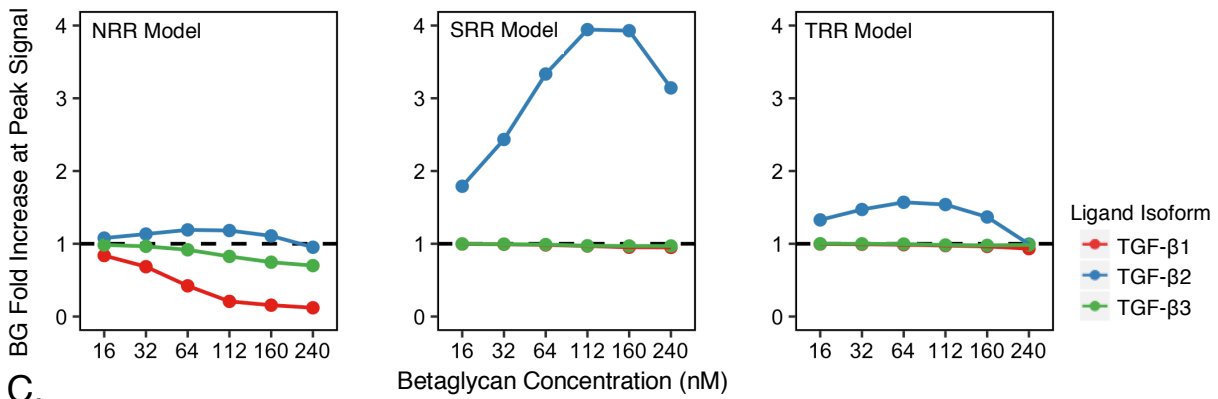
ligand. If the predicted behavior is wrong and TGF- β 2/BG/T β RII/T β RI (species circled in red, Figure 4A) is not transient, then it would be able to contribute to overall signal. When we allowed this species to contribute to signal we observed, across an extremely wide combination of ligand concentrations and BG concentrations, that there is no biphasic effect present (Figure 4B). These results demonstrate if TGF- β 2/BG/T β RII/T β RI is not a transient species it cannot contribute to signal in order to recapitulate BG inhibitory effect on TGF- β 2 signaling. If the transient hypothesis is true, then the inconsistent accumulation of TGF- β /BG/T β RII/T β RI species may be a reason for the suboptimal TGF- β 2 signal recovery. A screen for the dissociation of BG-ZP domain in the TGF- β /BG/T β RII/T β RI species (reaction 17) was performed to test if the inferred SPR kinetics are a reason for the impeded rescue.

Figure 3: Poor performance in three models when BG is added. (A) The parameter sets with an SEF of 50 and a receptor concentration of 160 nM (colored dots) for each TGF- β 2 model are displayed together. A tradeoff between tetramer production and BG enhanced signal is present across all of the models. (B) The signaling enhancement of the three ligand isoforms by BG across the three models was greater in the TGF- β 2 (blue line) system than TGF- β 1/ β 3 (green and red lines) systems. The data was normalized to the amount of signal produced in each model with no BG present, therefore, the black dotted horizontal line represents no increase in signal by adding BG. (C) The absolute signaling concentrations (dashed lines) for the three ligand systems (same coloring as Figure 3C) across the three models are shown. The NRR model produced almost no TGF- β 2 signal and the TRR model produced two times more TGF- β 2 signal than the SRR model. (D) When BG was added (x-axis), the TRR model at 75% recovery, was the best at recapitulating TGF- β 2 signal to levels comparable to TGF- β 3 signal (blue dashed line). Higher concentrations of BG inhibit TGF- β 2 signal as seen by the bell shape curves on the graph. (E) TGF- β 2 species composition of the signaling species and TGF- β 2/BG/T β RII/T β RI across each model. The TRR model produced more tetramer (bright pink) than the NRR and SRR models, and the major species in all models is TGF- β 2/BG/T β RII/T β RI (light red).

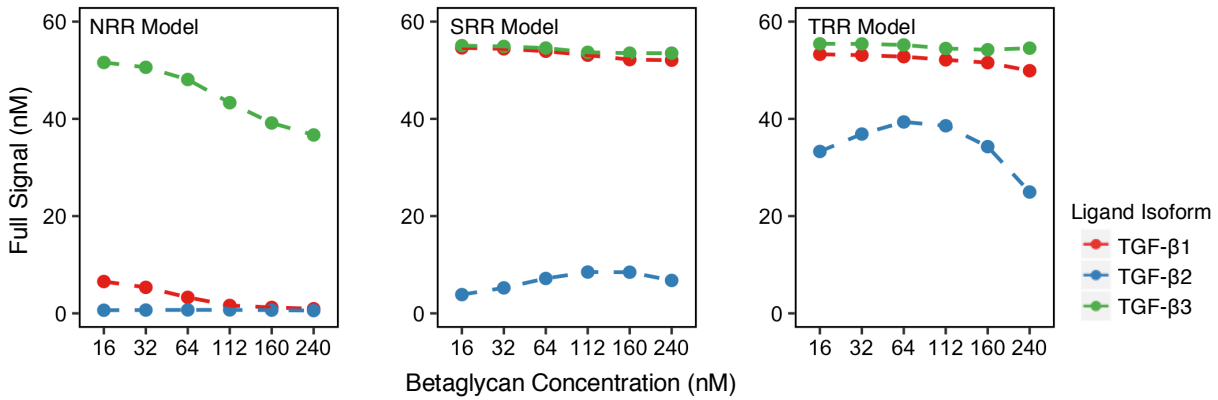
A.



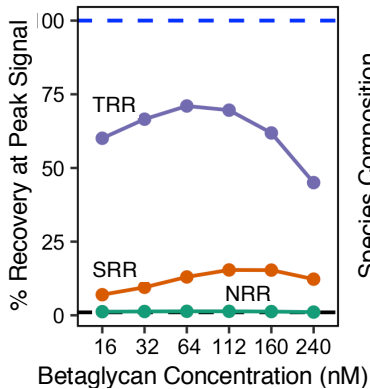
B.



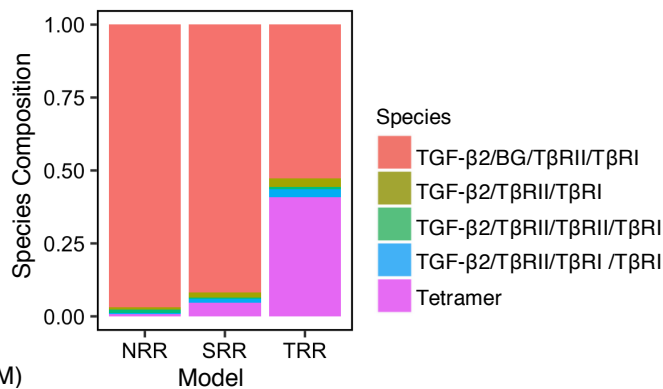
C.



D.



E.



Testing the effects of increasing BG-ZP dissociation

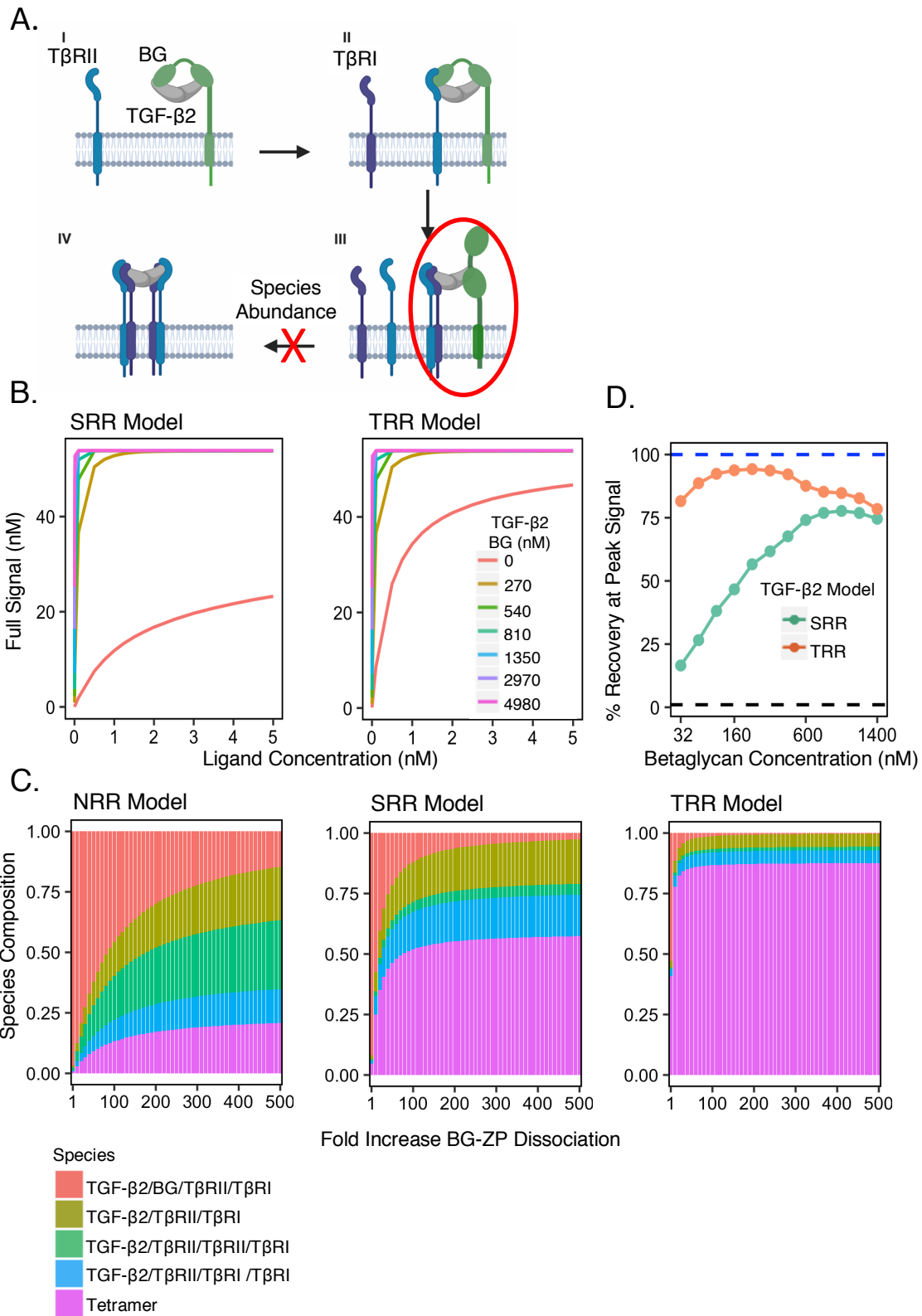
In order to further investigate how the two BG domains work together to enhance TGF- β 2 signal recovery, we increased the dissociation of the BG-ZP domain between a range of 1-500 to determine if the reduced abundance of TGF- β 2/BG/T β RII/T β RI-(species circled in red, Figure 4A) would lead to the formation of more signaling species and an increase in BG potentiated signal recovery for TGF- β 2 .

With greater than 100-fold increases in BG-ZP dissociation, the NRR model can produce results where the TGF- β 2/BG/T β RII/T β RI species is less than 50% of the signaling species (Figure 4C). With minimal increases in BG-ZP dissociation in the SRR and TRR models the abundance of TGF- β 2/BG/T β RII/T β RI was reduced, the prevalence of the heterotetramer increased, and it became the new major species in the receptor recruitment models (Figure 4B). Compared to the SRR and TRR models, the NRR model performs poorly at reducing the abundance of TGF- β 2/BG/T β RII/T β RI species. Due to this expected substandard performance and for the ease of comparison between the SRR and TRR models, the NRR model was left out of further analysis. For each model, we selected a fold increase in BG-ZP dissociation which produced at least 90% of the maximum signal for each model (100 and 30-fold increase for the SRR and TRR, respectively). Selecting a fold increase in BG-ZP dissociation beyond the selected value minimally affects the signaling results of each model. This idea is visualized by the logarithmic shaped curve in species composition graph as the fold change in BG-ZP dissociation increases (Figure 4C).

By minimally increasing the BG-ZP dissociation in the SRR and TRR models, a higher percent recovery in TGF- β 2 signal was observed. Using the same logic in Figure 3D, Figure 4D shows the TRR model can now achieve greater than 95% recovery of peak signal produced by TGF- β 3 while the SRR model produces roughly 75% with a wide range of BG concentrations tested (32 nM to 1400 nM). Comparing Figure 3D and Figure 4D, the signal recovery levels are higher for both the SRR and TRR models when TGF- β 2/BG/T β RII/T β RI is predicted to be transient and the dissociation of the species is minimally increased. These results support the conclusion that BG-ZP quickly dissociates when T β RI is bound and the TGF- β 2/BG/T β RII/T β RI species does not signal or minorly contributes to the overall signal of TGF- β 2 system. To test this experimentally, it will be important to further measure the impact of BG on TGF- β signaling under various amounts of BG overexpression..

Thus far, the proposed mechanism in Villarreal et al., 2016 with published rates from SPR experiments does not meet our evaluation criteria if the TGF- β 2/BG/T β RII/T β RI species is allowed to contribute to signal because there is no inhibitory effect when a wide range of BG was added. Furthermore, if the TGF- β 2/BG/T β RII/T β RI species is transient our results demonstrate that a minimal increase in the dissociation of this species allows for a higher percentage of TGF- β 2 signal rescue. When comparing two other system behaviors, percent tetramer and BG induced signal enhancement, the models that include the increase in BG-ZP dissociation outperform the previous models with the unchanged, inferred SPR data (Figure 5A). Figure 5B summarizes the effect of increasing BG-ZP dissociation on model performance at varying concentrations of BG (red to blue lines). This RMSE analysis not only compares the signaling differences between TGF- β 2 with BG to TGF- β 3 without BG, but also incorporates the expected signaling behavior of TGF- β 1 and β 3 systems with and without BG. The TRR model once again outperforms the SRR model at recapitulating the BG behaviors. Although the SRR model has been proven by SPR experimentations, it would be hasty to assume this is the only form of cooperative receptor recruitment present in the TGF- β system. A symmetric form of recruitment better facilitates the formation of the heterotetramer which follows the pattern in other protein systems (Chen and Privalsky 1995). The TRR model also outperforms the SRR model on almost all evaluation criteria of BG behavior. The work done in this paper suggest the TRR model is the most realistic model tested. To enable researchers to experimentally test the conclusions presented in this paper, differences between the SRR and TRR models were investigated with the following section.

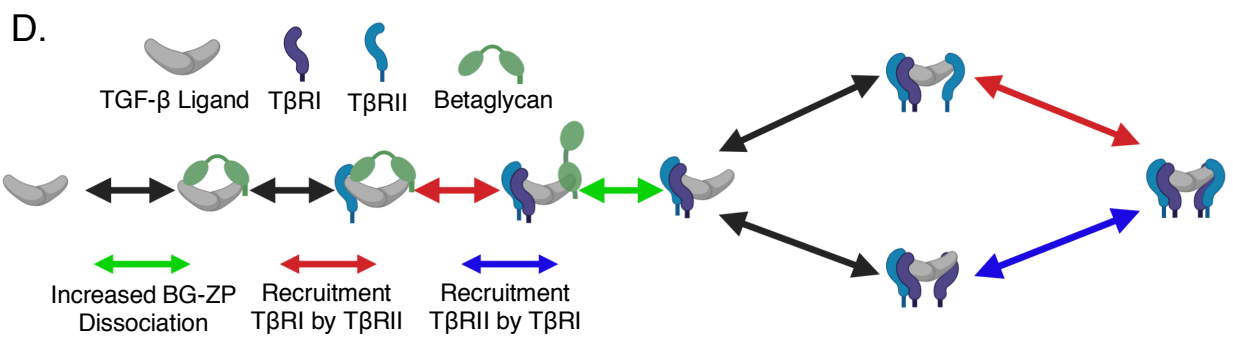
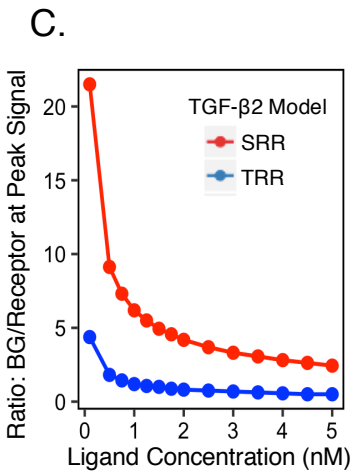
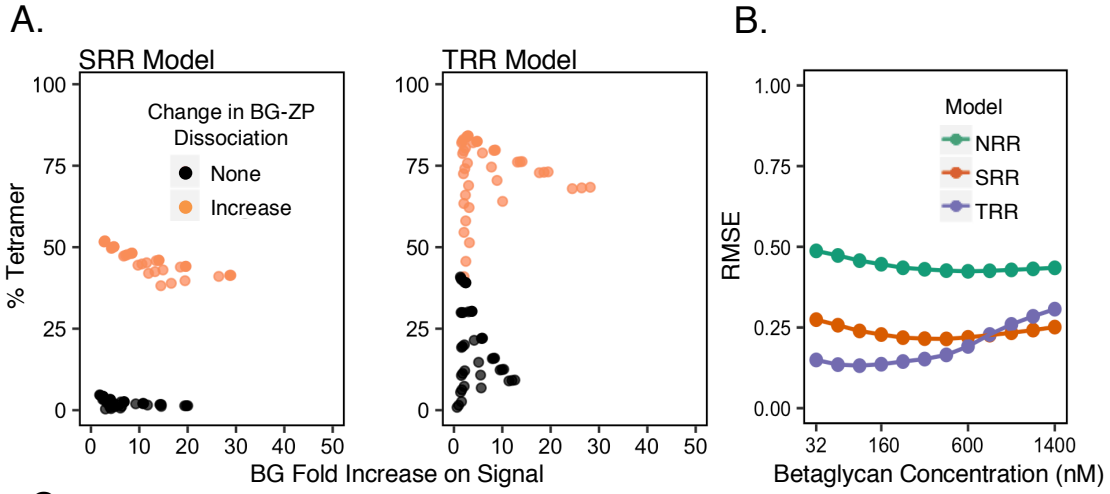
Figure 4: TGF- β 2/BG/T β RII/T β RI inconsistency solved by small increase in BG-ZP dissociation to ligand-complex. TRR model outperforms other models in recapitulating betaglycan behavior. (A) A depiction of the inconsistency previously found where TGF- β 2/BG/T β RII/T β RI complex (circled in red) was the most prevalent species out of all the species created. This abundance was hypothesized to inhibit the formation of signaling species. (B) When TGF- β 2/BG/T β RII/T β RI species is not required to be transient and contributes to signal, there is no biphasic effect across a wide range of ligand concentrations (x-axis) and BG concentrations (colored lines), 0.001 to 5 nM and 0 to 4980 nM, respectively. (C) A species composition analysis at peak signal, with a receptor concentration of 160 nM, and a SEF of 50, shows minimal increases in BG-ZP dissociation reduces the abundance of TGF- β 2/BG/T β RII/T β RI species in the SRR and TRR models. NRR model requires a larger increase in BG-ZP dissociation compared to SRR and NRR models. The BG-ZP dissociation fold increase selected for each model was when increasing the BG-ZP dissociation did not impacted the signaling results with the parameter ranges tested. This behavior is reached whenever 90% of the maximum signal is achieved. (D) TGF- β 2 signal in the TRR model (orange line) can recover greater than 95% of TGF- β 3 signal (blue dashed line) while the TGF- β 2 signal in the SRR model (green line) can recover roughly 75% of TGF- β 3 signal.



Investigating model differences

An observable difference between the SRR and TRR models is the varying betaglycan concentrations that are needed to induce an inhibitory effect on signal (Figure 4D). Therefore, we sought to determine the BG to receptor ratio that is required to produce a biphasic effect under the assumption that TGF- β 2/BG/T β RII/T β RI is transient with a model specific increase in the BG-ZP dissociation (discussed with Figure 4B). With a similar ligand concentration in each system, the SRR model needed a 2.44 to 21.5 BG to receptor ratio to induce a biphasic effect where the TRR model required a 0.50 to 4.38 BG to receptor ratio to induce a biphasic effect (Figure 5C). The SRR model needed a 4.7-4.9 times greater concentration of BG to receptor ratio than the TRR model. Experiments that seek to identify the molar ratios of receptors and betaglycan will provide useful data to discriminate between these alternatives.

Figure 5: Distinguishing between models and BG-mediated TGF- β 2 signal hypotheses. (A) Across a broad range of parameter sets, almost any increase in the dissociation of BG-ZP (orange points) outperforms the original parameter sets with no increase in BG-ZP dissociation (black points). (B) When requiring the TGF- β 2/BG/T β RII/T β RI species to be transient, the RMSE analysis captures how the models measure up to no BG and BG system requirements in all three ligand systems. The NRR model was incorporated again to show effectiveness of adding cooperative receptor recruitment into the TGF- β receptor signaling complex formation in the presence and absence of BG. Each model shows BG's inhibitory effect on TGF- β 's signal by the concave shape of the graphs. Across a wide range of BG concentrations (x-axis) the TRR model recapitulates no BG and BG behavior the best in all three ligand systems until BG inhibits TGF- β signal causing the RMSE to increase. (C) A testable distinction between the SRR and TRR models was found in the BG to receptor ratio required to achieve the biphasic effect on TGF- β 2 signal by BG. Across a wide range of ligand concentrations, 0.001-5 nM, the SRR model (red points) needs 4.7-4.9 time more BG to induce the biphasic effect than the TRR model (blue points). (D) Zoomed in diagram of the receptor complex assembly that highlights the final conclusions. The red and blue arrows represent the types of cooperative receptor recruitment that is hypothesized to be present and the green arrow indicates an increase in the dissociation of TGF- β 2/BG/T β RII/T β RI improves model performance under certain conditions.



3.4 Discussion

The role of BG in selectively facilitating TGF- β 2 signaling has been heavily investigated, but still remains unknown. In the absence of BG, TGF- β 2 cannot form a sufficient number of signal complexes to initiate targeted gene expression, ultimately leading to a disruption in associated developmental processes. The focus of this work was to identify conditions for selective enhancement of TGF- β 2 signaling and provide support for additional receptor binding cooperativity that is unable to be tested with current experimental tools. Through mathematical approaches, it appears that BG binding to TGF- β 2 ligand through two domains effectively potentiates TGF- β 2 signal and a symmetric cooperative receptor recruitment between T β RI and T β RII best explains the experimental data (TRR model). These findings are summarized with Figure 5D.

Computational modeling demonstrated the proposed mechanism for BG-mediated TGF- β 2 signaling with inferred SPR rates, produced suboptimal TGF- β 2 signal rescue as none of the models produced greater than 75% recovery in signal. With further investigation of model behavior, an inconsistent behavior with the proposed mechanism for BG-mediated TGF- β 2 signaling was identified in the abundance of TGF- β 2/BG/T β RII/T β RI species. This indicated that the transient hypothesis of the TGF- β 2/BG/T β RII/T β RI species from the proposed model may be incorrect or there may be a more complex biological interaction taking place between the macromolecules that the inferred SPR data could not accurately represent. If the TGF- β 2/BG/T β RII/T β RI species is allowed to signal, TGF- β 2 signal recovery can be increased, but there is no biphasic effect across a wide range of BG concentrations. Due to the inability for BG to inhibit signaling in a concentration dependent manner, we conclude that BG quaternary species is likely transient, and therefore, does not contribute to overall signal.

When the dissociation of the TGF- β 2/BG/T β RII/T β RI species was increased, through the increase of BG-ZP dissociation, the TRR model reach approximately 95% TGF- β 2 signal rescue and the SRR model reached approximately 75% TGF- β 2 signal rescue in the presence of BG. The improvement in TGF- β 2 signal rescue from minimal increases in BG-ZP dissociation highlights the importance of this step to predicting model performance and indicates the dissociation of TGF- β 2/BG/T β RII/T β RI complex may be more favored than originally inferred. With these findings, it is possible that the binding of T β RI to the TGF- β /BG/T β RII complex increases the dissociation of the BG-ZP domain through steric interactions or a conformational

change. This interaction cannot be measured in real time with experimental tools available today, but our models identified the importance of this reactions dissociation constant in determining model performance. These results support the hypothesis that there may be a more complex biological interaction taking place at this reaction than originally predicted. This hypothesis has downstream effects, as a change in structure in the BG quaternary species may also increase the affinity of the other receptor types. This hypothesis is not directly tested but could be one of the reasons why the TRR model performs better than the SRR model as it increases the affinity of other receptor interactions downstream.

The TRR Model with a minor increase in BG-ZP dissociation, meets all TGF- β predicted behavior with and without BG present. If the TRR model is present, then the BG to receptor concentration ratio will be from 0.5 to 4.38 whereas the SRR model has a BG to receptor ratio of 2.44 to 21.5. This is a testable difference between the two systems that could be performed to determine if T β RI does recruit T β RII. Modeling alone does not disprove or prove a model but suggests the TRR model should be further tested to determine estimated quantities relative to receptors in the system.

Simulations determining the biphasic effect of BG demonstrated that the TGF- β 2/BG/T β RII/T β RI species proposed in the mechanism meets betaglycan behaviors if the species has a transient quality and minimally contributes to overall signal. Therefore, if the proposed mechanism for BG-mediated TGF- β 2 signal enhancement is correct, the TGF- β 2/BG/T β RII/T β RI species is likely transient and is not a large contributor to overall signal.

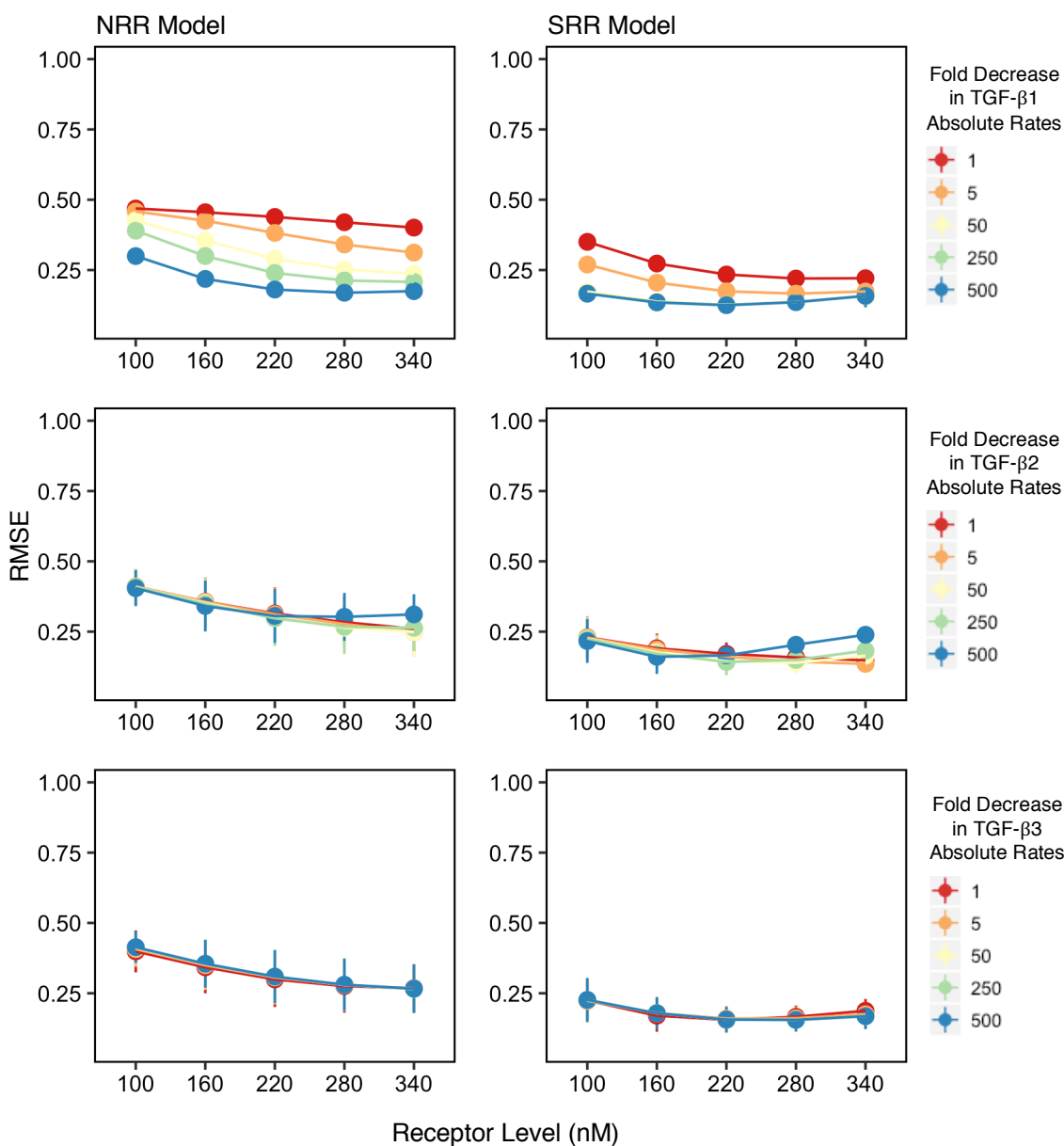
Even though BG's biphasic effect on TGF- β signaling is heavily supported, no direct experiments have been performed to show BG acts as a competitive inhibitor in a concentration dependent manner. To test this statement in our evaluation criteria, BG can be titrated into a cell culture to determine if TGF- β signaling activity is inhibited by BG in a concentration dependent manner.

Future work can be performed with stochastic simulations to investigate the purpose of BG-mediated TGF- β 2 signaling. Identifying if there are differences in noise and/ or transmission properties in the signaling dynamics between the three ligand systems could highlight potential signaling advantages in a system that utilizes a co-receptor for proper signaling.

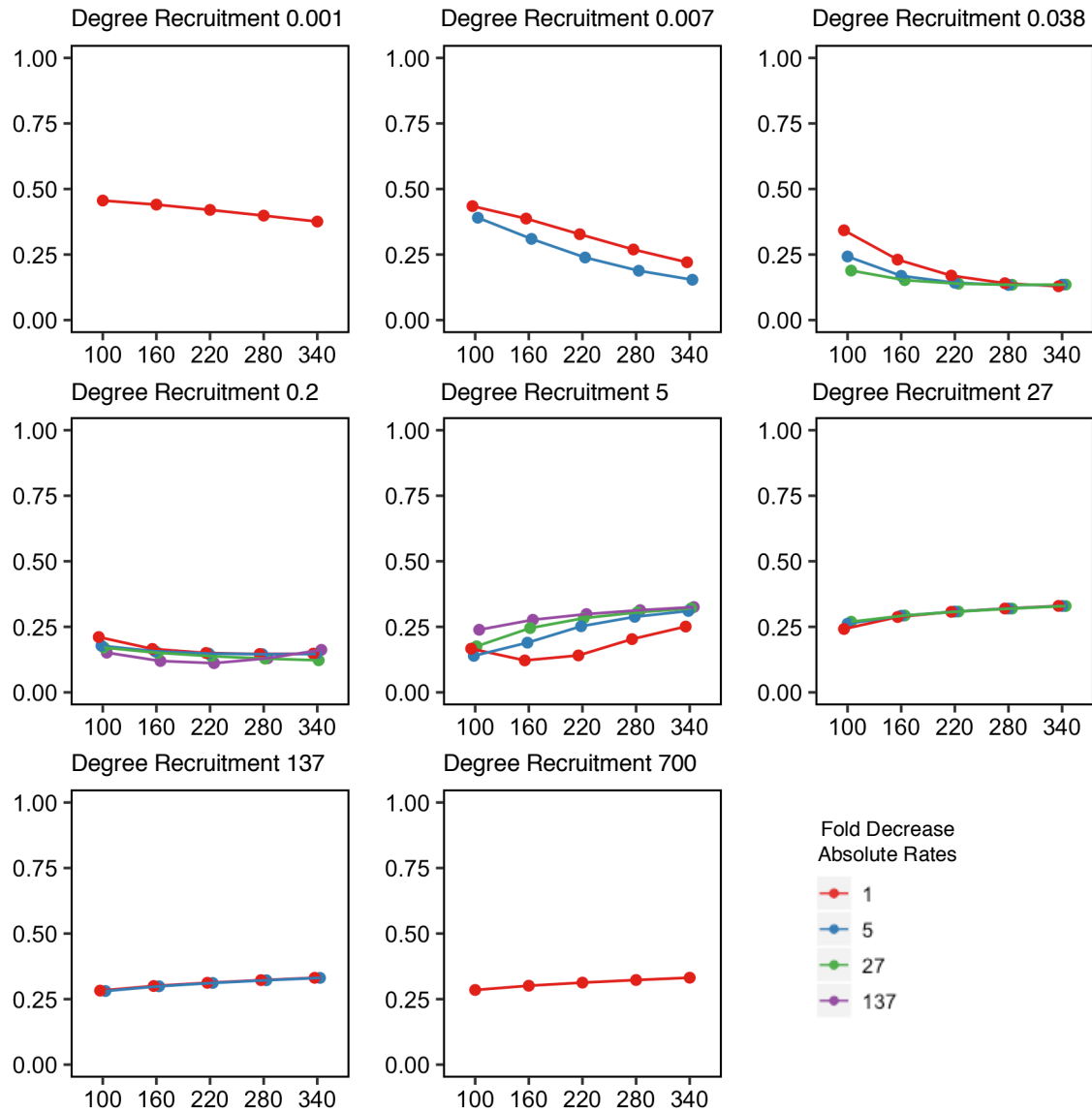
3.5 Methods

We carried out deterministic modeling using a python ODE solver program called pySB. PySB is a framework for building mathematical rule-based models of biochemical systems (Lopez et al., 2013). The deterministic model calculates a concentration of each individual species in simulation under different conditions. The nuclear pSmad signal from each TGF- β signaling species was calculated using a computational model of intracellular TGF- β signaling adapted from Schmierer et al., 2008 paper. The full pSmad signal used in RMSE analysis was calculated from a weighted sum of TGF- β signaling species. The detailed equation can be found in the supplemental material. PySB codes for the three receptor recruitment models can be found through GitHub (<https://github.com/ingle0/Thesis-Code>).

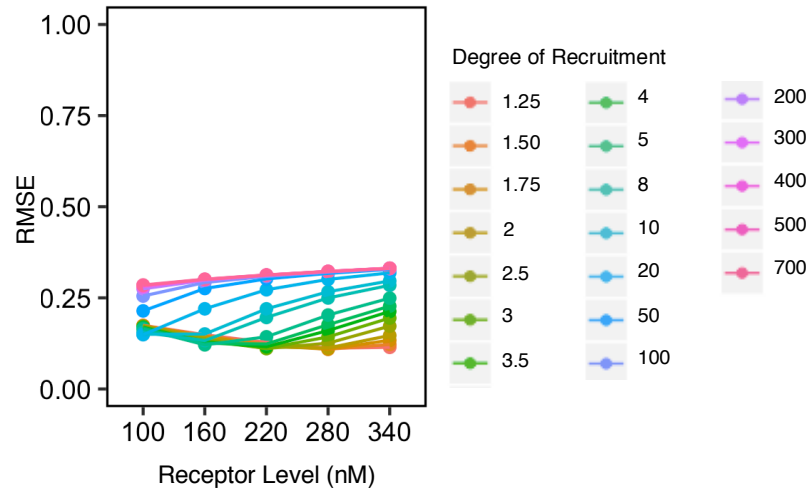
3.6 Supplementary Figures



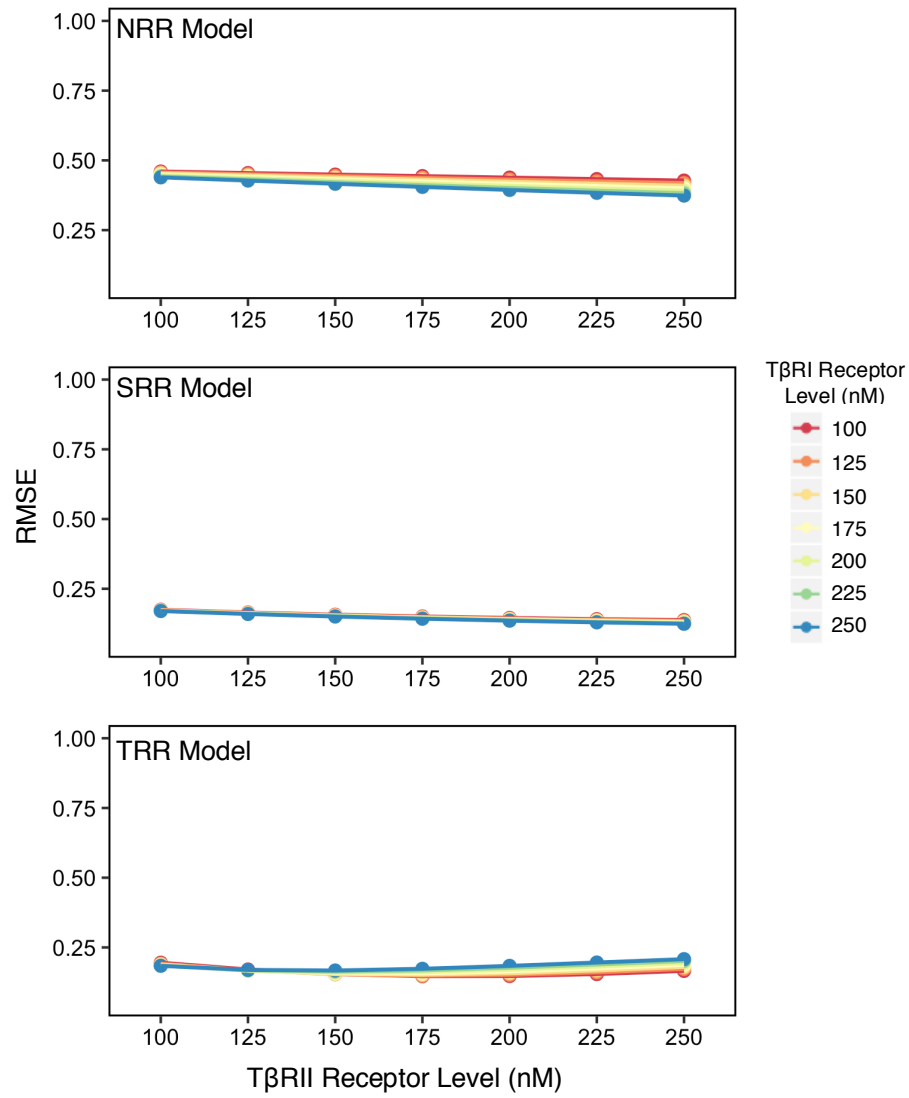
Supplemental Figure 1: There are minimal effects in decreasing the absolute rates of each ligand system independently across a range of receptor levels (100-340 nM). (A) In both the NRR and SRR models, when the fold decrease in TGF-β1 rates are held constant (red to blue lines) and TGF-β2 and TGF-β3 absolute rates are varied (bars present at each dot) there is minimal change in the RMSE value. (B) When the fold decrease in TGF-β2 rates are held constant (red to blue lines) and TGF-β1 and TGF-β3 absolute rates are varied (bars present at each dot) there is minimal change in the RMSE value. (C) When the fold decrease in TGF-β3 rates are held constant (red to blue lines) and TGF-β1 and TGF-β2 absolute rates are varied (bars present at each dot) there is minimal change in the RMSE value.



Supplemental Figure 2: Minimal impact in the RMSE value when decreasing the absolute rates (red, blue, green, and purple lines) across multiple values for $T\beta RI$'s recruitment of $T\beta RII$. Each graph represents one value for the degree of recruitment $T\beta RI$ has on $T\beta RII$ across a range of receptor levels (x-axis). Due to the computational screen set up, the median values of degree recruitment have more absolute rates tested than the end values. Degree recruitment of 0.001 and 700 has only one absolute rate (1-fold decrease) shown. Degree of recruitment 0.007 and 137 have two absolute rate values (1 and 5-fold decrease) shown. Degree of recruitment 0.038 and 27 have three absolute rate values (1, 5, and 27-fold decrease) shown. Degree of recruitment 0.2 and 5 have four absolute rate values (1, 5, 27, 137-fold decrease) shown.



Supplemental Figure 3: Across a broad range of values for the degree of recruitment T β RI has on T β RII (colored lines), a 5-fold degree recruitment produced the lowest RMSE at a receptor level of 160 nM.



Supplemental Figure 4: With no BG present, an SEF equal to 50, and specific absolute rates chosen, altering the concentrations of TβRI (red to blue lines) and TβRII (x-axis) independently, minimally affect the RMSE analysis (y-axis).

3.7 Supplementary Materials

Root mean square error analysis

Root mean square error (RMSE) measures model fit or how accurately the simulated model predicts the experimentally determined biological response. RMSE is the standard deviation of the unexplained variance between the models simulated output and the experimental data (Equation 1).

Equation 1:

$$RMSE = \sqrt{\frac{\sum_{i=1}^n (Simulated_i - Experimental_i)^2}{n}}$$

Lower RMSE values indicate a better model fit, or less unexplained variance between the simulated and experimental data points. This analysis indicates the absolute fit of the simulated models created to the experimental data found in Cheifetz et al., 1990. Experimental data was extracted from the graph using WebPlotDigitizer (Drevon et al., 2017).

Creating the models

We developed a deterministic model of the TGF- β receptor complex assembly that incorporated on-rates and off-rates for each reaction listed in Figure 1A and Supplemental Tables 1-9. Surface plasmon resonance (SPR) data found in literature was the biophysical data used as the starting point for each of the model's kinetic values. Supplemental Tables 1-9 show the kinetic rates used for each of the three models and their source (No Receptor Recruitment, Single-stage Recruitment, and Two-stage Recruitment).

TGF- β 's signal transduction pathway activates when one type II receptor and one type I receptor bind and continues to build towards full signaling capacity when a heterotetrameric complex of two type II (TBR_{II}) and two type I (TBR_I) receptors is formed on the cell membrane. The heterotetrameric signaling complex (TGF- β / TBR_{II}/TBR_{II}/TBR_I/TBR_I) has about four times the amount of nuclear pSmad accumulation than the dimeric signaling complexes (TGF- β /TBR_{II}/TBR_{II}/TBR_I, TGF- β /TBR_{II}/TBR_I/TBR_I, TGF- β /TBR_{II}/TBR_I) (Huang et al., 2011). This was reflected in the model by calculating a total receptor signal that included the full concentration of the TGF- β /TBR_{II}/TBR_{II}/TBR_I/TBR_I plus ¼ the concentration of the TGF-

β /T β RII/T β RI, TGF- β /T β RII/T β RII/T β RI, and TGF- β /T β RII/T β RI/T β RI, otherwise referred to as full signal (Equation 2).

Equation 2:

$$\begin{aligned} Full\ Signal &= [TGF-\beta \cdot T\beta RII \cdot T\beta RII \cdot T\beta RI \cdot T\beta RI] + \frac{1}{4} [TGF-\beta \cdot T\beta RII \cdot T\beta RI] \\ &+ \frac{1}{4} [TGF-\beta \cdot T\beta RII \cdot T\beta RII \cdot T\beta RI] + \frac{1}{4} [TGF-\beta \cdot T\beta RII \cdot T\beta RI \cdot T\beta RI] \end{aligned}$$

Surface enhancement factor justification

An important consideration in modeling any receptor complex assembly is considering the differences in reaction affinities between reactions that involve extracellular and cellular reactants (ligand plus membrane bound receptor) and reactions between two cellular reactants (ligand-receptor complex plus a membrane bound receptor). The magnitude of these reaction affinity differences, defined as surface enhancement factor (SEF), can be challenging to quantify and may seem arbitrary. However, when we examined the relative impact of high and low SEF values and checked with prior literature, we were confident that our SEF choice was valid. If the SEF value is too high it will improve the favorability of every reaction to a degree that washes out distinguishable signaling patterns between models or diminishes the appropriate effect of unfavorable reactions. If it is not applied to the system or is too low, the model will not produce enough signal to accurately fit the simulation data to experimental data. It would be unrealistic to say there is an exact number to fit this interaction, but a value of 50 has been used in previous papers with similar quantitative biological models which have been experimentally validated (Karim et al., 2012; Schmierer et al., 2008). Therefore, a value of 50 will be the baseline for our computational experiments. The No Receptor Recruitment model can also be used to partially validate the SEF selected. If the simulation results from the No Receptor Recruitment model looked exactly like the other two models, the SEF selected may be too high or low as it would wash out the important effects of altering certain reactions. This is not the case in the models presented.

In all the models and ligand systems, the SEF was applied to reactions 3 through 12 and reactions 14 through 17 and were modeled as second order reactions due to both reactants being located on the cell membrane. The SEF was not applied to reactions 1, 2 and 13 due to one of the

reactants, the TGF- β ligand, existing in the outside environment instead of on the cell membrane. Due to the creation of the products from a free-floating molecule and a membrane bound receptor, these reactions were modeled as pseudo-first order reactions.

Homologous reactions

The SPR data used for the reaction kinetics can only measure interactions between molecules/complexes it can isolate. Due to the unfavorable state of some complexes as well as their complex interactions, analyzing the reactions at these higher order intermediate states, like TGF- β /T β RII/T β RI/T β RI reacting with T β RII, is not yet possible. Therefore, we estimate these reactions by assuming they are homologous to lower order reactions that do have SPR data. Justification for homologous reactions are different for each of the receptor recruitment models and are further explained in the sections below describing the creation of each model in detail.

No Receptor Recruitment model creation

The No Receptor Recruitment (NRR) model was created as a control model to ensure that the receptor recruitment applied to SRR and TRR models was indeed required for effective signaling that met biologically known behaviors of the TGF- β system. The difference in signaling patterns between the NRR model and the SRR and TRR models also helps validate the SEF selected.

The justifications for the homologous reactions are the same across the three ligand systems for the NRR model, but the biophysical data is not (Supplemental Tables 1-3). Reactions 3, 5, 8, 10, and 12 are homologous to reaction 1 because there is an addition of a single T β RII to the ligand complex. Therefore, they will have the same dissociation, on-rate, and off-rate constants. Reactions 4, 6, 7, 9, and 11 are homologous to reaction 2 because there is an addition of a single T β RI to the ligand complex. Therefore, they will have the same dissociation, on-rate, and off-rate constants. Reaction 15 is homologous to reaction 13 because there is an addition of BG to the ligand complex.

Reactions 13 through 17 describe the interactions with BG involved in each of the ligand systems. Due to the limited biophysical data of BG interaction with TGF- β 1 and TGF- β 3, the rates and justifications for reactions 13, 14, 15, and 17 in the TGF- β 2 system were maintained. With the same kinetics applied across all three ligand systems we are able to test if our models

are robust to the knowledge that BG has an insignificant effect on TGF- β 1 and β 3 signaling especially in comparison to TGF- β 2. In the reactions 13 through 17, reaction 16 is the only rate that changed between the three ligand systems due to the homology to reaction 2 as mentioned previously.

Reaction 13's dissociation constant (K_D), on-rate, and off-rate values were taken from Kim et al., 2019 paper. Reaction 14's dissociation constant was taken from Villarreal et al., 2016. When BG is bound to TGF- β 2 it increases the affinity for T β RII. Through SPR data, reaction 14 is most similar to a type II receptors affinity for the TGF- β 3 ligand without BG present (Villarreal et al., 2016; Radaev et al., 2010). Therefore, the off-rate used for reaction 14 was from the addition of T β RII to TGF- β 3 in the TGF- β 3 system (Radaev et al., 2010: Table S2). The off-rate was then divided by the dissociation constant to find the on-rate. Reaction 17 is the addition of BG's zona pellucida domain to the ligand. The K_D , on-rate, and off-rate of this reaction were found in Kim et al., 2019. The reaction is represented as a second order reaction and is coded into the system as seen in the following tables to keep the kinetic integrity of the reactions.

Remaining reaction justifications for NRR model of TGF- β 1

Reaction biophysical data available and selected for the No Receptor Recruitment model of TGF- β 1 can be found in Supplemental Table 1. The dissociation constant, on and off-rates for reaction 1 were selected from Huang et al., 2014 publication based off of expertise knowledge as well as the latest and most abundant biophysical data available. The dissociation constant for reaction 2 was found in Radaev et al., 2010. Since the absolute rates (on and off-rates) were not published with the dissociation constant, a screen was run in order to determine if the uncertainty in the absolute rates needed further consideration and testing in our model. As previously demonstrated in Figure 2A, S1, and S3, changing the absolute rates did not significantly affect the results of the system, so rates close to the magnitude of previously observed SPR experiments were selected (Supplemental Table 1).

Remaining reaction justifications for NRR model of TGF- β 2

Reaction biophysical data available and selected for the No Receptor Recruitment model of TGF- β 2 can be found in Supplemental Table 2. The dissociation constant for reaction 1 was chosen by latest published rate and expertise advice, Villarreal et al., 2016. Since the absolute rates (on and off-rates) were not published with the dissociation constant, a screen was run in order to determine if the uncertainty in the absolute rates needed further consideration and testing in our model. The Absolute rates tested were between ranges that have been biologically recorded and observed through SPR analysis. As previously shown in Figure 2A, S1, and S3, changing the absolute rates did not significantly affect the results of the system, so rates close to the magnitude of previously observed SPR experiments were selected. The dissociation constant, on-rate, and off-rate for reaction 2 were found in Radaev et al., 2010 publication.

Remaining reaction justifications for NRR model of TGF- β 3

Reaction biophysical data available and selected for the No Receptor Recruitment model of TGF- β 3 can be found in Supplemental Table 3. The dissociation constant, on and off-rates for reaction 1 were selected from Huang et al., 2011 publication based off of expertise knowledge as well as the latest and most abundant biophysical data available. The dissociation constant for reaction 2 is 2400 nM taken from Radaev et al., 2010. Since the absolute rates (on and off-rates) were not published with the dissociation constant, a screen was run in order to determine if the uncertainty in the absolute rates needed further consideration and testing in our model. The values for the rates between the three ligand systems changed, but the fold decrease in the absolute rates were held constant for ease in RMSE analysis. As previously shown in Figure 2A, S1, and S3, changing the absolute rates did not significantly affect the results of the system, so rates close to the magnitude of previously observed SPR experiments were selected.

Supplemental Table 1: Available SPR data for No Receptor Recruitment model of TGF- β 1 ligand. The “A”, “B”, and “C” labels in the chart point to the specific source or test the data was obtained from per row. Bolded rates in reaction 1 are the values used in the final model.

No Receptor Recruitment Model: TGF- β 1					
#	Reaction	On-rate ($\text{nM}^{-1}\text{s}^{-1}$)	Off-rate (s^{-1})	Source	K_D (nM)
1	TGF- β 1 + T β RII \leftrightarrow TGF- β 1/T β RII	A) 1.16×10^{-3} C) 7.2×10^{-4}	A) 0.22 C) 0.121	A) Radaev 2010: Table 2 B) Groppe 2008: Table S1 C) Huang 2014: Table3	A) 190 B) 390 C) 170
2	TGF- β 1 + T β RI \leftrightarrow TGF- β 1/T β RI	A) 1.73×10^{-6}	A) 0.121	A) Screened B) Radaev 2010: Table2	B) 70000
3	TGF- β 1/T β RII + T β RII \leftrightarrow TGF- β 1/T β RII/T β RII			Homologous to Rxn1	
4	TGF- β 1/T β RII + T β RI \leftrightarrow TGF- β 1/T β RII/T β RI			Homologous to Rxn 2	
5	TGF- β 1/T β RI + T β RII \leftrightarrow TGF- β 1/T β RII/T β RI			Homologous to Rxn1	
6	TGF- β 1/T β RI + T β RI \leftrightarrow TGF- β 1/T β RI/T β RI			Homologous to Rxn2	
7	TGF- β 1/T β RII/T β RII + T β RI \leftrightarrow TGF- β 1/T β RII/T β RII/T β RI			Homologous to Rxn2	
8	TGF- β 1/T β RII/T β RI + T β RII \leftrightarrow TGF- β 1/T β RII/T β RII/T β RI			Homologous to Rxn1	
9	TGF- β 1/T β RII/T β RI + T β RI \leftrightarrow TGF- β 1/T β RII/T β RI/T β RI			Homologous to Rxn2	
10	TGF- β 1/T β RI/T β RI + T β RII \leftrightarrow TGF- β 1/T β RII/T β RI/T β RI			Homologous to Rxn1	
11	TGF- β 1/T β RII/T β RII/T β RI + T β RI \leftrightarrow TGF- β 1/T β RII/T β RII/T β RI/T β RI			Homologous to Rxn2	
12	TGF- β 1/T β RII/T β RI/T β RI + T β RII \leftrightarrow TGF- β 1/T β RII/T β RII/T β RI/T β RI			Homologous to Rxn1	
13	BG+TGF- β 1 \leftrightarrow TGF- β 1/BG	A) 1.5×10^{-3}	A) 7.6×10^{-4}	A) Kim 2019: Table 1	A) 0.51
14	TGF- β 1/BG + T β RII \leftrightarrow TGF- β 1/BG/T β RII	A) 2.24×10^{-4}	B) 0.24	A) Calculated in paper B) Radaev 2010: Table S2 C) Villarreal 2016: Table 2	C) 1070
15	TGF- β 1/T β RII + BG \leftrightarrow TGF- β 1/BG/T β RII			Homologous to Rxn13	
16	TGF- β 1/BG/T β RII + T β RI \leftrightarrow TGF- β 1/BG/T β RII/T β RI			Homologous to Rxn2	
17	TGF- β 1/T β RII/T β RI + BG \leftrightarrow TGF- β 1/BG/T β RII/T β RI	A) 3.3×10^{-5}	A) 2.9×10^{-3}	A) Kim 2019: Table1	90

Supplemental Table 2: Available SPR data for No Receptor Recruitment model of TGF- β 2 ligand. The “A”, “B”, and “C” labels in the chart point to the specific source the data was obtained from per row. The bolded rates in reaction 1 are the values used in the final model.

No Receptor Recruitment Model: TGF- β 2					
#	Reaction	On-rate ($\text{nM}^{-1}\text{s}^{-1}$)	Off-rate (s^{-1})	Source	K_D (nM)
1	TGF- β 2 + T β R _{II} \leftrightarrow TGF- β 2/T β R _{II}	C) 4.9×10^{-5} D) 4.9×10^{-5}	C) 1.10 D) 0.2554	A) Villarreal 2016: Table 5 B) Groppe 2008: Table S1 C) Radaev 2010: Table 2 D) Screened	A) 4600 B) 23000 C) 22449
2	TGF- β 2 + T β R _I \leftrightarrow TGF- β 2/T β R _I	A) 9.6×10^{-5}	A) 1.08	A) Radaev 2010: Table 2	A) 11250
3	TGF- β 2/T β R _{II} + T β R _{II} \leftrightarrow TGF- β 2/T β R _{II} /T β R _{II}			Homologous to Rxn1	
4	TGF- β 2/T β R _{II} + T β R _I \leftrightarrow TGF- β 2/T β R _{II} /T β R _I			Homologous to Rxn 2	
5	TGF- β 2/T β R _I + T β R _{II} \leftrightarrow TGF- β 2/T β R _I /T β R _{II}			Homologous to Rxn1	
6	TGF- β 2/T β R _I + T β R _I \leftrightarrow TGF- β 2/T β R _I /T β R _I			Homologous to Rxn2	
7	TGF- β 2/T β R _{II} /T β R _{II} + T β R _I \leftrightarrow TGF- β 2/T β R _{II} /T β R _{II} /T β R _I			Homologous to Rxn2	
8	TGF- β 2/T β R _{II} /T β R _I + T β R _{II} \leftrightarrow TGF- β 2/T β R _{II} /T β R _{II} /T β R _I			Homologous to Rxn1	
9	TGF- β 2/T β R _{II} /T β R _I + T β R _I \leftrightarrow TGF- β 2/T β R _{II} /T β R _I /T β R _I			Homologous to Rxn2	
10	TGF- β 2/T β R _I /T β R _I + T β R _{II} \leftrightarrow TGF- β 2/T β R _{II} /T β R _I /T β R _I			Homologous to Rxn1	
11	TGF- β 2/T β R _{II} /T β R _{II} /T β R _I + T β R _I \leftrightarrow TGF- β 2/T β R _{II} /T β R _{II} /T β R _I /T β R _I			Homologous to Rxn2	
12	TGF- β 2/T β R _{II} /T β R _I /T β R _I + T β R _{II} \leftrightarrow TGF- β 2/T β R _{II} /T β R _{II} /T β R _I /T β R _I			Homologous to Rxn1	
13	BG+TGF- β 2 \leftrightarrow TGF- β 2/BG	A) 1.5×10^{-3}	A) 7.6×10^{-4}	A) Kim 2019: Table 1	A) 0.51
14	TGF- β 2/BG + T β R _{II} \leftrightarrow TGF- β 2/BG/T β R _{II}	A) 2.24×10^{-4}	B) 0.24	A) Calculated in this paper B) Radaev 2010: Table S2 C) Villarreal 2016: Table 2	C)1070
15	TGF- β 2/T β R _{II} + BG \leftrightarrow TGF- β 2/BG/T β R _{II}			Homologous to Rxn13	
16	TGF- β 2/BG/T β R _{II} + T β R _I \leftrightarrow TGF- β 2/BG/T β R _{II} /T β R _I			Homologous to Rxn2	
17	TGF- β 2/T β R _{II} /T β R _I + BG \leftrightarrow TGF- β 2/BG/T β R _{II} /T β R _I	A) 3.3×10^{-5}	A) 2.9×10^{-3}	A) Kim 2019: Table1	90

Supplemental Table 3: Available SPR data for No Receptor Recruitment model of TGF- β 3 ligand. The “A”, “B”, and “C” labels in the chart point to the specific source the data was obtained from per row. Bolded rates in reaction 1 are the values used in the final model.

No Receptor Recruitment Model: TGF- β 3					
#	Reaction	On-rate ($\text{nM}^{-1}\text{s}^{-1}$)	Off-rate (s^{-1})	Source	K_D (nM)
1	TGF- β 3 + T β R II \leftrightarrow TGF- β 3/T β R II	A) 7.4×10^{-4} C) 1.8×10^{-3}	A) 0.10 C) 0.24	A) Huang 2011: Table1 B) Groppe 2008: TableS1 C) Radaev 2010: Table2	A) 140 B) 520 C) 140
2	TGF- β 3 + T β R I \leftrightarrow TGF- β 3/T β R I	A) 4.167×10^{-5}	A) 0.10	A) Screened B) Radaev 2010: Table2	B) 2400
3	TGF- β 3/T β R II + T β R II \leftrightarrow TGF- β 3/T β R II /T β R II			Homologous to Rxn1	
4	TGF- β 3/T β R II + T β R I \leftrightarrow TGF- β 3/T β R II /T β R I			Homologues to Rxn 2	
5	TGF- β 3/T β R I + T β R II \leftrightarrow TGF- β 3/T β R I /T β R II			Homologous to Rxn1	
6	TGF- β 3/T β R I + T β R I \leftrightarrow TGF- β 3/T β R I /T β R I			Homologous to Rxn2	
7	TGF- β 3/T β R II /T β R II + T β R I \leftrightarrow TGF- β 3/T β R II /T β R II /T β R I			Homologous to Rxn2	
8	TGF- β 3/T β R II /T β R I + T β R II \leftrightarrow TGF- β 3/T β R II /T β R II /T β R I			Homologous to Rxn1	
9	TGF- β 3/T β R II /T β R I + T β R I \leftrightarrow TGF- β 3/T β R II /T β R I /T β R I			Homologous to Rxn2	
10	TGF- β 3/T β R I /T β R I + T β R II \leftrightarrow TGF- β 3/T β R I /T β R I /T β R II			Homologous to Rxn1	
11	TGF- β 3/T β R II /T β R II /T β R I + T β R I \leftrightarrow TGF- β 3/T β R II /T β R II /T β R I /T β R I			Homologous to Rxn2	
12	TGF- β 3/T β R II /T β R I /T β R I + T β R II \leftrightarrow TGF- β 3/T β R II /T β R II /T β R I /T β R I			Homologous to Rxn1	
13	BG+TGF- β 3 \leftrightarrow TGF- β 3/BG	A) 1.5×10^{-3}	A) 7.6×10^{-4}	A) Kim 2019: Table 1	A) 0.51
14	TGF- β 3/BG + T β R II \leftrightarrow TGF- β 3/BG/T β R II	A) 2.24×10^{-4}	B) 0.24	A) Calculated in this paper B) Radaev 2010: Table S2 C) Villarreal 2016: Table 2	C)1070
15	TGF- β 3/T β R II + BG \leftrightarrow TGF- β 3/BG/T β R II			Homologous to Rxn13	
16	TGF- β 3/BG/T β R II + T β R I \leftrightarrow TGF- β 3/BG/T β R II /T β R I			Homologous to Rxn2	
17	TGF- β 3/T β R II /T β R I + BG \leftrightarrow TGF- β 3/BG/T β R II /T β R I	A) 3.3×10^{-5}	A) 2.9×10^{-3}	A) Kim 2019: Table1	A) 90

Single-stage Receptor Recruitment model creation

The justifications for the homologous reactions, screens, and reaction kinetics in the Single-stage Receptor Recruitment (SRR) model are the same as the NRR model except for the added receptor recruitment of T β RI by a ligand bound T β RII found in literature that affects reactions 4, 7, 11, and 16 (Supplemental Table 4-6). Reactions 7, 11, and 16 are homologous to reaction 4 because there is an addition of a single T β RI when a ligand bound T β RII is present and not already bound to T β RI. The justifications and kinetic rates for reactions 13 through 17 in the SRR model are still the same as the NRR model, but reaction 16's kinetics changed due to the homology to reaction 4 as mentioned previously.

Remaining reaction justifications for SRR model of TGF- β 1

Reaction biophysical data available and selected for the SRR model of TGF- β 1 can be found in Supplemental Table 4. The same absolute rate screen for reaction 2 carried out in the NRR model was performed in the SRR model. As previously shown in Figure 2A, S1, and S3, changing the absolute rates did not significantly affect the results of the system, so the same fold decrease in absolute rates chosen in the NRR model were also chosen for the SRR model to maintain comparison integrity. The dissociation constant, on and off-rates for reaction 4 were selected from Huang et al., 2014 publication based off of expertise knowledge as well as the latest and most abundant biophysical data available (Supplemental Table 4).

Remaining reaction justifications for SRR model of TGF- β 2

Reaction biophysical data available and selected for the SRR model of TGF- β 2 can be found in Supplemental Table 5. The same absolute rate screen for reaction 1 carried out in the NRR model was performed in the SRR model. As previously shown in Figure 2A, S1, and S3, changing the absolute rates did not significantly affect the results of the system, so the same rates chosen in the NRR model were also chosen for the SRR model to maintain comparison integrity. The dissociation constant, on-rate, and off-rate for reaction 4 were selected from Radaev et al., 2010 publication based off of expertise knowledge as well as the latest and most abundant biophysical data available in a single publication (Supplemental Table 5).

Remaining reaction justifications for SRR model of TGF- β 3

Reaction biophysical data available and selected for the SRR model of TGF- β 3 can be found in Supplemental Table 6. The same absolute rate screen for reaction 2 carried out in the NRR model was performed in the SRR model. As previously shown in Figure 2A, S1, and S3, changing the absolute rates did not significantly affect the results of the system, so the same rates chosen in the NRR model were also chosen for the SRR model to maintain comparison integrity. The dissociation constant, on and off-rates for reaction 4 were selected from Huang et al., 2011 publication based off of expertise knowledge as well as the latest and most abundant biophysical data available (Supplemental Table 6).

Supplemental Table 4: Available SPR data for Single-stage Receptor Recruitment model of TGF- β 1 ligand. The “A”, “B”, and “C” labels in the chart point to the specific source or test the data was obtained from per row. The rows highlighted in red show the reactions changed when adding the T β RII Recruitment of T β R1 of T β R1 by T β RII. Bolded rates in reaction 4 are the values used in the final model.

Single-stage Receptor Recruitment Model: TGF- β 1					
#	Reaction	On-rate ($\text{nM}^{-1}\text{s}^{-1}$)	Off-rate (s^{-1})	Source	K _D (nM)
1	TGF- β 1 + T β RII \leftrightarrow TGF- β 1/T β RII	A) 7.2×10^{-4}	A) 0.121	A) Huang 2014: Table3	A) 170
2	TGF- β 1 + T β R1 \leftrightarrow TGF- β 1/T β R1	A) 1.73×10^{-6}	A) 0.121	A) Screened B) Radaev 2010: Table2	B) 70000
3	TGF- β 1/T β RII + T β RII \leftrightarrow TGF- β 1/T β RII/T β RII			Homologous to Rxn1	
4	TGF- β 1/T β RII + T β R1 \leftrightarrow TGF- β 1/T β RII/T β R1	A) 9.7×10^{-5} C) 3.3×10^{-5}	A) 6.8×10^{-3} C) 7.6×10^{-3}	A) Radaev 2010: Table2 B) Groppe 2008: Table S1 C) Huang 2014: Table3	A) 70 B) 2530 C) 240
5	TGF- β 1/T β R1 + T β RII \leftrightarrow TGF- β 1/T β RII/T β R1			Homologous to Rxn1	
6	TGF- β 1/T β R1 + T β R1 \leftrightarrow TGF- β 1/T β R1/T β R1			Homologous to Rxn2	
7	TGF- β 1/T β RII/T β RII + T β R1 \leftrightarrow TGF- β 1/T β RII/T β RII/T β R1			Homologous to Rxn4	
8	TGF- β 1/T β RII/T β R1 + T β RII \leftrightarrow TGF- β 1/T β RII/T β RII/T β R1			Homologous to Rxn1	
9	TGF- β 1/T β RII/T β R1 + T β R1 \leftrightarrow TGF- β 1/T β RII/T β R1/T β R1			Homologous to Rxn2	
10	TGF- β 1/T β R1/T β R1 + T β RII \leftrightarrow TGF- β 1/T β RII/T β R1/T β R1			Homologous to Rxn1	
11	TGF- β 1/T β RII/T β RII/T β R1 + T β R1 \leftrightarrow TGF- β 1/T β RII/T β RII/T β R1/T β R1			Homologous to Rxn4	
12	TGF- β 1/T β RII/T β R1/T β R1 + T β RII \leftrightarrow TGF- β 1/T β RII/T β RII/T β R1/T β R1			Homologous to Rxn1	
13	BG+TGF- β 1 \leftrightarrow TGF- β 1/BG	A) 1.5×10^{-3}	A) 7.6×10^{-4}	A) Kim 2019: Table 1	A) 0.51
14	TGF- β 1/BG + T β RII \leftrightarrow TGF- β 1/BG/T β RII	A) 2.24×10^{-4}	B) 0.24	A) Calculated in paper B) Radaev 2010: Table S2 C) Villarreal 2016: Table 2	C) 1070
15	TGF- β 1/T β RII + BG \leftrightarrow TGF- β 1/BG/T β RII			Homologous to Rxn13	
16	TGF- β 1/BG/T β RII + T β R1 \leftrightarrow TGF- β 1/BG/T β RII/T β R1			Homologous to Rxn4	
17	TGF- β 1/T β RII/T β R1 + BG \leftrightarrow TGF- β 1/BG/T β RII/T β R1	A) 3.3×10^{-5}	A) 2.9×10^{-3}	A) Kim 2019: Table1	90

Supplemental Table 5: Available SPR data for Single-stage Receptor Recruitment model of TGF- β 2 ligand. The “A”, “B”, and “C” labels in the chart point to the specific source the data was obtained from per row. The rows highlighted in red show the reactions changed when adding the experimentally determined recruitment of T β RI by T β RII. The bolded rates in reaction 4 are the values used in the final model.

Single-stage Receptor Recruitment Model: TGF- β 2					
#	Reaction	On-rate ($\text{nM}^{-1}\text{s}^{-1}$)	Off-rate (s^{-1})	Source	K_D (nM)
1	TGF- β 2 + T β RII \leftrightarrow TGF- β 2/T β RII	A) 4.9×10^{-5}	A) 0.2554	A) Screened B) Villarreal 2016: Table 5	B) 4600
2	TGF- β 2 + T β RI \leftrightarrow TGF- β 2/T β RI	A) 9.6×10^{-5}	A) 1.08	A) Radaev 2010: Table 2	A) 11250
3	TGF- β 2/T β RII + T β RII \leftrightarrow TGF- β 2/T β RII/T β RII			Homologous to Rxn1	
4	TGF- β 2/T β RII + T β RI \leftrightarrow TGF- β 2/T β RII/T β RI	A) 1.8×10^{-4}	A) 2.9×10^{-3}	A) Radaev 2010: Table 2 B) Groppe 2008: Table S1	A) 16 B) 1170
5	TGF- β 2/T β RI + T β RII \leftrightarrow TGF- β 2/T β RII/T β RI			Homologous to Rxn1	
6	TGF- β 2/T β RI + T β RI \leftrightarrow TGF- β 2/T β RI/T β RI			Homologous to Rxn2	
7	TGF- β 2/T β RII/T β RII + T β RI \leftrightarrow TGF- β 2/T β RII/T β RII/T β RI			Homologous to Rxn4	
8	TGF- β 2/T β RII/T β RI + T β RII \leftrightarrow TGF- β 2/T β RII/T β RII/T β RI			Homologous to Rxn1	
9	TGF- β 2/T β RII/T β RI + T β RI \leftrightarrow TGF- β 2/T β RII/T β RI/T β RI			Homologous to Rxn2	
10	TGF- β 2/T β RI/T β RI + T β RII \leftrightarrow TGF- β 2/T β RII/T β RI/T β RI			Homologous to Rxn1	
11	TGF- β 2/T β RII/T β RII/T β RI + T β RI \leftrightarrow TGF- β 2/T β RII/T β RII/T β RI/T β RI			Homologous to Rxn4	
12	TGF- β 2/T β RII/T β RI/T β RI + T β RII \leftrightarrow TGF- β 2/T β RII/T β RII/T β RI/T β RI			Homologous to Rxn1	
13	BG+TGF- β 2 \leftrightarrow TGF- β 2/BG	A) 1.5×10^{-3}	A) 7.6×10^{-4}	A) Kim 2019: Table 1	A) 0.51
14	TGF- β 2/BG + T β RII \leftrightarrow TGF- β 2/BG/T β RII	A) 2.24×10^{-4}	B) 0.24	A) Calculated in this paper B) Radaev 2010: Table S2 C) Villarreal 2016: Table 2	C) 1070
15	TGF- β 2/T β RII + BG \leftrightarrow TGF- β 2/BG/T β RII			Homologous to Rxn13	
16	TGF- β 2/BG/T β RII + T β RI \leftrightarrow TGF- β 2/BG/T β RII/T β RI			Homologous to Rxn4	
17	TGF- β 2/T β RII/T β RI + BG \leftrightarrow TGF- β 2/BG/T β RII/T β RI	A) 3.3×10^{-5}	A) 2.9×10^{-3}	A) Kim 2019: Table 1	90

Supplemental Table 6: Available SPR data for Single-stage Receptor Recruitment model of TGF- β 3 ligand. The “A”, “B”, and “C” labels in the chart point to the specific source the data was obtained from per row. The rows highlighted in red show the reactions changed when adding the experimentally determined recruitment of T β RI by T β RII. The bolded rates in reaction 4 are the values used in the final model.

Single-stage Receptor Recruitment Model: TGF- β 3					
#	Reaction	On-rate ($\text{nM}^{-1}\text{s}^{-1}$)	Off-rate (s^{-1})	Source	K_D (nM)
1	TGF- β 3 + T β RII \leftrightarrow TGF- β 3/T β RII	A) 7.4×10^{-4}	A) 0.10	A) Huang 2011: Table1	A) 140
2	TGF- β 3 + T β RI \leftrightarrow TGF- β 3/T β RI	A) 4.167×10^{-5}	A) 0.10	A) Screened B) Radaev 2010: Table2	B) 2400
3	TGF- β 3/T β RII + T β RII \leftrightarrow TGF- β 3/T β RII/T β RII			Homologous to Rxn1	
4	TGF- β 3/T β RII + T β RI \leftrightarrow TGF- β 3/T β RII/T β RI	A) 3.5×10^{-5} C) 9.6×10^{-5}	A) 1.2×10^{-3} C) 1.3×10^{-3}	A) Huang 2011: Table 1 B) Groppe 2008: Table S1 C) Radaev 2010: Table2	A) 34 B) 600 C) 14.0
5	TGF- β 3/T β RI + T β RII \leftrightarrow TGF- β 3/T β RII/T β RI			Homologous to Rxn1	
6	TGF- β 3/T β RI + T β RI \leftrightarrow TGF- β 3/T β RI/T β RI			Homologous to Rxn2	
7	TGF- β 3/T β RII/T β RII + T β RI \leftrightarrow TGF- β 3/T β RII/T β RII/T β RI			Homologous to Rxn4	
8	TGF- β 3/T β RII/T β RI + T β RII \leftrightarrow TGF- β 3/T β RII/T β RII/T β RI			Homologous to Rxn1	
9	TGF- β 3/T β RII/T β RI + T β RI \leftrightarrow TGF- β 3/T β RII/T β RI/T β RI			Homologous to Rxn2	
10	TGF- β 3/T β RI/T β RI + T β RII \leftrightarrow TGF- β 3/T β RII/T β RI/T β RI			Homologous to Rxn1	
11	TGF- β 3/T β RII/T β RII/T β RI + T β RI \leftrightarrow TGF- β 3/T β RII/T β RII/T β RI/T β RI			Homologous to Rxn4	
12	TGF- β 3/T β RII/T β RI/T β RI + T β RII \leftrightarrow TGF- β 3/T β RII/T β RII/T β RI/T β RI			Homologous to Rxn1	
13	BG+TGF- β 3 \leftrightarrow TGF- β 3/BG	A) 1.5×10^{-3}	A) 7.6×10^{-4}	A) Kim 2019: Table 1	A) 0.51
14	TGF- β 3/BG + T β RII \leftrightarrow TGF- β 3/BG/T β RII	A) 2.24×10^{-4}	B) 0.24	A) Calculated in this paper B) Radaev 2010: Table S2 C) Villarreal 2016: Table 2	C) 1070
15	TGF- β 3/T β RII + BG \leftrightarrow TGF- β 3/BG/T β RII			Homologous to Rxn13	
16	TGF- β 3/BG/T β RII + T β RI \leftrightarrow TGF- β 3/BG/T β RII/T β RI			Homologous to Rxn4	
17	TGF- β 3/T β RII/T β RI + BG \leftrightarrow TGF- β 3/BG/T β RII/T β RI	A) 3.3×10^{-5}	A) 2.9×10^{-3}	A) Kim 2019: Table1	90

Two-stage Receptor Recruitment model creation

The Two-stage Receptor Recruitment (TRR) model continues to build off of the NRR and SRR models. The justifications for the homologous reactions and reaction kinetics are the same as the SRR model except for the added receptor recruitment of T β RII by a ligand bound T β RI that affects reactions 5, 10, and 12 (Supplemental Table 7-9). Reactions 10 and 12 are homologous to reaction 5 because there is an addition of a single T β RII when a ligand bound T β RI is present and not previously bound to a T β RII.

Remaining reaction justifications for TRR model for TGF- β 1, TGF- β 2, and TGF- β 3

Reaction biophysical data available and selected for the TRR model for TGF- β 1, TGF- β 2, TGF- β 3 can be found in Supplemental Tables 7, 8, and 9, respectfully. Screens were run to determine the optimal degree of recruitment for T β RI on T β RII (range of 1 to 700 degrees of recruitment) and to determine the effect of changing the absolute rates (range of 1 to 500-fold decrease in absolute rates) on all three ligand systems. The values for the rates between the three ligand systems changed, but the fold decrease in the absolute rates were held constant for the RMSE analysis, these value differences can be found in the supplemental tables. As previously shown in Figures 2B and 3S, simultaneously decreasing the magnitude of the absolute rates did not appreciably affect the RMSE analysis. Due to the minimal impact of changing the absolute rates simultaneously, the absolute rates selected were close to the magnitude of previously observed SPR experiments. Next, a more detailed screen on the degree of receptor recruitment of reactions 5, 10, and 12 were tested as shown in Figure 4S. A degree recruitment of roughly 5 across all of the ligand systems produces the lowest RMSE, therefore, the dissociation constant chosen was five-fold more favorable than reaction 1's dissociation constant in each of the ligand systems (Supplemental Table 7, 8, and 9).

Supplemental Table 7: Available SPR data for Two-stage Receptor Recruitment model of TGF- β 1 ligand. The “A”, “B”, and “C” labels in the chart point to the specific source or test the data was obtained from per row. The rows highlighted in red show the reactions changed when adding the experimentally determined recruitment of T β RI by T β RII. The rows highlighted in blue show the reactions affected when adding the theorized recruitment of T β RII by T β RI.

Two-stage Receptor Recruitment Model: TGF- β 1					
#	Reaction	On-rate ($\text{nM}^{-1}\text{s}^{-1}$)	Off-rate (s^{-1})	Source	K_D (nM)
1	TGF- β 1 + T β RII \leftrightarrow TGF- β 1/T β RII	A) 7.2×10^{-4}	A) 0.121	A) Huang 2014: Table3	A) 170
2	TGF- β 1 + T β RI \leftrightarrow TGF- β 1/T β RI	B) 1.73×10^{-6}	B) 0.121	A) Radaev 2010: Table2 B) Screened	A) 70000
3	TGF- β 1/T β RII + T β RII \leftrightarrow TGF- β 1/T β RII/T β RII			Homologous to Rxn1	
4	TGF- β 1/T β RII + T β RI \leftrightarrow TGF- β 1/T β RII/T β RI	A) 3.3×10^{-5}	A) 7.6×10^{-3}	A) Huang 2014: Table3	A) 240
5	TGF- β 1/T β RI + T β RII \leftrightarrow TGF- β 1/T β RI/T β RI	A) 3.83547×10^{-3}	A) 0.12516	A) Screened	A) 33
6	TGF- β 1/T β RI + T β RI \leftrightarrow TGF- β 1/T β RI/T β RI			Homologous to Rxn2	
7	TGF- β 1/T β RII/T β RII + T β RI \leftrightarrow TGF- β 1/T β RII/T β RII/T β RI			Homologous to Rxn4	
8	TGF- β 1/T β RII/T β RI + T β RII \leftrightarrow TGF- β 1/T β RII/T β RII/T β RI			Homologous to Rxn1	
9	TGF- β 1/T β RII/T β RI + T β RI \leftrightarrow TGF- β 1/T β RII/T β RI/T β RI			Homologous to Rxn2	
10	TGF- β 1/T β RI/T β RI + T β RII \leftrightarrow TGF- β 1/T β RII/T β RI/T β RI			Homologous to Rxn5	
11	TGF- β 1/T β RII/T β RII/T β RI + T β RI \leftrightarrow TGF- β 1/T β RII/T β RII/T β RI/T β RI			Homologous to Rxn4	
12	TGF- β 1/T β RII/T β RI/T β RI + T β RII \leftrightarrow TGF- β 1/T β RII/T β RII/T β RI/T β RI			Homologous to Rxn5	
13	BG+TGF- β 1 \leftrightarrow TGF- β 1/BG	A) 1.5×10^{-3}	A) 7.6×10^{-4}	A) Kim 2019: Table 1	A) 0.51
14	TGF- β 1/BG + T β RII \leftrightarrow TGF- β 1/BG/T β RII	A) 2.24×10^{-4}	B) 0.24	A) Calculated in paper B) Radaev 2010: Table S2 C) Villarreal 2016: Table 2	C)1070
15	TGF- β 1/T β RII + BG \leftrightarrow TGF- β 1/BG/T β RII			Homologous to Rxn13	
16	TGF- β 1/BG/T β RII + T β RI \leftrightarrow TGF- β 1/BG/T β RII/T β RI			Homologous to Rxn4	
17	TGF- β 1/T β RII/T β RI + BG \leftrightarrow TGF- β 1/BG/T β RII/T β RI	A) 3.3×10^{-5}	A) 2.9×10^{-3}	A) Kim 2019: Table1	90

Supplemental Table 8: Available SPR data for Two-stage Receptor Recruitment model of TGF- β 2 ligand. The “A”, “B”, and “C” labels in the chart point to the specific source the data was obtained from per row. The rows highlighted in red show the reactions changed when adding the experimentally determined recruitment of T β RI by T β RII. The rows highlighted in blue show the reactions affected when adding the theorized recruitment of T β RII by T β RI.

Two-stage Receptor Recruitment Model: TGF- β 2					
#	Reaction	On-rate ($\text{nM}^{-1}\text{s}^{-1}$)	Off-rate (s^{-1})	Source	K_D (nM)
1	TGF- β 2 + T β RII \leftrightarrow TGF- β 2/T β RII	A) 4.9×10^{-5}	A) 0.2554	A) Screened B) Villarreal 2016:Table 5	B) 4600
2	TGF- β 2 + T β RI \leftrightarrow TGF- β 2/T β RI	A) 9.6×10^{-5}	A) 1.08	A) Radaev 2010: Table 2	A) 11250
3	TGF- β 2/T β RII + T β RII \leftrightarrow TGF- β 2/T β RII/T β RII			Homologous to Rxn1	
4	TGF- β 2/T β RII + T β RI \leftrightarrow TGF- β 2/T β RII/T β RI	A) 1.8×10^{-4}	A) 2.9×10^{-3}	A) Radaev 2010: Table 2	A) 16
5	TGF- β 2/T β RI + T β RII \leftrightarrow TGF- β 2/T β RI/T β RII	A) 4.9×10^{-5}	A) 0.0438	A) Screened	A) 893
6	TGF- β 2/T β RI + T β RI \leftrightarrow TGF- β 2/T β RI/T β RI			Homologous to Rxn2	
7	TGF- β 2/T β RII/T β RII + T β RI \leftrightarrow TGF- β 2/T β RII/T β RII/T β RI			Homologous to Rxn4	
8	TGF- β 2/T β RII/T β RI + T β RII \leftrightarrow TGF- β 2/T β RII/T β RII/T β RI			Homologous to Rxn1	
9	TGF- β 2/T β RII/T β RI + T β RI \leftrightarrow TGF- β 2/T β RII/T β RI/T β RI			Homologous to Rxn2	
10	TGF- β 2/T β RI/T β RI + T β RII \leftrightarrow TGF- β 2/T β RII/T β RI/T β RI			Homologous to Rxn5	
11	TGF- β 2/T β RII/T β RII/T β RI + T β RI \leftrightarrow TGF- β 2/T β RII/T β RII/T β RI/T β RI			Homologous to Rxn4	
12	TGF- β 2/T β RII/T β RI/T β RI + T β RII \leftrightarrow TGF- β 2/T β RII/T β RII/T β RI/T β RI			Homologous to Rxn5	
13	BG+TGF- β 2 \leftrightarrow TGF- β 2/BG	A) 1.5×10^{-3}	A) 7.6×10^{-4}	A) Kim 2019: Table 1	A) 0.51
14	TGF- β 2/BG + T β RII \leftrightarrow TGF- β 2/BG/T β RII	A) 2.24×10^{-4}	B) 0.24	A) Calculated in this paper B) Radaev 2010: Table S2 C) Villarreal 2016: Table 2	C)1070
15	TGF- β 2/T β RII + BG \leftrightarrow TGF- β 2/BG/T β RII			Homologous to Rxn13	
16	TGF- β 2/BG/T β RII + T β RI \leftrightarrow TGF- β 2/BG/T β RII/T β RI			Homologous to Rxn4	
17	TGF- β 2/T β RII/T β RI + BG \leftrightarrow TGF- β 2/BG/T β RII/T β RI	A) 3.3×10^{-5}	A) 2.9×10^{-3}	A) Kim 2019: Table1	90

Supplemental Table 9: Available SPR data for Two-stage Receptor Recruitment model of TGF- β 3 ligand. The “A”, “B”, and “C” labels in the chart point to the specific source the data was obtained from per row. The rows highlighted in red show the reactions changed when adding the experimentally determined recruitment of T β RI by T β RII. The rows highlighted in blue show the reactions affected when adding the theorized recruitment of T β RII by T β RI.

Two-stage Receptor Recruitment Model: TGF- β 3					
#	Reaction	On-rate ($\text{nM}^{-1}\text{s}^{-1}$)	Off-rate (s^{-1})	Source	K_D (nM)
1	TGF- β 3 + T β RII \leftrightarrow TGF- β 3/T β RII	A) 7.4×10^{-4}	A) 0.10	A) Huang 2011: Table1	A) 140
2	TGF- β 3 + T β RI \leftrightarrow TGF- β 3/T β RI	A) 4.167×10^{-5}	A) 0.10	A) Screened B) Radaev 2010: Table2	B) 2400
3	TGF- β 3/T β RII + T β RII \leftrightarrow TGF- β 3/T β RII/T β RII			Homologous to Rxn1	
4	TGF- β 3/T β RII + T β RI \leftrightarrow TGF- β 3/T β RII/T β RI	A) 3.5×10^{-5}	A) 1.2×10^{-3}	A) Huang 2011: Table 1	A) 34
5	TGF- β 3/T β RI + T β RII \leftrightarrow TGF- β 3/T β RI/T β RI	A) 3.94×10^{-3}	A) 0.103	A) Screened	A) 27
6	TGF- β 3/T β RI + T β RI \leftrightarrow TGF- β 3/T β RI/T β RI			Homologous to Rxn2	
7	TGF- β 3/T β RII/T β RII + T β RI \leftrightarrow TGF- β 3/T β RII/T β RII/T β RI			Homologous to Rxn4	
8	TGF- β 3/T β RII/T β RI + T β RII \leftrightarrow TGF- β 3/T β RII/T β RII/T β RI			Homologous to Rxn1	
9	TGF- β 3/T β RII/T β RI + T β RI \leftrightarrow TGF- β 3/T β RII/T β RI/T β RI			Homologous to Rxn2	
10	TGF- β 3/T β RI/T β RI + T β RII \leftrightarrow TGF- β 3/T β RII/T β RI/T β RI			Homologous to Rxn5	
11	TGF- β 3/T β RII/T β RII/T β RI + T β RI \leftrightarrow TGF- β 3/T β RII/T β RII/T β RI/T β RI			Homologous to Rxn4	
12	TGF- β 3/T β RII/T β RI/T β RI + T β RII \leftrightarrow TGF- β 3/T β RII/T β RII/T β RI/T β RI			Homologous to Rxn5	
13	BG+TGF- β 3 \leftrightarrow TGF- β 3/BG	A) 1.5×10^{-3}	A) 7.6×10^{-4}	A) Kim 2019: Table 1	A) 0.51
14	TGF- β 3/BG + T β RII \leftrightarrow TGF- β 3/BG/T β RII	A) 2.24×10^{-4}	B) 0.24	A) Calculated in this paper B) Radaev 2010: Table S2 C) Villarreal 2016: Table 2	C) 1070
15	TGF- β 3/T β RII + BG \leftrightarrow TGF- β 3/BG/T β RII			Homologous to Rxn13	
16	TGF- β 3/BG/T β RII + T β RI \leftrightarrow TGF- β 3/BG/T β RII/T β RI			Homologous to Rxn4	
17	TGF- β 3/T β RII/T β RI + BG \leftrightarrow TGF- β 3/BG/T β RII/T β RI	A) 3.3×10^{-5}	A) 2.9×10^{-3}	A) Kim 2019: Table1	90

Receptor justification

From Wakefield et al., 1987, a median value of 10,000 is used for TGF- β receptors found per epithelial cell. Equimolar receptor concentrations were applied, 5000 Type I and Type II receptors with 10% at the surface of cell membrane (Vilar et al., 2006; Di Guglielmo et al., 2003; Chung et al., 2009). Therefore, the starting point for the simulations will be 500 Type I and II receptors which is equal to about 160 nM with the cell volume determined in Equation 3.

Equation 3:

$$\begin{aligned} \text{Volume} &= 10.2\mu\text{m} \times 10.2\mu\text{m} \times 0.05\mu\text{m} = 5.2\mu\text{m}^3 = 5.2 \times 10^{-6^3}\text{m}^3 = 5.2 \times 10^{-18}\text{m}^3 \\ &= 5.2 \times 10^{-18} \times \left(\frac{1}{0.001}\right)\text{Litre} = 5.2 \times 10^{-15}\text{Litre} \\ \text{conversion} &= \frac{500\text{ molecules}}{((6.022 \times 10^{23}\text{ molecules}) \times 5.2 \times 10^{-15}\text{Litre})} \times 1 \frac{\text{Mole}}{\text{Litre}} = 159.67\text{nM} \end{aligned}$$

The volume selected was a value similar to those used in other computational models of growth factors (Karim et al., 2012) and was informed by recorded data for the diameter size of common epithelial cells and the size of epithelial cells apical membrane (Devalia et al., 1990; Mitra et al., 2004). Although maintaining a volume close to the proposed extracellular space in question is important to drawing biological conclusions, narrowing in on the exact volume is time exhaustive because changing the volume does not significantly alter the signaling pattern. If the receptor concentration is held constant, decreasing the simulated extracellular volume around the cell will increase the number of receptors per milliliter (mL). This volume change will lead to a model more sensitive to detecting signaling patterns at lower receptor levels but altering the volume does not significantly change the trend of the signaling pattern. The trends of the simulation results are more dependent on the ratios of receptor to ligand levels and BG to receptor levels which are tested and analyzed in this paper.

In our computational models, endocytosis and receptor recycling were combined into one step. Drawing from the knowledge of a previous paper and expert knowledge, we used a very slow rate for this combined step (Karim et al., 2012). The TGF- β receptor complex assembly does not have a strong accumulation of higher order intermediate complexes. If the complexes were not able to dissociate when formed, this rate may need to be faster, but with the kinetic rates used for the reactions in these models, the intermediate complexes are able to dissociate

freely. Including this in our model does not significantly affect the results but does make the model more biological relevant by considering endocytosis and receptor recycling.

4. CONCLUSIONS AND FUTURE DIRECTIONS

Elucidating the mechanism by which BG potentiates TGF- β 2 signaling has been attempted through experimental measures for the purpose of uncovering BG's role and importance in the TGF- β system. Although the experimental measures have been successful at formulating a hypothesis for BG potentiation of TGF- β 2 signal, some of the assumptions from the hypothesis are difficult to test with the experimental technology available today. The mathematical modeling performed in this work was able to refine and validate some of the assumptions of the hypothesized BG potentiation of TGF- β 2 signal. This work also supports symmetric receptor recruitment and presents computational approaches that can be used to discover the system wide importance of BG in the TGF- β system.

Absence of betaglycan simulations

Running simulations with no BG present in the system was essential to support or refute a model. With no BG present in the system, all three models (NRR, SRR, TRR) can recapitulate experimental behavior as demonstrated by low RMSE values. The NRR model had the highest RMSE values out of the three models which supported the SEF value selected and indicated the cooperative receptor recruitment applied to the models was effective in altering the signaling results. The SRR and TRR models were almost indistinguishable in their RMSE values suggesting there may not be a need for symmetric receptor recruitment. By comparing model behavior to experimental behavior in the absence of BG, we were able to evaluate the accuracy of the starting parameters for the models before analyzing the role of BG in TGF- β signaling.

Betaglycan present simulations

When BG was first added to the three models of varying receptor recruitment, the TRR model outperformed the other models in the predetermined evaluation criteria for BG behavior— (i) BG increases signal production in TGF- β 2 to a greater degree than TGF- β 1/3, (ii) BG recovers TGF- β 2 signaling to levels comparable to TGF- β 1/3 signaling (iii) BG can inhibit TGF- β signaling in a concentration dependent manner. However, all the models sub-optimally performed in rescuing TGF- β 2 signal to levels comparable to TGF- β 1/3 signal. Further

simulation analysis revealed all of the models contradicted one of the assumed behaviors in the proposed mechanism for BG-mediated TGF- β 2 signal— the TGF- β 2/BG/T β RII/T β RI species is transient, and therefore, does not contribute to signal. This inconsistent simulation behavior led us to test the assumptions presented in the proposed mechanism for BG-mediated TGF- β 2 signaling to determine the cause of suboptimal signal recovery. This investigation demonstrated that the TGF- β 2/BG/T β RII/T β RI species cannot meet all the predetermined evaluation criteria for BG behaviors if the species is not transient, and therefore, does contribute to signal. Furthermore, when we tested the possibility that our inferred rate constants for TGF- β 2/BG/T β RII/T β RI species were inaccurate, the simulations showed that small increases in the dissociation of this species improved BG-mediated TGF- β 2 signal rescue to levels more aligned with experimental observations. In addition, the TRR model outperformed the SRR and NRR models in our established evaluation criteria no matter what assumptions were tested in the proposed BG mechanism. Although the TRR model outperformed the other models, mathematical modeling alone cannot definitively determine which model is present without further biological experimentation. Differences in the SRR model and TRR model were investigated in order to propose experiments to support or refute a specific model.

Final proposed experiments

Due to observed difference in BG to receptor ratios required to induce a biphasic effect between the SRR and TRR models, further computational analysis was performed to propose a validation experiment. If the TRR model is accurate, we expect that the ratio of BG to receptor concentration will fall between 0.5 to 4.38 whereas the SRR model predicts a BG to receptor ratio of 2.44 to 21.5. The SRR model required a 4.7-4.9 times higher concentration of BG to receptor ratio than the TRR model across a wide range of ligand concentrations (0.001 to 5 nM). This is a testable difference between the two systems that could be performed to determine if T β RI does recruit T β RII.

Future computational work can be performed alongside published single-molecule TIRF-based fluorescence imaging to further uncover the behavior of the TGF- β 2/BG/T β RII/T β RI species. This method measures the proportion of receptors that are monomeric (T β RII, TGF- β 2/T β RII, TGF- β 2/T β RII/T β RI, TGF- β 2/T β RII/T β RI/T β RI, and TGF- β 2/BG/T β RII/T β RI) or dimeric (TGF- β 2/T β RII/T β RII, TGF- β 2/T β RII/T β RII/T β RI, as well as heterotetramers) based on

the fraction of molecules that photo bleach in a single step versus those that bleach in two (Iino et al., 2001). This technique may aid in confirming or denying the transient quality of TGF- β 2/BG/T β RII/T β RI species by comparing the experimental stoichiometric ratios to the stoichiometric ratios calculated in simulations with different assumptions applied to the TGF- β 2/BG/T β RII/T β RI species. Furthermore, if these calculated stoichiometric ratios are different between the SRR and TRR models, they can be compared to the experimental stoichiometric ratios to further support or refute one of the models over the other.

Preliminary work is also being performed to determine the differences between the noise profiles of the SRR and TRR models as well as how the noise profiles are affected under the different perturbations in the BG-mediated TGF- β 2 signal enhancement. Initial results show there is not a significant difference between the noise profiles of SRR and TRR models, but further work is being performed to analyze the differences in the specific assumptions surrounding the BG-mediated TGF- β 2 signaling enhancement mechanism. Furthermore, creating mathematical models of the TGF- β 2 mutant developed in the Villarreal et al., 2016 paper is likely to be useful in distinguishing between the receptor recruitment models and to refine the conclusions regarding the TGF- β 2/BG/T β RII/T β RI species. More experimental and computational work is necessary to refute or support the models discussed in this work with biochemical data. However, the results demonstrate that we have successfully modeled published work with mathematical approaches and that this research will be able to shed light on the mechanisms at play in TGF- β signaling.

In addition to the conclusions formed from this work, the mathematical models provide a blueprint for more computational and experimental work to build from. Other membrane bound co-receptors such as endoglin, a TGF- β binding protein found in endothelial cells, could be modeled using a similar computational framework as presented in this thesis (McAllister et al., 1994). If one of these models is correct, then the models developed in this work may also be used as a starting point to aid in development of improved therapeutics for TGF- β -related disorders.

In conclusion, the computational work performed in this thesis supports a hypothesized model of BG potentiation of TGF- β 2 signaling, underscoring the requirement of symmetrical receptor recruitment, and provides a baseline model to further investigate various aspects of the TGF- β receptor complex assembly that are still unknown.

APPENDIX

#No Receptor Recruitment (NRR) model for TGF-beta1

#Importing functions for model creation

from __future__ import print_function

from pysb import *

_pysb_doctest_suppress_modelexistswarning = True

#Create the model

Model()

Monomer('BG')

Monomer('TBRII')

Monomer('TBRI')

Monomer('TB1_BG')

Monomer('TB1_BG_TBRII')

Monomer('TB1_BG_TBRII_TBRI')

Monomer('TB1_TBRI_TBRI')

Monomer('TB1_TBRII_TBRI')

Monomer('TB1_TBRII_TBRI_TBRI')

Monomer('TB1_TBRII_TBRII_TBRI')

Monomer('TB1_TBRII_TBRII_TBRI_TBRI')

Monomer('TB1_TBRII')

Monomer('TB1_TBRI')

Monomer('TB1_TBRII_TBRII')

#List out the reactions involved in the system

#Reaction rates used for this system can be seen in Supplemental Table 1

#Rxn 13a

Parameter('k13a_on', MF * Z)

Parameter('k13a_off', MR)

#BG + TB1 <-> TB1_BG

Rule('TB1_to_BG', BG() <> TB1_BG(), k13a_on, k13a_off)

#Rxn 14a

Parameter('k14a_on', NF*SEF)

Parameter('k14a_off', NR)

#TB1_BG + TBRII <-> TB1_BG_TBRII

Rule('TB1_BG_to_TB1_BG_TBRII', TB1_BG() + TBRII() <> TB1_BG_TBRII(), k14a_on, k14a_off)

#Rxn 16

Parameter('k16a_on', QF*SEF)

Parameter('k16a_off', QR)

```

#TB1_BG_TBRII + TBRI <-> TB1_BG_TBRII_TBRI
Rule('TB1_BG_TBRII_to_TB1_BG_TBRII_TBRI', TB1_BG_TBRII() + TBRI() <>
TB1_BG_TBRII_TBRI(), k16a_on, k16a_off)

#Rxn 17a # inverted reaction
Parameter('k17a_on', SF*SEF)
Parameter('k17a_off', SR)
#TB1_BG_TBRII_TBRI <-> TB1_TBRII_TBRI + BG
Rule('TB1_BG_TBRII_TBRI_to_TB1_TBRII_TBRI', TB1_TBRII_TBRI() + BG() <>
TB1_BG_TBRII_TBRI(), k17a_on, k17a_off)

#Rxn 8a
Parameter('k8a_on', HF*SEF)
Parameter('k8a_off', HR)
#TB1_TBRII_TBRI + TBRII <-> TB1_TBRII_TBRII_TBRI
Rule('TB1_TBRII_TBRI_to_TB1_TBRII_TBRII_TBRI', TB1_TBRII_TBRI() + TBRII() <>
TB1_TBRII_TBRII_TBRI(), k8a_on, k8a_off)

#Rxn 9a
Parameter('k9a_on', IF*SEF)
Parameter('k9a_off', IR)
#TB1_TBRII_TBRI + TBRI <-> TB1_TBRII_TBRI_TBRI
Rule('TB1_TBRII_TBRI_to_TB1_TBRII_TBRI_TBRI', TB1_TBRII_TBRI() + TBRI() <>
TB1_TBRII_TBRI_TBRI(), k9a_on, k9a_off)

#Rxn 11a
Parameter('k11a_on', KF*SEF)
Parameter('k11a_off', KR)
#TB1_TBRII_TBRII_TBRI + TBRI <-> TB1_TBRII_TBRII_TBRI_TBRI
Rule('TB1_TBRII_TBRII_TBRI_to_TB1_TBRII_TBRII_TBRI_TBRI',
TB1_TBRII_TBRII_TBRI() + TBRI() <> TB1_TBRII_TBRII_TBRI_TBRI(), k11a_on,
k11a_off)

#Rxn 12a
Parameter('k12a_on', LF*SEF)
Parameter('k12a_off', LR)
#TB1_TBRII_TBRI_TBRI + TBRII <-> TB1_TBRII_TBRII_TBRI_TBRI
Rule('TB1_TBRII_TBRI_TBRI_to_TB1_TBRII_TBRII_TBRI_TBRI',
TB1_TBRII_TBRI_TBRI() + TBRII() <> TB1_TBRII_TBRII_TBRI_TBRI(), k12a_on,
k12a_off)

#Rxn 1
Parameter('k1a_on', AF*Z)
Parameter('k1a_off', AR)
#TB1 + TBRII <-> TB1_TBRII
Rule('TB1_to_TB1_TBRII', TBRII() <> TB1_TBRII(), k1a_on, k1a_off)

```

```

#Rxn 4
Parameter('k4a_on', DF*SEF)
Parameter('k4a_off', DR)
#TB1_TBRII + TBRI <-> TB1_TBRII_TBRI
Rule('TB1_TBRII_to_TB1_TBRII_TBRI', TB1_TBRII() + TBRI() <> TB1_TBRII_TBRI(),
k4a_on, k4a_off)

#Rxn 3
Parameter('k3a_on', CF*SEF)
Parameter('k3a_off', CR)
#TB1_TBRII + TBRII <-> TB1_TBRII_TBRII
Rule('TB1_TBRII_to_TB1_TBRII_TBRII', TB1_TBRII() +TBRII() <> TB1_TBRII_TBRII(),
k3a_on, k3a_off)

#Rxn 7
Parameter('k7a_on', GF*SEF)
Parameter('k7a_off', GR)
#TB1_TBRII_TBRII +TBRI <> TB1_TBRII_TBRII_TBRI
Rule('TB1_TBRII_TBRII_to_TB1_TBRII_TBRII', TB1_TBRII_TBRII() +TBRI() <>
TB1_TBRII_TBRII_TBRI(), k7a_on, k7a_off)

#Rxn 2
Parameter('k2a_on', BF*Z)
Parameter('k2a_off', BR)
#TB1 + TBRI <-> TB1_TBRI
Rule('TB1_to_TB1_TBRI', TBRI() <> TB1_TBRI(), k2a_on, k2a_off)

#Rxn 5
Parameter('k5a_on', EF*SEF)
Parameter('k5a_off', ER)
#TB1_TBRI + TBRII <-> TB1_TBRI_TBRI
Rule('TB1_TBRI_to_TB1_TBRII_TBRI', TB1_TBRI() + TBRII() <> TB1_TBRII_TBRI(),
k5a_on, k5a_off)

#Rxn 6
Parameter('k6a_on', FF*SEF)
Parameter('k6a_off', FR)
#TB1_TBRI + TBRI <-> TB1_TBRI_TBRI
Rule('TB1_TBRI_to_TB1_TBRI_TBRI', TB1_TBRI() + TBRI() <> TB1_TBRI_TBRI(),
k6a_on, k6a_off)

#Rxn 10
Parameter('k10a_on', JF*SEF)
Parameter('k10a_off', JR)
#TB1_TBRI_TBRI + TBRII <-> TB1_TBRII_TBRI_TBRI

```

```
Rule('TB1_TBRI_TBRI_to_TB1_TBRII_TBRI_TBRI', TB1_TBRI_TBRI() + TBRII() <>
TB1_TBRII_TBRI_TBRI(), k10a_on, k10a_off)
```

```
#Rxn 15
```

```
Parameter('k15a_on', PF*SEF)
```

```
Parameter('k15a_off', PR)
```

```
#TB1_TBRI + TBRI <-> TB1_TBRI_TBRI
```

```
Rule('TB1_TBRII_to_TB1_BG_TBRII', TB1_TBRII() + BG() <> TB1_BG_TBRII(), k15a_on,
k15a_off)
```

```
#Receptor Recycling and Endocytosis in one step
```

```
#Rxn1001
```

```
Parameter('kendo', kendo)
```

```
#TB1_BG -> BG + TB1
```

```
Rule('TB1_BG_Endo1', TB1_BG() >> BG(), kendo)
```

```
#Rxn1002
```

```
#TB1_BG_TBRII -> BG + TBRII + TB1
```

```
Rule('TB1_BG_TBRII_Endo2', TB1_BG_TBRII() >> BG() + TBRII(), kendo)
```

```
#Rxn1003
```

```
#TB1_TBRII -> TB1 + TBRII
```

```
Rule('TB1_TBRII_Endo3', TB1_TBRII() >> TBRII(), kendo)
```

```
#Rxn1004
```

```
#TB1_TBRI -> TBRI + TB1
```

```
Rule('TB1_TBRI_Endo4', TB1_TBRI() >> TBRI(), kendo)
```

```
#Rxn1005
```

```
#TB1_BG_TBRII_TBRI ->
```

```
Rule('TB1_BG_TBRII_TBRI_Endo5', TB1_BG_TBRII_TBRI() >> BG() + TBRII() + TBRI(),
kendo)
```

```
#Rxn1006
```

```
#TB1_TBRII_TBRI -> TBRII + TBRI + TB1
```

```
Rule('TB1_TBRII_TBRI_Endo6', TB1_TBRII_TBRI() >> TBRII() + TBRI(), kendo)
```

```
#Rxn1007
```

```
#TB1_TBRII_TBRII_TBRI -> TBRII(2) + TBRI + TB1
```

```
Rule('TB1_TBRII_TBRII_TBRI_Endo7', TB1_TBRII_TBRII_TBRI() >> TBRII() + TBRII() + TBRI(), kendo)
```

```
#Rxn1008
```

```
#TB1_TBRII_TBRI_TBRI -> TBRII + TBRI + TBRI + TB1  
Rule('TB1_TBRII_TBRI_TBRI_Endo8', TB1_TBRII_TBRI_TBRI() >> TBRII() + TBRI() + TBRI(), kendo)
```

```
#Rxn1009
```

```
#TB1_TBRII_TBRII_TBRI_TBRI -> TBRII + TBRII + TBRI + TBRI + TB1  
Rule('TB1_TBRII_TBRII_TBRI_TBRI_Endo9', TB1_TBRII_TBRII_TBRI_TBRI() >> TBRII() + TBRII() + TBRI() + TBRI(), kendo)
```

```
#Rxn1010
```

```
#TB1_TBRII_TBRII -> TBRII + TBRII + TB1  
Rule('TB1_TBRII_TBRII_Endo10', TB1_TBRII_TBRII() >> TBRII() + TBRII(), kendo)
```

```
#Rxn1011
```

```
Rule('TB1_TBRI_TBRI_Endo11', TB1_TBRI_TBRI() >> TBRI() + TBRI(), kendo)
```

```
#Defining parameters that are not rates
```

```
Parameter('BG_0', Z2)  
Parameter('TBRII_0', RII)  
Parameter('TBRI_0', RI)
```

```
#Initial Values
```

```
#These values would vary depending on our screen  
Initial(BG(), BG_0)  
Initial(TBRII(), TBRII_0)  
Initial(TBRI(), TBRI_0)
```

```
#Observable Amount of Monomer
```

```
Observable('BG', BG());  
Observable('TBRII', TBRII());  
Observable('TBRI', TBRI());  
Observable('TB1_TBRI_TBRI', TB1_TBRI_TBRI());  
Observable('TB1_BG', TB1_BG());  
Observable('TB1_TBRI', TB1_TBRI());  
Observable('TB1_TBRII', TB1_TBRII());  
Observable('TB1_TBRII_TBRII', TB1_TBRII_TBRII());  
Observable('TB1_BG_TBRII', TB1_BG_TBRII());  
Observable('TB1_BG_TBRII_TBRI', TB1_BG_TBRII_TBRI());
```

```

Observable('TB1_TBRII_TBRI', TB1_TBRII_TBRI());
Observable('TB1_TBRII_TBRII_TBRI', TB1_TBRII_TBRII_TBRI());
Observable('TB1_TBRII_TBRI_TBRI', TB1_TBRII_TBRI_TBRI());
Observable('TB1_TBRII_TBRII_TBRI_TBRI', TB1_TBRII_TBRII_TBRI_TBRI());

#import functions for data analysis
from matplotlib.pyplot import *
from numpy import linspace, array
from pysb.simulator import ScipyOdeSimulator

# We will integrate from t=0 to t=86400
t = linspace(0, 186400, 186401)
y = ScipyOdeSimulator(model, rtol=1e-4, atol=[1e-8, 1e-14, 1e-6]).run(tspan=t).all

# Gather the observables of interest into a matrix
yobs = array([y[obs] for obs in ('BG', 'TBRII', 'TBRI', 'TB1_BG', 'TB1_TBRI', 'TB1_TBRII',
'TB1_TBRII_TBRII', 'TB1_BG_TBRII', 'TB1_BG_TBRII_TBRI', 'TB1_TBRII_TBRI',
'TB1_TBRII_TBRII_TBRI', 'TB1_TBRII_TBRI_TBRI', 'TB1_TBRII_TBRII_TBRI_TBRI',
'TB1_TBRI_TBRI')]).T

#Recording the concentrations of individual species at 186400 seconds
TetramerShot = ((y['TB1_TBRII_TBRII_TBRI_TBRI'][186400]))
Shot_BG = ((y['BG'][186400]))
ShotTBRII = ((y['TBRII'][186400]))
ShotTBRI = ((y['TBRI'][186400]))
ShotTB1_BG = ((y['TB1_BG'][186400]))
ShotTB1_TBRI = ((y['TB1_TBRI'][186400]))
ShotTB1_TBRII = ((y['TB1_TBRII'][186400]))
ShotTB1_TBRI_TBRI = ((y['TB1_TBRI_TBRI'][186400]))
ShotTB1_TBRII_TBRII = ((y['TB1_TBRII_TBRII'][186400]))
ShotTB1_BG_TBRII = ((y['TB1_BG_TBRII'][186400]))
ShotTB1_BG_TBRII_TBRI = ((y['TB1_BG_TBRII_TBRI'][186400]))
ShotTB1_TBRII_TBRI = ((y['TB1_TBRII_TBRI'][186400]))
ShotTB1_TBRII_TBRII_TBRI = ((y['TB1_TBRII_TBRII_TBRI'][186400]))
ShotTB1_TBRII_TBRI_TBRI = ((y['TB1_TBRII_TBRI_TBRI'][186400]))
ShotTB1_TBRII_TBRII_TBRI_TBRI = ((y['TB1_TBRII_TBRII_TBRI_TBRI'][186400]))

#End of NRR model for TGF-beta1

```

```

#No Receptor Recruitment (NRR) model for TGF-beta2

#Importing functions for model creation
from __future__ import print_function
from pysb import *
_pysb_doctest_suppress_modelexistswarning = True

#Create model
Model()

Monomer('BG')
Monomer('TBRII')
Monomer('TBRI')
Monomer('TB2_BG')
Monomer('TB2_BG_TBRII')
Monomer('TB2_BG_TBRII_TBRI')
Monomer('TB2_TBRI_TBRI')
Monomer('TB2_TBRII_TBRI')
Monomer('TB2_TBRII_TBRI_TBRI')
Monomer('TB2_TBRII_TBRII_TBRI')
Monomer('TB2_TBRII_TBRII_TBRI_TBRI')
Monomer('TB2_TBRII')
Monomer('TB2_TBRI')
Monomer('TB2_TBRII_TBRII')

#Listing reactions
#Reaction rates for this system can be found in Supplemental Table 2

#Rxn 13a
Parameter('k13a_on', MF * Z)
Parameter('k13a_off', MR)
#BG + TB2 <-> TB2_BG
Rule('TB2_to_BG', BG() <> TB2_BG(), k13a_on, k13a_off)

#Rxn 14a
Parameter('k14a_on', NF*SEF)
Parameter('k14a_off', NR)
#TB2_BG + TBRII <-> TB2_BG_TBRII
Rule('TB2_BG_to_TB2_BG_TBRII', TB2_BG() + TBRII() <> TB2_BG_TBRII(), k14a_on,
k14a_off)

#Rxn 16
Parameter('k16a_on', QF*SEF)
Parameter('k16a_off', QR)
#TB2_BG_TBRII + TBRI <-> TB2_BG_TBRII_TBRI

```

Rule('TB2_BG_TBRII_to_TB2_BG_TBRII_TBRI', TB2_BG_TBRII() + TBRI() <>
TB2_BG_TBRII_TBRI(), k16a_on, k16a_off)

#Rxn 17a # inverted reaction

Parameter('k17a_on', SF*SEF)

Parameter('k17a_off', SR)

#TB2_BG_TBRII_TBRI <-> TB2_TBRII_TBRI + BG

Rule('TB2_BG_TBRII_TBRI_to_TB2_TBRII_TBRI', TB2_TBRII_TBRI() + BG() <>
TB2_BG_TBRII_TBRI(), k17a_on, k17a_off)

#Rxn 8a

Parameter('k8a_on', HF*SEF)

Parameter('k8a_off', HR)

#TB2_TBRII_TBRI + TBRII <-> TB2_TBRII_TBRII_TBRI

Rule('TB2_TBRII_TBRI_to_TB2_TBRII_TBRII_TBRI', TB2_TBRII_TBRI() + TBRII() <>
TB2_TBRII_TBRII_TBRI(), k8a_on, k8a_off)

#Rxn 9a

Parameter('k9a_on', IF*SEF)

Parameter('k9a_off', IR)

#TB2_TBRII_TBRI + TBRI <-> TB2_TBRII_TBRI_TBRI

Rule('TB2_TBRII_TBRI_to_TB2_TBRII_TBRI_TBRI', TB2_TBRII_TBRI() + TBRI() <>
TB2_TBRII_TBRI_TBRI(), k9a_on, k9a_off)

#Rxn 11a

Parameter('k11a_on', KF*SEF)

Parameter('k11a_off', KR)

#TB2_TBRII_TBRII_TBRI + TBRI <-> TB2_TBRII_TBRII_TBRI_TBRI

Rule('TB2_TBRII_TBRII_TBRI_to_TB2_TBRII_TBRII_TBRI_TBRI',
TB2_TBRII_TBRII_TBRI() + TBRI() <> TB2_TBRII_TBRII_TBRI_TBRI(), k11a_on,
k11a_off)

#Rxn 12a

Parameter('k12a_on', LF*SEF)

Parameter('k12a_off', LR)

#TB2_TBRII_TBRI_TBRI + TBRII <-> TB2_TBRII_TBRII_TBRI_TBRI

Rule('TB2_TBRII_TBRI_TBRI_to_TB2_TBRII_TBRII_TBRI_TBRI',
TB2_TBRII_TBRI_TBRI() + TBRII() <> TB2_TBRII_TBRII_TBRI_TBRI(), k12a_on,
k12a_off)

#Rxn 1

Parameter('k1a_on', AF*Z)

Parameter('k1a_off', AR)

#TB2 + TBRII <-> TB2_TBRII

Rule('TB2_to_TB2_TBRII', TBRII() <> TB2_TBRII(), k1a_on, k1a_off)

```

#Rxn 4
Parameter('k4a_on', DF*SEF)
Parameter('k4a_off', DR)
#TB2_TBRII + TBRI <-> TB2_TBRII_TBRI
Rule('TB2_TBRII_to_TB2_TBRII_TBRI', TB2_TBRII() + TBRI() <> TB2_TBRII_TBRI(),
k4a_on, k4a_off)

#Rxn 3
Parameter('k3a_on', CF*SEF)
Parameter('k3a_off', CR)
#TB2_TBRII + TBRII <-> TB2_TBRII_TBRII
Rule('TB2_TBRII_to_TB2_TBRII_TBRII', TB2_TBRII() + TBRII() <> TB2_TBRII_TBRII(),
k3a_on, k3a_off)

#Rxn 7
Parameter('k7a_on', GF*SEF)
Parameter('k7a_off', GR)
#TB2_TBRII_TBRII + TBRI <> TB2_TBRII_TBRII_TBRI
Rule('TB2_TBRII_TBRII_to_TB2_TBRII_TBRII', TB2_TBRII_TBRII() + TBRI() <>
TB2_TBRII_TBRII_TBRI(), k7a_on, k7a_off)

#Rxn 2
Parameter('k2a_on', BF*Z)
Parameter('k2a_off', BR)
#TB2 + TBRI <-> TB2_TBRI
Rule('TB2_to_TB2_TBRI', TBRI() <> TB2_TBRI(), k2a_on, k2a_off)

#Rxn 5
Parameter('k5a_on', EF*SEF)
Parameter('k5a_off', ER)
#TB2_TBRI + TBRII <-> TB2_TBRI_TBRI
Rule('TB2_TBRI_to_TB2_TBRII_TBRI', TB2_TBRI() + TBRII() <> TB2_TBRII_TBRI(),
k5a_on, k5a_off)

#Rxn 6
Parameter('k6a_on', FF*SEF)
Parameter('k6a_off', FR)
#TB2_TBRI + TBRI <-> TB2_TBRI_TBRI
Rule('TB2_TBRI_to_TB2_TBRI_TBRI', TB2_TBRI() + TBRI() <> TB2_TBRI_TBRI(),
k6a_on, k6a_off)

#Rxn 10
Parameter('k10a_on', JF*SEF)
Parameter('k10a_off', JR)
#TB2_TBRI_TBRI + TBRII <-> TB2_TBRII_TBRI_TBRI

```

```
Rule('TB2_TBRI_TBRI_to_TB2_TBRII_TBRI_TBRI', TB2_TBRI_TBRI() + TBRII() <>
TB2_TBRII_TBRI_TBRI(), k10a_on, k10a_off)
```

```
#Rxn 15
```

```
Parameter('k15a_on', PF*SEF)
```

```
Parameter('k15a_off', PR)
```

```
#TB2_TBRI + TBRI <-> TB2_TBRI_TBRI
```

```
Rule('TB2_TBRII_to_TB2_BG_TBRII', TB2_TBRII() + BG() <> TB2_BG_TBRII(), k15a_on,
k15a_off)
```

```
#Receptor Recycling and Endocytosis in one step
```

```
#Rxn1001
```

```
Parameter('kendo', kendo)
```

```
#TB2_BG -> BG + TB2
```

```
Rule('TB2_BG_Endo1', TB2_BG() >> BG(), kendo)
```

```
#Rxn1002
```

```
#TB2_BG_TBRII -> BG + TBRII + TB2
```

```
Rule('TB2_BG_TBRII_Endo2', TB2_BG_TBRII() >> BG() + TBRII(), kendo)
```

```
#Rxn1003
```

```
#TB2_TBRII -> TB2 + TBRII
```

```
Rule('TB2_TBRII_Endo3', TB2_TBRII() >> TBRII(), kendo)
```

```
#Rxn1004
```

```
#TB2_TBRI -> TBRI + TB2
```

```
Rule('TB2_TBRI_Endo4', TB2_TBRI() >> TBRI(), kendo)
```

```
#Rxn1005
```

```
#TB2_BG_TBRII_TBRI ->
```

```
Rule('TB2_BG_TBRII_TBRI_Endo5', TB2_BG_TBRII_TBRI() >> BG() + TBRII() + TBRI(),
kendo)
```

```
#Rxn1006
```

```
#TB2_TBRII_TBRI -> TBRII + TBRI + TB2
```

```
Rule('TB2_TBRII_TBRI_Endo6', TB2_TBRII_TBRI() >> TBRII() + TBRI(), kendo)
```

```
#Rxn1007
```

```
#TB2_TBRII_TBRII_TBRI -> TBRII(2) + TBRI + TB2
```

```
Rule('TB2_TBRII_TBRII_TBRI_Endo7', TB2_TBRII_TBRII_TBRI() >> TBRII() + TBRII() + TBRI(), kendo)
```

```
#Rxn1008
```

```
#TB2_TBRII_TBRI_TBRI -> TBRII + TBRI + TBRI + TB2  
Rule('TB2_TBRII_TBRI_TBRI_Endo8', TB2_TBRII_TBRI_TBRI() >> TBRII() + TBRI() + TBRI(), kendo)
```

```
#Rxn1009
```

```
#TB2_TBRII_TBRII_TBRI_TBRI -> TBRII + TBRII + TBRI + TBRI + TB2  
Rule('TB2_TBRII_TBRII_TBRI_TBRI_Endo9', TB2_TBRII_TBRII_TBRI_TBRI() >> TBRII() + TBRII() + TBRI() + TBRI(), kendo)
```

```
#Rxn1010
```

```
#TB2_TBRII_TBRII -> TBRII + TBRII + TB2  
Rule('TB2_TBRII_TBRII_Endo10', TB2_TBRII_TBRII() >> TBRII() + TBRII(), kendo)
```

```
#Rxn1011
```

```
Rule('TB2_TBRI_TBRI_Endo11', TB2_TBRI_TBRI() >> TBRI() + TBRI(), kendo)
```

```
#Defining parameters that are not rates
```

```
Parameter('BG_0', Z2)  
Parameter('TBRII_0', RII)  
Parameter('TBRI_0', RI)
```

```
#Initial Values
```

```
#These values would vary depending on screen performed
```

```
Initial(BG(), BG_0)  
Initial(TBRII(), TBRII_0)  
Initial(TBRI(), TBRI_0)
```

```
#Observable Amount of Monomer
```

```
Observable('BG', BG());  
Observable('TBRII', TBRII());  
Observable('TBRI', TBRI());  
Observable('TB2_TBRI_TBRI', TB2_TBRI_TBRI());  
Observable('TB2_BG', TB2_BG());  
Observable('TB2_TBRI', TB2_TBRI());  
Observable('TB2_TBRII', TB2_TBRII());  
Observable('TB2_TBRII_TBRII', TB2_TBRII_TBRII());  
Observable('TB2_BG_TBRII', TB2_BG_TBRII());  
Observable('TB2_BG_TBRII_TBRI', TB2_BG_TBRII_TBRI());  
Observable('TB2_TBRII_TBRI', TB2_TBRII_TBRI());
```

```

Observable('TB2_TBRII_TBRII_TBRI', TB2_TBRII_TBRII_TBRI());
Observable('TB2_TBRII_TBRI_TBRI', TB2_TBRII_TBRI_TBRI());
Observable('TB2_TBRII_TBRII_TBRI_TBRI', TB2_TBRII_TBRII_TBRI_TBRI());

#Importing functions for data analysis
from matplotlib.pyplot import *
from numpy import linspace, array
from pysb.simulator import ScipyOdeSimulator

# We will integrate from t=0 to t=86400
t = linspace(0, 186400, 186401)
y = ScipyOdeSimulator(model, rtol=1e-4, atol=[1e-8, 1e-14, 1e-6]).run(tspan=t).all

# Gather the observables of interest into a matrix
yobs = array([y[obs] for obs in ('BG', 'TBRII', 'TBRI', 'TB2_BG', 'TB2_TBRI', 'TB2_TBRII',
'TB2_TBRII_TBRII', 'TB2_BG_TBRII', 'TB2_BG_TBRII_TBRI', 'TB2_TBRII_TBRI',
'TB2_TBRII_TBRII_TBRI', 'TB2_TBRII_TBRI_TBRI', 'TB2_TBRII_TBRII_TBRI_TBRI',
'TB2_TBRI_TBRI')]).T

#Recording the concentrations of individual species at 186400 seconds
TetramerShot = ((y['TB2_TBRII_TBRII_TBRI_TBRI'][186400]))
Shot_BG = ((y['BG'][186400]))
ShotTBRII = ((y['TBRII'][186400]))
ShotTBRI = ((y['TBRI'][186400]))
ShotTB2_BG = ((y['TB2_BG'][186400]))
ShotTB2_TBRI = ((y['TB2_TBRI'][186400]))
ShotTB2_TBRII = ((y['TB2_TBRII'][186400]))
ShotTB2_TBRI_TBRI = ((y['TB2_TBRI_TBRI'][186400]))
ShotTB2_TBRII_TBRII = ((y['TB2_TBRII_TBRII'][186400]))
ShotTB2_BG_TBRII = ((y['TB2_BG_TBRII'][186400]))
ShotTB2_BG_TBRII_TBRI = ((y['TB2_BG_TBRII_TBRI'][186400]))
ShotTB2_TBRII_TBRI = ((y['TB2_TBRII_TBRI'][186400]))
ShotTB2_TBRII_TBRII_TBRI = ((y['TB2_TBRII_TBRII_TBRI'][186400]))
ShotTB2_TBRII_TBRI_TBRI = ((y['TB2_TBRII_TBRI_TBRI'][186400]))
ShotTB2_TBRII_TBRII_TBRI_TBRI = ((y['TB2_TBRII_TBRII_TBRI_TBRI'][186400]))

#End of NRR model for TGF-beta2

```

```

#No Receptor Recruitment (NRR) model for TGF-beta3

#Importing functions for model creation
from __future__ import print_function
from pysb import *
_pysb_doctest_suppress_modelexistswarning = True

#Create Model
Model()

Monomer('BG')
Monomer('TBRII')
Monomer('TBRI')
Monomer('TB3_BG')
Monomer('TB3_BG_TBRII')
Monomer('TB3_BG_TBRII_TBRI')
Monomer('TB3_TBRI_TBRI')
Monomer('TB3_TBRII_TBRI')
Monomer('TB3_TBRII_TBRI_TBRI')
Monomer('TB3_TBRII_TBRII_TBRI')
Monomer('TB3_TBRII_TBRII_TBRI_TBRI')
Monomer('TB3_TBRII')
Monomer('TB3_TBRI')
Monomer('TB3_TBRII_TBRII')

#Listing reactions
#Reaction rates for this system can be found in Supplemental Table 3

#Rxn 13a
Parameter('k13a_on', MF * Z)
Parameter('k13a_off', MR)
#BG + TB3 <-> TB3_BG
Rule('TB3_to_BG', BG() <> TB3_BG(), k13a_on, k13a_off)

#Rxn 14a
Parameter('k14a_on', NF*SEF)
Parameter('k14a_off', NR)
#TB3_BG + TBRII <-> TB3_BG_TBRII
Rule('TB3_BG_to_TB3_BG_TBRII', TB3_BG() + TBRII() <> TB3_BG_TBRII(), k14a_on,
k14a_off)

#Rxn 16
Parameter('k16a_on', QF*SEF)
Parameter('k16a_off', QR)
#TB3_BG_TBRII + TBRI <-> TB3_BG_TBRII_TBRI

```

Rule('TB3_BG_TBRII_to_TB3_BG_TBRII_TBRI', TB3_BG_TBRII() + TBRI() <>
TB3_BG_TBRII_TBRI(), k16a_on, k16a_off)

#Rxn 17a # inverted reaction

Parameter('k17a_on', SF*SEF)

Parameter('k17a_off', SR)

#TB3_BG_TBRII_TBRI <-> TB3_TBRII_TBRI + BG

Rule('TB3_BG_TBRII_TBRI_to_TB3_TBRII_TBRI', TB3_TBRII_TBRI() + BG() <>
TB3_BG_TBRII_TBRI(), k17a_on, k17a_off)

#Rxn 8a

Parameter('k8a_on', HF*SEF)

Parameter('k8a_off', HR)

#TB3_TBRII_TBRI + TBRII <-> TB3_TBRII_TBRII_TBRI

Rule('TB3_TBRII_TBRI_to_TB3_TBRII_TBRII_TBRI', TB3_TBRII_TBRI() + TBRII() <>
TB3_TBRII_TBRII_TBRI(), k8a_on, k8a_off)

#Rxn 9a

Parameter('k9a_on', IF*SEF)

Parameter('k9a_off', IR)

#TB3_TBRII_TBRI + TBRI <-> TB3_TBRII_TBRI_TBRI

Rule('TB3_TBRII_TBRI_to_TB3_TBRII_TBRI_TBRI', TB3_TBRII_TBRI() + TBRI() <>
TB3_TBRII_TBRI_TBRI(), k9a_on, k9a_off)

#Rxn 11a

Parameter('k11a_on', KF*SEF)

Parameter('k11a_off', KR)

#TB3_TBRII_TBRII_TBRI + TBRI <-> TB3_TBRII_TBRII_TBRI_TBRI

Rule('TB3_TBRII_TBRII_TBRI_to_TB3_TBRII_TBRII_TBRI_TBRI',
TB3_TBRII_TBRII_TBRI() + TBRI() <> TB3_TBRII_TBRII_TBRI_TBRI(), k11a_on,
k11a_off)

#Rxn 12a

Parameter('k12a_on', LF*SEF)

Parameter('k12a_off', LR)

#TB3_TBRII_TBRI_TBRI + TBRII <-> TB3_TBRII_TBRII_TBRI_TBRI

Rule('TB3_TBRII_TBRI_TBRI_to_TB3_TBRII_TBRII_TBRI_TBRI',
TB3_TBRII_TBRI_TBRI() + TBRII() <> TB3_TBRII_TBRII_TBRI_TBRI(), k12a_on,
k12a_off)

#Rxn 1

Parameter('k1a_on', AF*Z)

Parameter('k1a_off', AR)

#TB3 + TBRII <-> TB3_TBRII

Rule('TB3_to_TB3_TBRII', TBRII() <> TB3_TBRII(), k1a_on, k1a_off)

```

#Rxn 4
Parameter('k4a_on', DF*SEF)
Parameter('k4a_off', DR)
#TB3_TBRII + TBRI <-> TB3_TBRII_TBRI
Rule('TB3_TBRII_to_TB3_TBRII_TBRI', TB3_TBRII() + TBRI() <> TB3_TBRII_TBRI(),
k4a_on, k4a_off)

#Rxn 3
Parameter('k3a_on', CF*SEF)
Parameter('k3a_off', CR)
#TB3_TBRII + TBRII <-> TB3_TBRII_TBRII
Rule('TB3_TBRII_to_TB3_TBRII_TBRII', TB3_TBRII() + TBRII() <> TB3_TBRII_TBRII(),
k3a_on, k3a_off)

#Rxn 7
Parameter('k7a_on', GF*SEF)
Parameter('k7a_off', GR)
#TB3_TBRII_TBRII + TBRI <> TB3_TBRII_TBRII_TBRI
Rule('TB3_TBRII_TBRII_to_TB3_TBRII_TBRII', TB3_TBRII_TBRII() + TBRI() <>
TB3_TBRII_TBRII_TBRI(), k7a_on, k7a_off)

#Rxn 2
Parameter('k2a_on', BF*Z)
Parameter('k2a_off', BR)
#TB3 + TBRI <-> TB3_TBRI
Rule('TB3_to_TB3_TBRI', TBRI() <> TB3_TBRI(), k2a_on, k2a_off)

#Rxn 5
Parameter('k5a_on', EF*SEF)
Parameter('k5a_off', ER)
#TB3_TBRI + TBRII <-> TB3_TBRI_TBRI
Rule('TB3_TBRI_to_TB3_TBRII_TBRI', TB3_TBRI() + TBRII() <> TB3_TBRII_TBRI(),
k5a_on, k5a_off)

#Rxn 6
Parameter('k6a_on', FF*SEF)
Parameter('k6a_off', FR)
#TB3_TBRI + TBRI <-> TB3_TBRI_TBRI
Rule('TB3_TBRI_to_TB3_TBRI_TBRI', TB3_TBRI() + TBRI() <> TB3_TBRI_TBRI(),
k6a_on, k6a_off)

#Rxn 10
Parameter('k10a_on', JF*SEF)
Parameter('k10a_off', JR)
#TB3_TBRI_TBRI + TBRII <-> TB3_TBRII_TBRI_TBRI

```

```

Rule('TB3_TBRI_TBRI_to_TB3_TBRII_TBRI_TBRI', TB3_TBRI_TBRI() + TBRII() <>
TB3_TBRII_TBRI_TBRI(), k10a_on, k10a_off)

#Rxn 15
Parameter('k15a_on', PF*SEF)
Parameter('k15a_off', PR)
#TB3_TBRI + TBRI <-> TB3_TBRI_TBRI
Rule('TB3_TBRII_to_TB3_BG_TBRII', TB3_TBRII() + BG() <> TB3_BG_TBRII(), k15a_on,
k15a_off)

#Receptor Recycling and Endocytosis in one step

#Rxn1001
Parameter('kendo', kendo)
#TB3_BG -> BG + TB3
Rule('TB3_BG_Endo1', TB3_BG() >> BG(), kendo)

#Rxn1002

#TB3_BG_TBRII -> BG +TBRII + TB3
Rule('TB3_BG_TBRII_Endo2', TB3_BG_TBRII() >> BG() + TBRII(), kendo)

#Rxn1003

#TB3_TBRII -> TB3 + TBRII
Rule('TB3_TBRII_Endo3', TB3_TBRII() >> TBRII(), kendo)

#Rxn1004

#TB3_TBRI -> TBRI + TB3
Rule('TB3_TBRI_Endo4', TB3_TBRI() >> TBRI(), kendo)

#Rxn1005
#TB3_BG_TBRII_TBRI ->
Rule('TB3_BG_TBRII_TBRI_Endo5', TB3_BG_TBRII_TBRI() >> BG() + TBRII() + TBRI(),
kendo)

#Rxn1006

#TB3_TBRII_TBRI -> TBRII + TBRI + TB3
Rule('TB3_TBRII_TBRI_Endo6', TB3_TBRII_TBRI() >> TBRII() + TBRI(), kendo)

#Rxn1007

#TB3_TBRII_TBRII_TBRI -> TBRII(2) + TBRI + TB3

```

```
Rule('TB3_TBRII_TBRII_TBRI_Endo7', TB3_TBRII_TBRII_TBRI() >> TBRII() + TBRII() + TBRI(), kendo)
```

```
#Rxn1008
```

```
#TB3_TBRII_TBRI_TBRI -> TBRII + TBRI + TBRI + TB3  
Rule('TB3_TBRII_TBRI_TBRI_Endo8', TB3_TBRII_TBRI_TBRI() >> TBRII() + TBRI() + TBRI(), kendo)
```

```
#Rxn1009
```

```
#TB3_TBRII_TBRII_TBRI_TBRI -> TBRII + TBRII + TBRI + TBRI + TB3  
Rule('TB3_TBRII_TBRII_TBRI_TBRI_Endo9', TB3_TBRII_TBRII_TBRI_TBRI() >> TBRII() + TBRII() + TBRI() + TBRI(), kendo)
```

```
#Rxn1010
```

```
#TB3_TBRII_TBRII -> TBRII + TBRII + TB3  
Rule('TB3_TBRII_TBRII_Endo10', TB3_TBRII_TBRII() >> TBRII() + TBRII(), kendo)
```

```
#Rxn1011
```

```
Rule('TB3_TBRI_TBRI_Endo11', TB3_TBRI_TBRI() >> TBRI() + TBRI(), kendo)
```

```
#Defining parameters that are not rates
```

```
Parameter('BG_0', Z2)  
Parameter('TBRII_0', RII)  
Parameter('TBRI_0', RI)
```

```
#Initial Values
```

```
#These values would vary depending on screen performed  
Initial(BG(), BG_0)  
Initial(TBRII(), TBRII_0)  
Initial(TBRI(), TBRI_0)
```

```
#Observable Amount of Monomer
```

```
Observable('BG', BG());  
Observable('TBRII', TBRII());  
Observable('TBRI', TBRI());  
Observable('TB3_TBRI_TBRI', TB3_TBRI_TBRI());  
Observable('TB3_BG', TB3_BG());  
Observable('TB3_TBRI', TB3_TBRI());  
Observable('TB3_TBRII', TB3_TBRII());  
Observable('TB3_TBRII_TBRII', TB3_TBRII_TBRII());  
Observable('TB3_BG_TBRII', TB3_BG_TBRII());  
Observable('TB3_BG_TBRII_TBRI', TB3_BG_TBRII_TBRI());
```

```

Observable('TB3_TBRII_TBRI', TB3_TBRII_TBRI());
Observable('TB3_TBRII_TBRII_TBRI', TB3_TBRII_TBRII_TBRI());
Observable('TB3_TBRII_TBRI_TBRI', TB3_TBRII_TBRI_TBRI());
Observable('TB3_TBRII_TBRII_TBRI_TBRI', TB3_TBRII_TBRII_TBRI_TBRI());

#Importing functions for data analysis
from matplotlib.pyplot import *
from numpy import linspace, array
from pysb.simulator import ScipyOdeSimulator

# We will integrate from t=0 to t=86400
t = linspace(0, 186400, 186401)
y = ScipyOdeSimulator(model, rtol=1e-4, atol=[1e-8, 1e-14, 1e-6]).run(tspan=t).all

# Gather the observables of interest into a matrix
yobs = array([y[obs] for obs in ('BG', 'TBRII', 'TBRI', 'TB3_BG', 'TB3_TBRI', 'TB3_TBRII',
'TB3_TBRII_TBRII', 'TB3_BG_TBRII', 'TB3_BG_TBRII_TBRI', 'TB3_TBRII_TBRI',
'TB3_TBRII_TBRII_TBRI', 'TB3_TBRII_TBRI_TBRI', 'TB3_TBRII_TBRII_TBRI_TBRI',
'TB3_TBRI_TBRI')]).T

#Recording the concentrations of individual species at 186400 seconds
TetramerShot = ((y['TB3_TBRII_TBRII_TBRI_TBRI'][186400]))
Shot_BG = ((y['BG'][186400]))
ShotTBRII = ((y['TBRII'][186400]))
ShotTBRI = ((y['TBRI'][186400]))
ShotTB3_BG = ((y['TB3_BG'][186400]))
ShotTB3_TBRI = ((y['TB3_TBRI'][186400]))
ShotTB3_TBRII = ((y['TB3_TBRII'][186400]))
ShotTB3_TBRI_TBRI = ((y['TB3_TBRI_TBRI'][186400]))
ShotTB3_TBRII_TBRII = ((y['TB3_TBRII_TBRII'][186400]))
ShotTB3_BG_TBRII = ((y['TB3_BG_TBRII'][186400]))
ShotTB3_BG_TBRII_TBRI = ((y['TB3_BG_TBRII_TBRI'][186400]))
ShotTB3_TBRII_TBRI = ((y['TB3_TBRII_TBRI'][186400]))
ShotTB3_TBRII_TBRII_TBRI = ((y['TB3_TBRII_TBRII_TBRI'][186400]))
ShotTB3_TBRII_TBRI_TBRI = ((y['TB3_TBRII_TBRI_TBRI'][186400]))
ShotTB3_TBRII_TBRII_TBRI_TBRI = ((y['TB3_TBRII_TBRII_TBRI_TBRI'][186400]))

#End of NRR model for TGF-beta3

```

```
#Single-stage Receptor Recruitment (SRR) model for TGF-beta1
```

```
#Import functions for model creation  
from __future__ import print_function  
from pysb import *  
_pysb_doctest_suppress_modelexistswarning = True
```

```
#Create model  
Model()
```

```
Monomer('BG')  
Monomer('TBRII')  
Monomer('TBRI')  
Monomer('TB1_BG')  
Monomer('TB1_BG_TBRII')  
Monomer('TB1_BG_TBRII_TBRI')  
Monomer('TB1_TBRI_TBRI')  
Monomer('TB1_TBRII_TBRI')  
Monomer('TB1_TBRII_TBRI_TBRI')  
Monomer('TB1_TBRII_TBRII_TBRI')  
Monomer('TB1_TBRII_TBRII_TBRI_TBRI')  
Monomer('TB1_TBRII')  
Monomer('TB1_TBRI')  
Monomer('TB1_TBRII_TBRII')
```

```
#Listing reactions  
#Reaction rates for this system can be found in Supplemental Table 4
```

```
#Rxn 13a  
Parameter('k13a_on', MF * Z)  
Parameter('k13a_off', MR)  
#BG + TB1 <-> TB1_BG  
Rule('TB1_to_BG', BG() <> TB1_BG(), k13a_on, k13a_off)
```

```
#Rxn 14a  
Parameter('k14a_on', NF*SEF)  
Parameter('k14a_off', NR)  
#TB1_BG + TBRII <-> TB1_BG_TBRII  
Rule('TB1_BG_to_TB1_BG_TBRII', TB1_BG() + TBRII() <> TB1_BG_TBRII(), k14a_on,  
k14a_off)
```

```
#Rxn 16  
Parameter('k16a_on', QF*SEF)  
Parameter('k16a_off', QR)  
#TB1_BG_TBRII + TBRI <-> TB1_BG_TBRII_TBRI
```

Rule('TB1_BG_TBRII_to_TB1_BG_TBRII_TBRI', TB1_BG_TBRII() + TBRI() <>
TB1_BG_TBRII_TBRI(), k16a_on, k16a_off)

#Rxn 17a # inverted reaction

Parameter('k17a_on', SF*SEF)

Parameter('k17a_off', SR)

#TB1_BG_TBRII_TBRI <-> TB1_TBRII_TBRI + BG

Rule('TB1_BG_TBRII_TBRI_to_TB1_TBRII_TBRI', TB1_TBRII_TBRI() + BG() <>
TB1_BG_TBRII_TBRI(), k17a_on, k17a_off)

#Rxn 8a

Parameter('k8a_on', HF*SEF)

Parameter('k8a_off', HR)

#TB1_TBRII_TBRI + TBRII <-> TB1_TBRII_TBRII_TBRI

Rule('TB1_TBRII_TBRI_to_TB1_TBRII_TBRII_TBRI', TB1_TBRII_TBRI() + TBRII() <>
TB1_TBRII_TBRII_TBRI(), k8a_on, k8a_off)

#Rxn 9a

Parameter('k9a_on', IF*SEF)

Parameter('k9a_off', IR)

#TB1_TBRII_TBRI + TBRI <-> TB1_TBRII_TBRI_TBRI

Rule('TB1_TBRII_TBRI_to_TB1_TBRII_TBRI_TBRI', TB1_TBRII_TBRI() + TBRI() <>
TB1_TBRII_TBRI_TBRI(), k9a_on, k9a_off)

#Rxn 11a

Parameter('k11a_on', KF*SEF)

Parameter('k11a_off', KR)

#TB1_TBRII_TBRII_TBRI + TBRI <-> TB1_TBRII_TBRII_TBRI_TBRI

Rule('TB1_TBRII_TBRII_TBRI_to_TB1_TBRII_TBRII_TBRI_TBRI',
TB1_TBRII_TBRII_TBRI() + TBRI() <> TB1_TBRII_TBRII_TBRI_TBRI(), k11a_on,
k11a_off)

#Rxn 12a

Parameter('k12a_on', LF*SEF)

Parameter('k12a_off', LR)

#TB1_TBRII_TBRI_TBRI + TBRII <-> TB1_TBRII_TBRII_TBRI_TBRI

Rule('TB1_TBRII_TBRI_TBRI_to_TB1_TBRII_TBRII_TBRI_TBRI',
TB1_TBRII_TBRI_TBRI() + TBRII() <> TB1_TBRII_TBRII_TBRI_TBRI(), k12a_on,
k12a_off)

#Rxn 1

Parameter('k1a_on', AF*Z)

Parameter('k1a_off', AR)

#TB1 + TBRII <-> TB1_TBRII

Rule('TB1_to_TB1_TBRII', TBRII() <> TB1_TBRII(), k1a_on, k1a_off)

#Rxn 4

Parameter('k4a_on', DF*SEF)

Parameter('k4a_off', DR)

#TB1_TBRII + TBRI <-> TB1_TBRII_TBRI

Rule('TB1_TBRII_to_TB1_TBRII_TBRI', TB1_TBRII() + TBRI() <> TB1_TBRII_TBRI(),
k4a_on, k4a_off)

#Rxn 3

Parameter('k3a_on', CF*SEF)

Parameter('k3a_off', CR)

#TB1_TBRII + TBRII <-> TB1_TBRII_TBRII

Rule('TB1_TBRII_to_TB1_TBRII_TBRII', TB1_TBRII() + TBRII() <> TB1_TBRII_TBRII(),
k3a_on, k3a_off)

#Rxn 7

Parameter('k7a_on', GF*SEF)

Parameter('k7a_off', GR)

#TB1_TBRII_TBRII + TBRI <> TB1_TBRII_TBRII_TBRI

Rule('TB1_TBRII_TBRII_to_TB1_TBRII_TBRII', TB1_TBRII_TBRII() + TBRI() <>
TB1_TBRII_TBRII_TBRI(), k7a_on, k7a_off)

#Rxn 2

Parameter('k2a_on', BF*Z)

Parameter('k2a_off', BR)

#TB1 + TBRI <-> TB1_TBRI

Rule('TB1_to_TB1_TBRI', TBRI() <> TB1_TBRI(), k2a_on, k2a_off)

#Rxn 5

Parameter('k5a_on', EF*SEF)

Parameter('k5a_off', ER)

#TB1_TBRI + TBRII <-> TB1_TBRI_TBRI

Rule('TB1_TBRI_to_TB1_TBRII_TBRI', TB1_TBRI() + TBRII() <> TB1_TBRII_TBRI(),
k5a_on, k5a_off)

#Rxn 6

Parameter('k6a_on', FF*SEF)

Parameter('k6a_off', FR)

#TB1_TBRI + TBRI <-> TB1_TBRI_TBRI

Rule('TB1_TBRI_to_TB1_TBRI_TBRI', TB1_TBRI() + TBRI() <> TB1_TBRI_TBRI(),
k6a_on, k6a_off)

#Rxn 10

Parameter('k10a_on', JF*SEF)

Parameter('k10a_off', JR)

#TB1_TBRI_TBRI + TBRII <-> TB1_TBRII_TBRI_TBRI

```
Rule('TB1_TBRI_TBRI_to_TB1_TBRII_TBRI_TBRI', TB1_TBRI_TBRI() + TBRII() <>
TB1_TBRII_TBRI_TBRI(), k10a_on, k10a_off)
```

```
#Rxn 15
```

```
Parameter('k15a_on', PF*SEF)
```

```
Parameter('k15a_off', PR)
```

```
#TB1_TBRI + TBRI <-> TB1_TBRI_TBRI
```

```
Rule('TB1_TBRII_to_TB1_BG_TBRII', TB1_TBRII() + BG() <> TB1_BG_TBRII(), k15a_on,
k15a_off)
```

```
#Receptor Recycling and Endocytosis in one step
```

```
#Rxn1001
```

```
Parameter('kendo', kendo)
```

```
#TB1_BG -> BG + TB1
```

```
Rule('TB1_BG_Endo1', TB1_BG() >> BG(), kendo)
```

```
#Rxn1002
```

```
#TB1_BG_TBRII -> BG + TBRII + TB1
```

```
Rule('TB1_BG_TBRII_Endo2', TB1_BG_TBRII() >> BG() + TBRII(), kendo)
```

```
#Rxn1003
```

```
#TB1_TBRII -> TB1 + TBRII
```

```
Rule('TB1_TBRII_Endo3', TB1_TBRII() >> TBRII(), kendo)
```

```
#Rxn1004
```

```
#TB1_TBRI -> TBRI + TB1
```

```
Rule('TB1_TBRI_Endo4', TB1_TBRI() >> TBRI(), kendo)
```

```
#Rxn1005
```

```
#TB1_BG_TBRII_TBRI ->
```

```
Rule('TB1_BG_TBRII_TBRI_Endo5', TB1_BG_TBRII_TBRI() >> BG() + TBRII() + TBRI(),
kendo)
```

```
#Rxn1006
```

```
#TB1_TBRII_TBRI -> TBRII + TBRI + TB1
```

```
Rule('TB1_TBRII_TBRI_Endo6', TB1_TBRII_TBRI() >> TBRII() + TBRI(), kendo)
```

```
#Rxn1007
```

```
#TB1_TBRII_TBRII_TBRI -> TBRII(2) + TBRI + TB1
```

```
Rule('TB1_TBRII_TBRII_TBRI_Endo7', TB1_TBRII_TBRII_TBRI() >> TBRII() + TBRII() + TBRI(), kendo)
```

```
#Rxn1008
```

```
#TB1_TBRII_TBRI_TBRI -> TBRII + TBRI + TBRI + TB1  
Rule('TB1_TBRII_TBRI_TBRI_Endo8', TB1_TBRII_TBRI_TBRI() >> TBRII() + TBRI() + TBRI(), kendo)
```

```
#Rxn1009
```

```
#TB1_TBRII_TBRII_TBRI_TBRI -> TBRII + TBRII + TBRI + TBRI + TB1  
Rule('TB1_TBRII_TBRII_TBRI_TBRI_Endo9', TB1_TBRII_TBRII_TBRI_TBRI() >> TBRII() + TBRII() + TBRI() + TBRI(), kendo)
```

```
#Rxn1010
```

```
#TB1_TBRII_TBRII -> TBRII + TBRII + TB1  
Rule('TB1_TBRII_TBRII_Endo10', TB1_TBRII_TBRII() >> TBRII() + TBRII(), kendo)
```

```
#Rxn1011
```

```
Rule('TB1_TBRI_TBRI_Endo11', TB1_TBRI_TBRI() >> TBRI() + TBRI(), kendo)
```

```
#Defining parameters that are not rates
```

```
Parameter('BG_0', Z2)  
Parameter('TBRII_0', RII)  
Parameter('TBRI_0', RI)
```

```
#Initial Values
```

```
#These values would vary depending on screen performed
```

```
Initial(BG(), BG_0)  
Initial(TBRII(), TBRII_0)  
Initial(TBRI(), TBRI_0)
```

```
#Observable Amount of Monomer
```

```
Observable('BG', BG());  
Observable('TBRII', TBRII());  
Observable('TBRI', TBRI());  
Observable('TB1_TBRI_TBRI', TB1_TBRI_TBRI());  
Observable('TB1_BG', TB1_BG());  
Observable('TB1_TBRI', TB1_TBRI());  
Observable('TB1_TBRII', TB1_TBRII());  
Observable('TB1_TBRII_TBRII', TB1_TBRII_TBRII());  
Observable('TB1_BG_TBRII', TB1_BG_TBRII());  
Observable('TB1_BG_TBRII_TBRI', TB1_BG_TBRII_TBRI());  
Observable('TB1_TBRII_TBRI', TB1_TBRII_TBRI());
```

```

Observable('TB1_TBRII_TBRII_TBRI', TB1_TBRII_TBRII_TBRI());
Observable('TB1_TBRII_TBRI_TBRI', TB1_TBRII_TBRI_TBRI());
Observable('TB1_TBRII_TBRII_TBRI_TBRI', TB1_TBRII_TBRII_TBRI_TBRI());

#Importin functions for data analysis
from matplotlib.pyplot import *
from numpy import linspace, array
from pysb.simulator import ScipyOdeSimulator

# We will integrate from t=0 to t=86400
t = linspace(0, 186400, 186401)
y = ScipyOdeSimulator(model, rtol=1e-4, atol=[1e-8, 1e-14, 1e-6]).run(tspan=t).all

# Gather the observables of interest into a matrix
yobs = array([y[obs] for obs in ('BG', 'TBRII', 'TBRI', 'TB1_BG', 'TB1_TBRI', 'TB1_TBRII',
'TB1_TBRII_TBRII', 'TB1_BG_TBRII', 'TB1_BG_TBRII_TBRI', 'TB1_TBRII_TBRI',
'TB1_TBRII_TBRII_TBRI', 'TB1_TBRII_TBRI_TBRI', 'TB1_TBRII_TBRII_TBRI_TBRI',
'TB1_TBRI_TBRI')]).T

#Recording the concentrations of individual species at 186400 seconds
TetramerShot = ((y['TB1_TBRII_TBRII_TBRI_TBRI'][186400]))
Shot_BG = ((y['BG'][186400]))
ShotTBRII = ((y['TBRII'][186400]))
ShotTBRI = ((y['TBRI'][186400]))
ShotTB1_BG = ((y['TB1_BG'][186400]))
ShotTB1_TBRI = ((y['TB1_TBRI'][186400]))
ShotTB1_TBRII = ((y['TB1_TBRII'][186400]))
ShotTB1_TBRI_TBRI = ((y['TB1_TBRI_TBRI'][186400]))
ShotTB1_TBRII_TBRII = ((y['TB1_TBRII_TBRII'][186400]))
ShotTB1_BG_TBRII = ((y['TB1_BG_TBRII'][186400]))
ShotTB1_BG_TBRII_TBRI = ((y['TB1_BG_TBRII_TBRI'][186400]))
ShotTB1_TBRII_TBRI = ((y['TB1_TBRII_TBRI'][186400]))
ShotTB1_TBRII_TBRII_TBRI = ((y['TB1_TBRII_TBRII_TBRI'][186400]))
ShotTB1_TBRII_TBRI_TBRI = ((y['TB1_TBRII_TBRI_TBRI'][186400]))
ShotTB1_TBRII_TBRII_TBRI_TBRI = ((y['TB1_TBRII_TBRII_TBRI_TBRI'][186400]))

#End of SRR model for TGF-beta1

```

```
#Single-stage Receptor Recruitment (SRR) model for TGF-beta2
```

```
#Importing functions for model creation  
from __future__ import print_function  
from pysb import *  
_pysb_doctest_suppress_modelexistswarning = True
```

```
#Create model  
Model()
```

```
Monomer('BG')  
Monomer('TBRII')  
Monomer('TBRI')  
Monomer('TB2_BG')  
Monomer('TB2_BG_TBRII')  
Monomer('TB2_BG_TBRII_TBRI')  
Monomer('TB2_TBRI_TBRI')  
Monomer('TB2_TBRII_TBRI')  
Monomer('TB2_TBRII_TBRI_TBRI')  
Monomer('TB2_TBRII_TBRII_TBRI')  
Monomer('TB2_TBRII_TBRII_TBRI_TBRI')  
Monomer('TB2_TBRII')  
Monomer('TB2_TBRI')  
Monomer('TB2_TBRII_TBRII')
```

```
#Listing reactions  
#Reaction rates for this system can be found in Supplemental Table 5
```

```
#Rxn 13a  
Parameter('k13a_on', MF * Z)  
Parameter('k13a_off', MR)  
#BG + TB2 <-> TB2_BG  
Rule('TB2_to_BG', BG() <> TB2_BG(), k13a_on, k13a_off)
```

```
#Rxn 14a  
Parameter('k14a_on', NF*SEF)  
Parameter('k14a_off', NR)  
#TB2_BG + TBRII <-> TB2_BG_TBRII  
Rule('TB2_BG_to_TB2_BG_TBRII', TB2_BG() + TBRII() <> TB2_BG_TBRII(), k14a_on,  
k14a_off)
```

```
#Rxn 16  
Parameter('k16a_on', QF*SEF)  
Parameter('k16a_off', QR)  
#TB2_BG_TBRII + TBRI <-> TB2_BG_TBRII_TBRI
```

Rule('TB2_BG_TBRII_to_TB2_BG_TBRII_TBRI', TB2_BG_TBRII() + TBRI() <>
TB2_BG_TBRII_TBRI(), k16a_on, k16a_off)

#Rxn 17a # inverted reaction

Parameter('k17a_on', SF*SEF)

Parameter('k17a_off', SR)

#TB2_BG_TBRII_TBRI <-> TB2_TBRII_TBRI + BG

Rule('TB2_BG_TBRII_TBRI_to_TB2_TBRII_TBRI', TB2_TBRII_TBRI() + BG() <>
TB2_BG_TBRII_TBRI(), k17a_on, k17a_off)

#Rxn 8a

Parameter('k8a_on', HF*SEF)

Parameter('k8a_off', HR)

#TB2_TBRII_TBRI + TBRII <-> TB2_TBRII_TBRII_TBRI

Rule('TB2_TBRII_TBRI_to_TB2_TBRII_TBRII_TBRI', TB2_TBRII_TBRI() + TBRII() <>
TB2_TBRII_TBRII_TBRI(), k8a_on, k8a_off)

#Rxn 9a

Parameter('k9a_on', IF*SEF)

Parameter('k9a_off', IR)

#TB2_TBRII_TBRI + TBRI <-> TB2_TBRII_TBRI_TBRI

Rule('TB2_TBRII_TBRI_to_TB2_TBRII_TBRI_TBRI', TB2_TBRII_TBRI() + TBRI() <>
TB2_TBRII_TBRI_TBRI(), k9a_on, k9a_off)

#Rxn 11a

Parameter('k11a_on', KF*SEF)

Parameter('k11a_off', KR)

#TB2_TBRII_TBRII_TBRI + TBRI <-> TB2_TBRII_TBRII_TBRI_TBRI

Rule('TB2_TBRII_TBRII_TBRI_to_TB2_TBRII_TBRII_TBRI_TBRI',
TB2_TBRII_TBRII_TBRI() + TBRI() <> TB2_TBRII_TBRII_TBRI_TBRI(), k11a_on,
k11a_off)

#Rxn 12a

Parameter('k12a_on', LF*SEF)

Parameter('k12a_off', LR)

#TB2_TBRII_TBRI_TBRI + TBRII <-> TB2_TBRII_TBRII_TBRI_TBRI

Rule('TB2_TBRII_TBRI_TBRI_to_TB2_TBRII_TBRII_TBRI_TBRI',
TB2_TBRII_TBRI_TBRI() + TBRII() <> TB2_TBRII_TBRII_TBRI_TBRI(), k12a_on,
k12a_off)

#Rxn 1

Parameter('k1a_on', AF*Z)

Parameter('k1a_off', AR)

#TB2 + TBRII <-> TB2_TBRII

Rule('TB2_to_TB2_TBRII', TBRII() <> TB2_TBRII(), k1a_on, k1a_off)

```

#Rxn 4
Parameter('k4a_on', DF*SEF)
Parameter('k4a_off', DR)
#TB2_TBRII + TBRI <-> TB2_TBRII_TBRI
Rule('TB2_TBRII_to_TB2_TBRII_TBRI', TB2_TBRII() + TBRI() <> TB2_TBRII_TBRI(),
k4a_on, k4a_off)

#Rxn 3
Parameter('k3a_on', CF*SEF)
Parameter('k3a_off', CR)
#TB2_TBRII + TBRII <-> TB2_TBRII_TBRII
Rule('TB2_TBRII_to_TB2_TBRII_TBRII', TB2_TBRII() + TBRII() <> TB2_TBRII_TBRII(),
k3a_on, k3a_off)

#Rxn 7
Parameter('k7a_on', GF*SEF)
Parameter('k7a_off', GR)
#TB2_TBRII_TBRII + TBRI <> TB2_TBRII_TBRII_TBRI
Rule('TB2_TBRII_TBRII_to_TB2_TBRII_TBRII', TB2_TBRII_TBRII() + TBRI() <>
TB2_TBRII_TBRII_TBRI(), k7a_on, k7a_off)

#Rxn 2
Parameter('k2a_on', BF*Z)
Parameter('k2a_off', BR)
#TB2 + TBRI <-> TB2_TBRI
Rule('TB2_to_TB2_TBRI', TBRI() <> TB2_TBRI(), k2a_on, k2a_off)

#Rxn 5
Parameter('k5a_on', EF*SEF)
Parameter('k5a_off', ER)
#TB2_TBRI + TBRII <-> TB2_TBRI_TBRI
Rule('TB2_TBRI_to_TB2_TBRII_TBRI', TB2_TBRI() + TBRII() <> TB2_TBRII_TBRI(),
k5a_on, k5a_off)

#Rxn 6
Parameter('k6a_on', FF*SEF)
Parameter('k6a_off', FR)
#TB2_TBRI + TBRI <-> TB2_TBRI_TBRI
Rule('TB2_TBRI_to_TB2_TBRI_TBRI', TB2_TBRI() + TBRI() <> TB2_TBRI_TBRI(),
k6a_on, k6a_off)

#Rxn 10
Parameter('k10a_on', JF*SEF)
Parameter('k10a_off', JR)
#TB2_TBRI_TBRI + TBRII <-> TB2_TBRII_TBRI_TBRI

```

```
Rule('TB2_TBRI_TBRI_to_TB2_TBRII_TBRI_TBRI', TB2_TBRI_TBRI() + TBRII() <>
TB2_TBRII_TBRI_TBRI(), k10a_on, k10a_off)
```

```
#Rxn 15
```

```
Parameter('k15a_on', PF*SEF)
```

```
Parameter('k15a_off', PR)
```

```
#TB2_TBRI + TBRI <-> TB2_TBRI_TBRI
```

```
Rule('TB2_TBRII_to_TB2_BG_TBRII', TB2_TBRII() + BG() <> TB2_BG_TBRII(), k15a_on,
k15a_off)
```

```
#Receptor Recycling and Endocytosis in one step
```

```
#Rxn1001
```

```
Parameter('kendo', kendo)
```

```
#TB2_BG -> BG + TB2
```

```
Rule('TB2_BG_Endo1', TB2_BG() >> BG(), kendo)
```

```
#Rxn1002
```

```
#TB2_BG_TBRII -> BG + TBRII + TB2
```

```
Rule('TB2_BG_TBRII_Endo2', TB2_BG_TBRII() >> BG() + TBRII(), kendo)
```

```
#Rxn1003
```

```
#TB2_TBRII -> TB2 + TBRII
```

```
Rule('TB2_TBRII_Endo3', TB2_TBRII() >> TBRII(), kendo)
```

```
#Rxn1004
```

```
#TB2_TBRI -> TBRI + TB2
```

```
Rule('TB2_TBRI_Endo4', TB2_TBRI() >> TBRI(), kendo)
```

```
#Rxn1005
```

```
#TB2_BG_TBRII_TBRI ->
```

```
Rule('TB2_BG_TBRII_TBRI_Endo5', TB2_BG_TBRII_TBRI() >> BG() + TBRII() + TBRI(),
kendo)
```

```
#Rxn1006
```

```
#TB2_TBRII_TBRI -> TBRII + TBRI + TB2
```

```
Rule('TB2_TBRII_TBRI_Endo6', TB2_TBRII_TBRI() >> TBRII() + TBRI(), kendo)
```

```
#Rxn1007
```

```
#TB2_TBRII_TBRII_TBRI -> TBRII(2) + TBRI + TB2
```

```
Rule('TB2_TBRII_TBRII_TBRI_Endo7', TB2_TBRII_TBRII_TBRI() >> TBRII() + TBRII() + TBRI(), kendo)
```

```
#Rxn1008
```

```
#TB2_TBRII_TBRI_TBRI -> TBRII + TBRI + TBRI + TB2  
Rule('TB2_TBRII_TBRI_TBRI_Endo8', TB2_TBRII_TBRI_TBRI() >> TBRII() + TBRI() + TBRI(), kendo)
```

```
#Rxn1009
```

```
#TB2_TBRII_TBRII_TBRI_TBRI -> TBRII + TBRII + TBRI + TBRI + TB2  
Rule('TB2_TBRII_TBRII_TBRI_TBRI_Endo9', TB2_TBRII_TBRII_TBRI_TBRI() >> TBRII() + TBRII() + TBRI() + TBRI(), kendo)
```

```
#Rxn1010
```

```
#TB2_TBRII_TBRII -> TBRII + TBRII + TB2  
Rule('TB2_TBRII_TBRII_Endo10', TB2_TBRII_TBRII() >> TBRII() + TBRII(), kendo)
```

```
#Rxn1011
```

```
Rule('TB2_TBRI_TBRI_Endo11', TB2_TBRI_TBRI() >> TBRI() + TBRI(), kendo)
```

```
#Defining the parameters that are not rates
```

```
Parameter('BG_0', Z2)  
Parameter('TBRII_0', RII)  
Parameter('TBRI_0', RI)
```

```
#Initial Values
```

```
#These values would vary depending on screen performed
```

```
Initial(BG(), BG_0)  
Initial(TBRII(), TBRII_0)  
Initial(TBRI(), TBRI_0)
```

```
#Observable Amount of Monomer
```

```
Observable('BG', BG());  
Observable('TBRII', TBRII());  
Observable('TBRI', TBRI());  
Observable('TB2_TBRI_TBRI', TB2_TBRI_TBRI());  
Observable('TB2_BG', TB2_BG());  
Observable('TB2_TBRI', TB2_TBRI());  
Observable('TB2_TBRII', TB2_TBRII());  
Observable('TB2_TBRII_TBRII', TB2_TBRII_TBRII());  
Observable('TB2_BG_TBRII', TB2_BG_TBRII());  
Observable('TB2_BG_TBRII_TBRI', TB2_BG_TBRII_TBRI());  
Observable('TB2_TBRII_TBRI', TB2_TBRII_TBRI());
```

```

Observable('TB2_TBRII_TBRII_TBRI', TB2_TBRII_TBRII_TBRI());
Observable('TB2_TBRII_TBRI_TBRI', TB2_TBRII_TBRI_TBRI());
Observable('TB2_TBRII_TBRII_TBRI_TBRI', TB2_TBRII_TBRII_TBRI_TBRI());

#Importing functions for data analysis
from matplotlib.pyplot import *
from numpy import linspace, array
from pysb.simulator import ScipyOdeSimulator

# We will integrate from t=0 to t=86400
t = linspace(0, 186400, 186401)
y = ScipyOdeSimulator(model, rtol=1e-4, atol=[1e-8, 1e-14, 1e-6]).run(tspan=t).all

# Gather the observables of interest into a matrix
yobs = array([y[obs] for obs in ('BG', 'TBRII', 'TBRI', 'TB2_BG', 'TB2_TBRI', 'TB2_TBRII',
'TB2_TBRII_TBRII', 'TB2_BG_TBRII', 'TB2_BG_TBRII_TBRI', 'TB2_TBRII_TBRI',
'TB2_TBRII_TBRII_TBRI', 'TB2_TBRII_TBRI_TBRI', 'TB2_TBRII_TBRII_TBRI_TBRI',
'TB2_TBRI_TBRI')]).T

#Recording the concentrations of individual species at 186400 seconds
TetramerShot = ((y['TB2_TBRII_TBRII_TBRI_TBRI'][186400]))
Shot_BG = ((y['BG'][186400]))
ShotTBRII = ((y['TBRII'][186400]))
ShotTBRI = ((y['TBRI'][186400]))

ShotTB2_BG = ((y['TB2_BG'][186400]))
ShotTB2_TBRI = ((y['TB2_TBRI'][186400]))
ShotTB2_TBRII = ((y['TB2_TBRII'][186400]))
ShotTB2_TBRI_TBRI = ((y['TB2_TBRI_TBRI'][186400]))
ShotTB2_TBRII_TBRII = ((y['TB2_TBRII_TBRII'][186400]))
ShotTB2_BG_TBRII = ((y['TB2_BG_TBRII'][186400]))
ShotTB2_BG_TBRII_TBRI = ((y['TB2_BG_TBRII_TBRI'][186400]))
ShotTB2_TBRII_TBRI = ((y['TB2_TBRII_TBRI'][186400]))
ShotTB2_TBRII_TBRII_TBRI = ((y['TB2_TBRII_TBRII_TBRI'][186400]))
ShotTB2_TBRII_TBRI_TBRI = ((y['TB2_TBRII_TBRI_TBRI'][186400]))
ShotTB2_TBRII_TBRII_TBRI_TBRI = ((y['TB2_TBRII_TBRII_TBRI_TBRI'][186400]))

#End of SRR model for TGF-beta2

```

```
#Single-stage Receptor Recruitment (SRR) model for TGF-beta3
```

```
#Importing functions for model creation
```

```
from __future__ import print_function
```

```
from pysb import *
```

```
_pysb_doctest_suppress_modelexistswarning = True
```

```
#Create model
```

```
Model()
```

```
Monomer('BG')
```

```
Monomer('TBRII')
```

```
Monomer('TBRI')
```

```
Monomer('TB3_BG')
```

```
Monomer('TB3_BG_TBRII')
```

```
Monomer('TB3_BG_TBRII_TBRI')
```

```
Monomer('TB3_TBRI_TBRI')
```

```
Monomer('TB3_TBRII_TBRI')
```

```
Monomer('TB3_TBRII_TBRI_TBRI')
```

```
Monomer('TB3_TBRII_TBRII_TBRI')
```

```
Monomer('TB3_TBRII_TBRII_TBRI_TBRI')
```

```
Monomer('TB3_TBRII')
```

```
Monomer('TB3_TBRI')
```

```
Monomer('TB3_TBRII_TBRII')
```

```
#List reactions
```

```
#Reaction rates for this system can be found in Supplemental Table 6
```

```
#Rxn 13a
```

```
Parameter('k13a_on', MF * Z)
```

```
Parameter('k13a_off', MR)
```

```
#BG + TB3 <-> TB3_BG
```

```
Rule('TB3_to_BG', BG() <> TB3_BG(), k13a_on, k13a_off)
```

```
#Rxn 14a
```

```
Parameter('k14a_on', NF*SEF)
```

```
Parameter('k14a_off', NR)
```

```
#TB3_BG + TBRII <-> TB3_BG_TBRII
```

```
Rule('TB3_BG_to_TB3_BG_TBRII', TB3_BG() + TBRII() <> TB3_BG_TBRII(), k14a_on, k14a_off)
```

```
#Rxn 16
```

```
Parameter('k16a_on', QF*SEF)
```

```
Parameter('k16a_off', QR)
```

```
#TB3_BG_TBRII + TBRI <-> TB3_BG_TBRII_TBRI
```

Rule('TB3_BG_TBRII_to_TB3_BG_TBRII_TBRI', TB3_BG_TBRII() + TBRI() <>
TB3_BG_TBRII_TBRI(), k16a_on, k16a_off)

#Rxn 17a # inverted reaction

Parameter('k17a_on', SF*SEF)

Parameter('k17a_off', SR)

#TB3_BG_TBRII_TBRI <-> TB3_TBRII_TBRI + BG

Rule('TB3_BG_TBRII_TBRI_to_TB3_TBRII_TBRI', TB3_TBRII_TBRI() + BG() <>
TB3_BG_TBRII_TBRI(), k17a_on, k17a_off)

#Rxn 8a

Parameter('k8a_on', HF*SEF)

Parameter('k8a_off', HR)

#TB3_TBRII_TBRI + TBRII <-> TB3_TBRII_TBRII_TBRI

Rule('TB3_TBRII_TBRI_to_TB3_TBRII_TBRII_TBRI', TB3_TBRII_TBRI() + TBRII() <>
TB3_TBRII_TBRII_TBRI(), k8a_on, k8a_off)

#Rxn 9a

Parameter('k9a_on', IF*SEF)

Parameter('k9a_off', IR)

#TB3_TBRII_TBRI + TBRI <-> TB3_TBRII_TBRI_TBRI

Rule('TB3_TBRII_TBRI_to_TB3_TBRII_TBRI_TBRI', TB3_TBRII_TBRI() + TBRI() <>
TB3_TBRII_TBRI_TBRI(), k9a_on, k9a_off)

#Rxn 11a

Parameter('k11a_on', KF*SEF)

Parameter('k11a_off', KR)

#TB3_TBRII_TBRII_TBRI + TBRI <-> TB3_TBRII_TBRII_TBRI_TBRI

Rule('TB3_TBRII_TBRII_TBRI_to_TB3_TBRII_TBRII_TBRI_TBRI',
TB3_TBRII_TBRII_TBRI() + TBRI() <> TB3_TBRII_TBRII_TBRI_TBRI(), k11a_on,
k11a_off)

#Rxn 12a

Parameter('k12a_on', LF*SEF)

Parameter('k12a_off', LR)

#TB3_TBRII_TBRI_TBRI + TBRII <-> TB3_TBRII_TBRII_TBRI_TBRI

Rule('TB3_TBRII_TBRI_TBRI_to_TB3_TBRII_TBRII_TBRI_TBRI',
TB3_TBRII_TBRI_TBRI() + TBRII() <> TB3_TBRII_TBRII_TBRI_TBRI(), k12a_on,
k12a_off)

#Rxn 1

Parameter('k1a_on', AF*Z)

Parameter('k1a_off', AR)

#TB3 + TBRII <-> TB3_TBRII

Rule('TB3_to_TB3_TBRII', TBRII() <> TB3_TBRII(), k1a_on, k1a_off)

```

#Rxn 4
Parameter('k4a_on', DF*SEF)
Parameter('k4a_off', DR)
#TB3_TBRII + TBRI <-> TB3_TBRII_TBRI
Rule('TB3_TBRII_to_TB3_TBRII_TBRI', TB3_TBRII() + TBRI() <> TB3_TBRII_TBRI(),
k4a_on, k4a_off)

#Rxn 3
Parameter('k3a_on', CF*SEF)
Parameter('k3a_off', CR)
#TB3_TBRII + TBRII <-> TB3_TBRII_TBRII
Rule('TB3_TBRII_to_TB3_TBRII_TBRII', TB3_TBRII() + TBRII() <> TB3_TBRII_TBRII(),
k3a_on, k3a_off)

#Rxn 7
Parameter('k7a_on', GF*SEF)
Parameter('k7a_off', GR)
#TB3_TBRII_TBRII + TBRI <> TB3_TBRII_TBRII_TBRI
Rule('TB3_TBRII_TBRII_to_TB3_TBRII_TBRII', TB3_TBRII_TBRII() + TBRI() <>
TB3_TBRII_TBRII_TBRI(), k7a_on, k7a_off)

#Rxn 2
Parameter('k2a_on', BF*Z)
Parameter('k2a_off', BR)
#TB3 + TBRI <-> TB3_TBRI
Rule('TB3_to_TB3_TBRI', TBRI() <> TB3_TBRI(), k2a_on, k2a_off)

#Rxn 5
Parameter('k5a_on', EF*SEF)
Parameter('k5a_off', ER)
#TB3_TBRI + TBRII <-> TB3_TBRI_TBRI
Rule('TB3_TBRI_to_TB3_TBRII_TBRI', TB3_TBRI() + TBRII() <> TB3_TBRII_TBRI(),
k5a_on, k5a_off)

#Rxn 6
Parameter('k6a_on', FF*SEF)
Parameter('k6a_off', FR)
#TB3_TBRI + TBRI <-> TB3_TBRI_TBRI
Rule('TB3_TBRI_to_TB3_TBRI_TBRI', TB3_TBRI() + TBRI() <> TB3_TBRI_TBRI(),
k6a_on, k6a_off)

#Rxn 10
Parameter('k10a_on', JF*SEF)
Parameter('k10a_off', JR)
#TB3_TBRI_TBRI + TBRII <-> TB3_TBRII_TBRI_TBRI

```

```
Rule('TB3_TBRI_TBRI_to_TB3_TBRII_TBRI_TBRI', TB3_TBRI_TBRI() + TBRII() <>
TB3_TBRII_TBRI_TBRI(), k10a_on, k10a_off)
```

```
#Rxn 15
```

```
Parameter('k15a_on', PF*SEF)
```

```
Parameter('k15a_off', PR)
```

```
#TB3_TBRI + TBRI <-> TB3_TBRI_TBRI
```

```
Rule('TB3_TBRII_to_TB3_BG_TBRII', TB3_TBRII() + BG() <> TB3_BG_TBRII(), k15a_on,
k15a_off)
```

```
#Receptor Recycling and Endocytosis in one step
```

```
#Rxn1001
```

```
Parameter('kendo', kendo)
```

```
#TB3_BG -> BG + TB3
```

```
Rule('TB3_BG_Endo1', TB3_BG() >> BG(), kendo)
```

```
#Rxn1002
```

```
#TB3_BG_TBRII -> BG + TBRII + TB3
```

```
Rule('TB3_BG_TBRII_Endo2', TB3_BG_TBRII() >> BG() + TBRII(), kendo)
```

```
#Rxn1003
```

```
#TB3_TBRII -> TB3 + TBRII
```

```
Rule('TB3_TBRII_Endo3', TB3_TBRII() >> TBRII(), kendo)
```

```
#Rxn1004
```

```
#TB3_TBRI -> TBRI + TB3
```

```
Rule('TB3_TBRI_Endo4', TB3_TBRI() >> TBRI(), kendo)
```

```
#Rxn1005
```

```
#TB3_BG_TBRII_TBRI ->
```

```
Rule('TB3_BG_TBRII_TBRI_Endo5', TB3_BG_TBRII_TBRI() >> BG() + TBRII() + TBRI(),
kendo)
```

```
#Rxn1006
```

```
#TB3_TBRII_TBRI -> TBRII + TBRI + TB3
```

```
Rule('TB3_TBRII_TBRI_Endo6', TB3_TBRII_TBRI() >> TBRII() + TBRI(), kendo)
```

```
#Rxn1007
```

```
#TB3_TBRII_TBRII_TBRI -> TBRII(2) + TBRI + TB3
```

```
Rule('TB3_TBRII_TBRII_TBRI_Endo7', TB3_TBRII_TBRII_TBRI() >> TBRII() + TBRII() + TBRI(), kendo)
```

```
#Rxn1008
```

```
#TB3_TBRII_TBRI_TBRI -> TBRII + TBRI + TBRI + TB3  
Rule('TB3_TBRII_TBRI_TBRI_Endo8', TB3_TBRII_TBRI_TBRI() >> TBRII() + TBRI() + TBRI(), kendo)
```

```
#Rxn1009
```

```
#TB3_TBRII_TBRII_TBRI_TBRI -> TBRII + TBRII + TBRI + TBRI + TB3  
Rule('TB3_TBRII_TBRII_TBRI_TBRI_Endo9', TB3_TBRII_TBRII_TBRI_TBRI() >> TBRII() + TBRII() + TBRI() + TBRI(), kendo)
```

```
#Rxn1010
```

```
#TB3_TBRII_TBRII -> TBRII + TBRII + TB3  
Rule('TB3_TBRII_TBRII_Endo10', TB3_TBRII_TBRII() >> TBRII() + TBRII(), kendo)
```

```
#Rxn1011
```

```
Rule('TB3_TBRI_TBRI_Endo11', TB3_TBRI_TBRI() >> TBRI() + TBRI(), kendo)
```

```
#Defining parameter values that are not rates
```

```
Parameter('BG_0', Z2)  
Parameter('TBRII_0', RII)  
Parameter('TBRI_0', RI)
```

```
#Initial Values
```

```
#These values would vary depending on screen performed
```

```
Initial(BG(), BG_0)  
Initial(TBRII(), TBRII_0)  
Initial(TBRI(), TBRI_0)
```

```
#Observable Amount of Monomer
```

```
Observable('BG', BG());  
Observable('TBRII', TBRII());  
Observable('TBRI', TBRI());  
Observable('TB3_TBRI_TBRI', TB3_TBRI_TBRI());  
Observable('TB3_BG', TB3_BG());  
Observable('TB3_TBRI', TB3_TBRI());  
Observable('TB3_TBRII', TB3_TBRII());  
Observable('TB3_TBRII_TBRII', TB3_TBRII_TBRII());  
Observable('TB3_BG_TBRII', TB3_BG_TBRII());  
Observable('TB3_BG_TBRII_TBRI', TB3_BG_TBRII_TBRI());  
Observable('TB3_TBRII_TBRI', TB3_TBRII_TBRI());
```

```

Observable('TB3_TBRII_TBRII_TBRI', TB3_TBRII_TBRII_TBRI());
Observable('TB3_TBRII_TBRI_TBRI', TB3_TBRII_TBRI_TBRI());
Observable('TB3_TBRII_TBRII_TBRI_TBRI', TB3_TBRII_TBRII_TBRI_TBRI());

#importing functions for data analysis
from matplotlib.pyplot import *
from numpy import linspace, array
from pysb.simulator import ScipyOdeSimulator

# We will integrate from t=0 to t=86400
t = linspace(0, 186400, 186401)
y = ScipyOdeSimulator(model, rtol=1e-4, atol=[1e-8, 1e-14, 1e-6]).run(tspan=t).all

# Gather the observables of interest into a matrix
yobs = array([y[obs] for obs in ('BG', 'TBRII', 'TBRI', 'TB3_BG', 'TB3_TBRI', 'TB3_TBRII',
'TB3_TBRII_TBRII', 'TB3_BG_TBRII', 'TB3_BG_TBRII_TBRI', 'TB3_TBRII_TBRI',
'TB3_TBRII_TBRII_TBRI', 'TB3_TBRII_TBRI_TBRI', 'TB3_TBRII_TBRII_TBRI_TBRI',
'TB3_TBRI_TBRI')]).T

#Recording the concentrations of individual species at 186400 seconds
TetramerShot = ((y['TB3_TBRII_TBRII_TBRI_TBRI'][186400]))
Shot_BG = ((y['BG'][186400]))
ShotTBRII = ((y['TBRII'][186400]))
ShotTBRI = ((y['TBRI'][186400]))
ShotTB3_BG = ((y['TB3_BG'][186400]))
ShotTB3_TBRI = ((y['TB3_TBRI'][186400]))
ShotTB3_TBRII = ((y['TB3_TBRII'][186400]))
ShotTB3_TBRI_TBRI = ((y['TB3_TBRI_TBRI'][186400]))
ShotTB3_TBRII_TBRII = ((y['TB3_TBRII_TBRII'][186400]))
ShotTB3_BG_TBRII = ((y['TB3_BG_TBRII'][186400]))
ShotTB3_BG_TBRII_TBRI = ((y['TB3_BG_TBRII_TBRI'][186400]))
ShotTB3_TBRII_TBRI = ((y['TB3_TBRII_TBRI'][186400]))
ShotTB3_TBRII_TBRII_TBRI = ((y['TB3_TBRII_TBRII_TBRI'][186400]))
ShotTB3_TBRII_TBRI_TBRI = ((y['TB3_TBRII_TBRI_TBRI'][186400]))
ShotTB3_TBRII_TBRII_TBRI_TBRI = ((y['TB3_TBRII_TBRII_TBRI_TBRI'][186400]))

#End of SRR model for TGF-beta3

```

```

#Two-stage Receptor Recruitment (TRR) model for TGF-beta1

#Importing functions for model creation
from __future__ import print_function
from pysb import *
_pysb_doctest_suppress_modelexistswarning = True

#Create model
Model()

Monomer('BG')
Monomer('TBRII')
Monomer('TBRI')
Monomer('TB1_BG')
Monomer('TB1_BG_TBRII')
Monomer('TB1_BG_TBRII_TBRI')
Monomer('TB1_TBRI_TBRI')
Monomer('TB1_TBRII_TBRI')
Monomer('TB1_TBRII_TBRI_TBRI')
Monomer('TB1_TBRII_TBRII_TBRI')
Monomer('TB1_TBRII_TBRII_TBRI_TBRI')
Monomer('TB1_TBRII')
Monomer('TB1_TBRI')
Monomer('TB1_TBRII_TBRII')

#List reactions
#Reaction rates for this system can be found in Supplemental Table 7

#Rxn 13a
Parameter('k13a_on', MF * Z)
Parameter('k13a_off', MR)
#BG + TB1 <-> TB1_BG
Rule('TB1_to_BG', BG() <> TB1_BG(), k13a_on, k13a_off)

#Rxn 14a
Parameter('k14a_on', NF*SEF)
Parameter('k14a_off', NR)
#TB1_BG + TBRII <-> TB1_BG_TBRII
Rule('TB1_BG_to_TB1_BG_TBRII', TB1_BG() + TBRII() <> TB1_BG_TBRII(), k14a_on,
k14a_off)

#Rxn 16
Parameter('k16a_on', QF*SEF)
Parameter('k16a_off', QR)
#TB1_BG_TBRII + TBRI <-> TB1_BG_TBRII_TBRI

```

Rule('TB1_BG_TBRII_to_TB1_BG_TBRII_TBRI', TB1_BG_TBRII() + TBRI() <>
TB1_BG_TBRII_TBRI(), k16a_on, k16a_off)

#Rxn 17a # inverted reaction

Parameter('k17a_on', SF*SEF)

Parameter('k17a_off', SR)

#TB1_BG_TBRII_TBRI <-> TB1_TBRII_TBRI + BG

Rule('TB1_BG_TBRII_TBRI_to_TB1_TBRII_TBRI', TB1_TBRII_TBRI() + BG() <>
TB1_BG_TBRII_TBRI(), k17a_on, k17a_off)

#Rxn 8a

Parameter('k8a_on', HF*SEF)

Parameter('k8a_off', HR)

#TB1_TBRII_TBRI + TBRII <-> TB1_TBRII_TBRII_TBRI

Rule('TB1_TBRII_TBRI_to_TB1_TBRII_TBRII_TBRI', TB1_TBRII_TBRI() + TBRII() <>
TB1_TBRII_TBRII_TBRI(), k8a_on, k8a_off)

#Rxn 9a

Parameter('k9a_on', IF*SEF)

Parameter('k9a_off', IR)

#TB1_TBRII_TBRI + TBRI <-> TB1_TBRII_TBRI_TBRI

Rule('TB1_TBRII_TBRI_to_TB1_TBRII_TBRI_TBRI', TB1_TBRII_TBRI() + TBRI() <>
TB1_TBRII_TBRI_TBRI(), k9a_on, k9a_off)

#Rxn 11a

Parameter('k11a_on', KF*SEF)

Parameter('k11a_off', KR)

#TB1_TBRII_TBRII_TBRI + TBRI <-> TB1_TBRII_TBRII_TBRI_TBRI

Rule('TB1_TBRII_TBRII_TBRI_to_TB1_TBRII_TBRII_TBRI_TBRI',
TB1_TBRII_TBRII_TBRI() + TBRI() <> TB1_TBRII_TBRII_TBRI_TBRI(), k11a_on,
k11a_off)

#Rxn 12a

Parameter('k12a_on', LF*SEF)

Parameter('k12a_off', LR)

#TB1_TBRII_TBRI_TBRI + TBRII <-> TB1_TBRII_TBRII_TBRI_TBRI

Rule('TB1_TBRII_TBRI_TBRI_to_TB1_TBRII_TBRII_TBRI_TBRI',
TB1_TBRII_TBRI_TBRI() + TBRII() <> TB1_TBRII_TBRII_TBRI_TBRI(), k12a_on,
k12a_off)

#Rxn 1

Parameter('k1a_on', AF*Z)

Parameter('k1a_off', AR)

#TB1 + TBRII <-> TB1_TBRII

Rule('TB1_to_TB1_TBRII', TBRII() <> TB1_TBRII(), k1a_on, k1a_off)

#Rxn 4

Parameter('k4a_on', DF*SEF)

Parameter('k4a_off', DR)

#TB1_TBRII + TBRI <-> TB1_TBRII_TBRI

Rule('TB1_TBRII_to_TB1_TBRII_TBRI', TB1_TBRII() + TBRI() <> TB1_TBRII_TBRI(),
k4a_on, k4a_off)

#Rxn 3

Parameter('k3a_on', CF*SEF)

Parameter('k3a_off', CR)

#TB1_TBRII + TBRII <-> TB1_TBRII_TBRII

Rule('TB1_TBRII_to_TB1_TBRII_TBRII', TB1_TBRII() + TBRII() <> TB1_TBRII_TBRII(),
k3a_on, k3a_off)

#Rxn 7

Parameter('k7a_on', GF*SEF)

Parameter('k7a_off', GR)

#TB1_TBRII_TBRII + TBRI <> TB1_TBRII_TBRII_TBRI

Rule('TB1_TBRII_TBRII_to_TB1_TBRII_TBRII', TB1_TBRII_TBRII() + TBRI() <>
TB1_TBRII_TBRII_TBRI(), k7a_on, k7a_off)

#Rxn 2

Parameter('k2a_on', BF*Z)

Parameter('k2a_off', BR)

#TB1 + TBRI <-> TB1_TBRI

Rule('TB1_to_TB1_TBRI', TBRI() <> TB1_TBRI(), k2a_on, k2a_off)

#Rxn 5

Parameter('k5a_on', EF*SEF)

Parameter('k5a_off', ER)

#TB1_TBRI + TBRII <-> TB1_TBRI_TBRI

Rule('TB1_TBRI_to_TB1_TBRII_TBRI', TB1_TBRI() + TBRII() <> TB1_TBRII_TBRI(),
k5a_on, k5a_off)

#Rxn 6

Parameter('k6a_on', FF*SEF)

Parameter('k6a_off', FR)

#TB1_TBRI + TBRI <-> TB1_TBRI_TBRI

Rule('TB1_TBRI_to_TB1_TBRI_TBRI', TB1_TBRI() + TBRI() <> TB1_TBRI_TBRI(),
k6a_on, k6a_off)

#Rxn 10

Parameter('k10a_on', JF*SEF)

Parameter('k10a_off', JR)

#TB1_TBRI_TBRI + TBRII <-> TB1_TBRII_TBRI_TBRI

```
Rule('TB1_TBRI_TBRI_to_TB1_TBRII_TBRI_TBRI', TB1_TBRI_TBRI() + TBRII() <>
TB1_TBRII_TBRI_TBRI(), k10a_on, k10a_off)
```

```
#Rxn 15
```

```
Parameter('k15a_on', PF*SEF)
```

```
Parameter('k15a_off', PR)
```

```
#TB1_TBRI + TBRI <-> TB1_TBRI_TBRI
```

```
Rule('TB1_TBRII_to_TB1_BG_TBRII', TB1_TBRII() + BG() <> TB1_BG_TBRII(), k15a_on,
k15a_off)
```

```
#Receptor Recycling and Endocytosis in one step
```

```
#Rxn1001
```

```
Parameter('kendo', kendo)
```

```
#TB1_BG -> BG + TB1
```

```
Rule('TB1_BG_Endo1', TB1_BG() >> BG(), kendo)
```

```
#Rxn1002
```

```
#TB1_BG_TBRII -> BG + TBRII + TB1
```

```
Rule('TB1_BG_TBRII_Endo2', TB1_BG_TBRII() >> BG() + TBRII(), kendo)
```

```
#Rxn1003
```

```
#TB1_TBRII -> TB1 + TBRII
```

```
Rule('TB1_TBRII_Endo3', TB1_TBRII() >> TBRII(), kendo)
```

```
#Rxn1004
```

```
#TB1_TBRI -> TBRI + TB1
```

```
Rule('TB1_TBRI_Endo4', TB1_TBRI() >> TBRI(), kendo)
```

```
#Rxn1005
```

```
#TB1_BG_TBRII_TBRI ->
```

```
Rule('TB1_BG_TBRII_TBRI_Endo5', TB1_BG_TBRII_TBRI() >> BG() + TBRII() + TBRI(),
kendo)
```

```
#Rxn1006
```

```
#TB1_TBRII_TBRI -> TBRII + TBRI + TB1
```

```
Rule('TB1_TBRII_TBRI_Endo6', TB1_TBRII_TBRI() >> TBRII() + TBRI(), kendo)
```

```
#Rxn1007
```

```
#TB1_TBRII_TBRII_TBRI -> TBRII(2) + TBRI + TB1
```

```
Rule('TB1_TBRII_TBRII_TBRI_Endo7', TB1_TBRII_TBRII_TBRI() >> TBRII() + TBRII() + TBRI(), kendo)
```

```
#Rxn1008
```

```
#TB1_TBRII_TBRI_TBRI -> TBRII + TBRI + TBRI + TB1  
Rule('TB1_TBRII_TBRI_TBRI_Endo8', TB1_TBRII_TBRI_TBRI() >> TBRII() + TBRI() + TBRI(), kendo)
```

```
#Rxn1009
```

```
#TB1_TBRII_TBRII_TBRI_TBRI -> TBRII + TBRII + TBRI + TBRI + TB1  
Rule('TB1_TBRII_TBRII_TBRI_TBRI_Endo9', TB1_TBRII_TBRII_TBRI_TBRI() >> TBRII() + TBRII() + TBRI() + TBRI(), kendo)
```

```
#Rxn1010
```

```
#TB1_TBRII_TBRII -> TBRII + TBRII + TB1  
Rule('TB1_TBRII_TBRII_Endo10', TB1_TBRII_TBRII() >> TBRII() + TBRII(), kendo)
```

```
#Rxn1011
```

```
Rule('TB1_TBRI_TBRI_Endo11', TB1_TBRI_TBRI() >> TBRI() + TBRI(), kendo)
```

```
#Defining parameters that are not rates
```

```
Parameter('BG_0', Z2)  
Parameter('TBRII_0', RII)  
Parameter('TBRI_0', RI)
```

```
#Initial Values
```

```
#These values would vary depending on screen performed
```

```
Initial(BG(), BG_0)  
Initial(TBRII(), TBRII_0)  
Initial(TBRI(), TBRI_0)
```

```
#Observable Amount of Monomer
```

```
Observable('BG', BG());  
Observable('TBRII', TBRII());  
Observable('TBRI', TBRI());  
Observable('TB1_TBRI_TBRI', TB1_TBRI_TBRI());  
Observable('TB1_BG', TB1_BG());  
Observable('TB1_TBRI', TB1_TBRI());  
Observable('TB1_TBRII', TB1_TBRII());  
Observable('TB1_TBRII_TBRII', TB1_TBRII_TBRII());  
Observable('TB1_BG_TBRII', TB1_BG_TBRII());  
Observable('TB1_BG_TBRII_TBRI', TB1_BG_TBRII_TBRI());  
Observable('TB1_TBRII_TBRI', TB1_TBRII_TBRI());
```

```

Observable('TB1_TBRII_TBRII_TBRI', TB1_TBRII_TBRII_TBRI());
Observable('TB1_TBRII_TBRI_TBRI', TB1_TBRII_TBRI_TBRI());
Observable('TB1_TBRII_TBRII_TBRI_TBRI', TB1_TBRII_TBRII_TBRI_TBRI());

#Importing functions for data analysis
from matplotlib.pyplot import *
from numpy import linspace, array
from pysb.simulator import ScipyOdeSimulator

# We will integrate from t=0 to t=86400
t = linspace(0, 186400, 186401)
y = ScipyOdeSimulator(model, rtol=1e-4, atol=[1e-8, 1e-14, 1e-6]).run(tspan=t).all

# Gather the observables of interest into a matrix
yobs = array([y[obs] for obs in ('BG', 'TBRII', 'TBRI', 'TB1_BG', 'TB1_TBRI', 'TB1_TBRII',
'TB1_TBRII_TBRII', 'TB1_BG_TBRII', 'TB1_BG_TBRII_TBRI', 'TB1_TBRII_TBRI',
'TB1_TBRII_TBRII_TBRI', 'TB1_TBRII_TBRI_TBRI', 'TB1_TBRII_TBRII_TBRI_TBRI',
'TB1_TBRI_TBRI')]).T

#Recording the concentrations of individual species at 186400 seconds
TetramerShot = ((y['TB1_TBRII_TBRII_TBRI_TBRI'][186400]))
Shot_BG = ((y['BG'][186400]))
ShotTBRII = ((y['TBRII'][186400]))
ShotTBRI = ((y['TBRI'][186400]))
ShotTB1_BG = ((y['TB1_BG'][186400]))
ShotTB1_TBRI = ((y['TB1_TBRI'][186400]))
ShotTB1_TBRII = ((y['TB1_TBRII'][186400]))
ShotTB1_TBRI_TBRI = ((y['TB1_TBRI_TBRI'][186400]))
ShotTB1_TBRII_TBRII = ((y['TB1_TBRII_TBRII'][186400]))
ShotTB1_BG_TBRII = ((y['TB1_BG_TBRII'][186400]))
ShotTB1_BG_TBRII_TBRI = ((y['TB1_BG_TBRII_TBRI'][186400]))
ShotTB1_TBRII_TBRI = ((y['TB1_TBRII_TBRI'][186400]))
ShotTB1_TBRII_TBRII_TBRI = ((y['TB1_TBRII_TBRII_TBRI'][186400]))
ShotTB1_TBRII_TBRI_TBRI = ((y['TB1_TBRII_TBRI_TBRI'][186400]))
ShotTB1_TBRII_TBRII_TBRI_TBRI = ((y['TB1_TBRII_TBRII_TBRI_TBRI'][186400]))

#End of TRR model for TGF-beta1

```

```

#Two-stage Receptor Recruitment (TRR) model for TGF-beta2

#Importing functions for model creation
from __future__ import print_function
from pysb import *
_pysb_doctest_suppress_modelexistswarning = True

#Create model
Model()

Monomer('BG')
Monomer('TBRII')
Monomer('TBRI')
Monomer('TB2_BG')
Monomer('TB2_BG_TBRII')
Monomer('TB2_BG_TBRII_TBRI')
Monomer('TB2_TBRI_TBRI')
Monomer('TB2_TBRII_TBRI')
Monomer('TB2_TBRII_TBRI_TBRI')
Monomer('TB2_TBRII_TBRII_TBRI')
Monomer('TB2_TBRII_TBRII_TBRI_TBRI')
Monomer('TB2_TBRII')
Monomer('TB2_TBRI')
Monomer('TB2_TBRII_TBRII')

#List reactions
#Reaction rates for this system can be found in Supplemental Table 8

#Rxn 13a
Parameter('k13a_on', MF * Z)
Parameter('k13a_off', MR)
#BG + TB2 <-> TB2_BG
Rule('TB2_to_BG', BG() <> TB2_BG(), k13a_on, k13a_off)

#Rxn 14a
Parameter('k14a_on', NF*SEF)
Parameter('k14a_off', NR)
#TB2_BG + TBRII <-> TB2_BG_TBRII
Rule('TB2_BG_to_TB2_BG_TBRII', TB2_BG() + TBRII() <> TB2_BG_TBRII(), k14a_on,
k14a_off)

#Rxn 16
Parameter('k16a_on', QF*SEF)
Parameter('k16a_off', QR)
#TB2_BG_TBRII + TBRI <-> TB2_BG_TBRII_TBRI

```

Rule('TB2_BG_TBRII_to_TB2_BG_TBRII_TBRI', TB2_BG_TBRII() + TBRI() <>
TB2_BG_TBRII_TBRI(), k16a_on, k16a_off)

#Rxn 17a # inverted reaction

Parameter('k17a_on', SF*SEF)

Parameter('k17a_off', SR)

#TB2_BG_TBRII_TBRI <-> TB2_TBRII_TBRI + BG

Rule('TB2_BG_TBRII_TBRI_to_TB2_TBRII_TBRI', TB2_TBRII_TBRI() + BG() <>
TB2_BG_TBRII_TBRI(), k17a_on, k17a_off)

#Rxn 8a

Parameter('k8a_on', HF*SEF)

Parameter('k8a_off', HR)

#TB2_TBRII_TBRI + TBRII <-> TB2_TBRII_TBRII_TBRI

Rule('TB2_TBRII_TBRI_to_TB2_TBRII_TBRII_TBRI', TB2_TBRII_TBRI() + TBRII() <>
TB2_TBRII_TBRII_TBRI(), k8a_on, k8a_off)

#Rxn 9a

Parameter('k9a_on', IF*SEF)

Parameter('k9a_off', IR)

#TB2_TBRII_TBRI + TBRI <-> TB2_TBRII_TBRI_TBRI

Rule('TB2_TBRII_TBRI_to_TB2_TBRII_TBRI_TBRI', TB2_TBRII_TBRI() + TBRI() <>
TB2_TBRII_TBRI_TBRI(), k9a_on, k9a_off)

#Rxn 11a

Parameter('k11a_on', KF*SEF)

Parameter('k11a_off', KR)

#TB2_TBRII_TBRII_TBRI + TBRI <-> TB2_TBRII_TBRII_TBRI_TBRI

Rule('TB2_TBRII_TBRII_TBRI_to_TB2_TBRII_TBRII_TBRI_TBRI',
TB2_TBRII_TBRII_TBRI() + TBRI() <> TB2_TBRII_TBRII_TBRI_TBRI(), k11a_on,
k11a_off)

#Rxn 12a

Parameter('k12a_on', LF*SEF)

Parameter('k12a_off', LR)

#TB2_TBRII_TBRI_TBRI + TBRII <-> TB2_TBRII_TBRII_TBRI_TBRI

Rule('TB2_TBRII_TBRI_TBRI_to_TB2_TBRII_TBRII_TBRI_TBRI',
TB2_TBRII_TBRI_TBRI() + TBRII() <> TB2_TBRII_TBRII_TBRI_TBRI(), k12a_on,
k12a_off)

#Rxn 1

Parameter('k1a_on', AF*Z)

Parameter('k1a_off', AR)

#TB2 + TBRII <-> TB2_TBRII

Rule('TB2_to_TB2_TBRII', TBRII() <> TB2_TBRII(), k1a_on, k1a_off)

```

#Rxn 4
Parameter('k4a_on', DF*SEF)
Parameter('k4a_off', DR)
#TB2_TBRII + TBRI <-> TB2_TBRII_TBRI
Rule('TB2_TBRII_to_TB2_TBRII_TBRI', TB2_TBRII() + TBRI() <> TB2_TBRII_TBRI(),
k4a_on, k4a_off)

#Rxn 3
Parameter('k3a_on', CF*SEF)
Parameter('k3a_off', CR)
#TB2_TBRII + TBRII <-> TB2_TBRII_TBRII
Rule('TB2_TBRII_to_TB2_TBRII_TBRII', TB2_TBRII() + TBRII() <> TB2_TBRII_TBRII(),
k3a_on, k3a_off)

#Rxn 7
Parameter('k7a_on', GF*SEF)
Parameter('k7a_off', GR)
#TB2_TBRII_TBRII + TBRI <> TB2_TBRII_TBRII_TBRI
Rule('TB2_TBRII_TBRII_to_TB2_TBRII_TBRII', TB2_TBRII_TBRII() + TBRI() <>
TB2_TBRII_TBRII_TBRI(), k7a_on, k7a_off)

#Rxn 2
Parameter('k2a_on', BF*Z)
Parameter('k2a_off', BR)
#TB2 + TBRI <-> TB2_TBRI
Rule('TB2_to_TB2_TBRI', TBRI() <> TB2_TBRI(), k2a_on, k2a_off)

#Rxn 5
Parameter('k5a_on', EF*SEF)
Parameter('k5a_off', ER)
#TB2_TBRI + TBRII <-> TB2_TBRI_TBRI
Rule('TB2_TBRI_to_TB2_TBRII_TBRI', TB2_TBRI() + TBRII() <> TB2_TBRII_TBRI(),
k5a_on, k5a_off)

#Rxn 6
Parameter('k6a_on', FF*SEF)
Parameter('k6a_off', FR)
#TB2_TBRI + TBRI <-> TB2_TBRI_TBRI
Rule('TB2_TBRI_to_TB2_TBRI_TBRI', TB2_TBRI() + TBRI() <> TB2_TBRI_TBRI(),
k6a_on, k6a_off)

#Rxn 10
Parameter('k10a_on', JF*SEF)
Parameter('k10a_off', JR)
#TB2_TBRI_TBRI + TBRII <-> TB2_TBRII_TBRI_TBRI

```

```
Rule('TB2_TBRI_TBRI_to_TB2_TBRII_TBRI_TBRI', TB2_TBRI_TBRI() + TBRII() <>
TB2_TBRII_TBRI_TBRI(), k10a_on, k10a_off)
```

```
#Rxn 15
```

```
Parameter('k15a_on', PF*SEF)
```

```
Parameter('k15a_off', PR)
```

```
#TB2_TBRI + TBRI <-> TB2_TBRI_TBRI
```

```
Rule('TB2_TBRII_to_TB2_BG_TBRII', TB2_TBRII() + BG() <> TB2_BG_TBRII(), k15a_on,
k15a_off)
```

```
#Receptor Recycling and Endocytosis in one step
```

```
#Rxn1001
```

```
Parameter('kendo', kendo)
```

```
#TB2_BG -> BG + TB2
```

```
Rule('TB2_BG_Endo1', TB2_BG() >> BG(), kendo)
```

```
#Rxn1002
```

```
#TB2_BG_TBRII -> BG + TBRII + TB2
```

```
Rule('TB2_BG_TBRII_Endo2', TB2_BG_TBRII() >> BG() + TBRII(), kendo)
```

```
#Rxn1003
```

```
#TB2_TBRII -> TB2 + TBRII
```

```
Rule('TB2_TBRII_Endo3', TB2_TBRII() >> TBRII(), kendo)
```

```
#Rxn1004
```

```
#TB2_TBRI -> TBRI + TB2
```

```
Rule('TB2_TBRI_Endo4', TB2_TBRI() >> TBRI(), kendo)
```

```
#Rxn1005
```

```
#TB2_BG_TBRII_TBRI ->
```

```
Rule('TB2_BG_TBRII_TBRI_Endo5', TB2_BG_TBRII_TBRI() >> BG() + TBRII() + TBRI(),
kendo)
```

```
#Rxn1006
```

```
#TB2_TBRII_TBRI -> TBRII + TBRI + TB2
```

```
Rule('TB2_TBRII_TBRI_Endo6', TB2_TBRII_TBRI() >> TBRII() + TBRI(), kendo)
```

```
#Rxn1007
```

```
#TB2_TBRII_TBRII_TBRI -> TBRII(2) + TBRI + TB2
```

```
Rule('TB2_TBRII_TBRII_TBRI_Endo7', TB2_TBRII_TBRII_TBRI() >> TBRII() + TBRII() + TBRI(), kendo)
```

```
#Rxn1008
```

```
#TB2_TBRII_TBRI_TBRI -> TBRII + TBRI + TBRI + TB2  
Rule('TB2_TBRII_TBRI_TBRI_Endo8', TB2_TBRII_TBRI_TBRI() >> TBRII() + TBRI() + TBRI(), kendo)
```

```
#Rxn1009
```

```
#TB2_TBRII_TBRII_TBRI_TBRI -> TBRII + TBRII + TBRI + TBRI + TB2  
Rule('TB2_TBRII_TBRII_TBRI_TBRI_Endo9', TB2_TBRII_TBRII_TBRI_TBRI() >> TBRII() + TBRII() + TBRI() + TBRI(), kendo)
```

```
#Rxn1010
```

```
#TB2_TBRII_TBRII -> TBRII + TBRII + TB2  
Rule('TB2_TBRII_TBRII_Endo10', TB2_TBRII_TBRII() >> TBRII() + TBRII(), kendo)
```

```
#Rxn1011
```

```
Rule('TB2_TBRI_TBRI_Endo11', TB2_TBRI_TBRI() >> TBRI() + TBRI(), kendo)
```

```
#Defining parameters that are not rates
```

```
Parameter('BG_0', Z2)  
Parameter('TBRII_0', RII)  
Parameter('TBRI_0', RI)
```

```
#Initial Values
```

```
#These values would vary depending on screen performed
```

```
Initial(BG(), BG_0)  
Initial(TBRII(), TBRII_0)  
Initial(TBRI(), TBRI_0)
```

```
#Observable Amount of Monomer
```

```
Observable('BG', BG());  
Observable('TBRII', TBRII());  
Observable('TBRI', TBRI());  
Observable('TB2_TBRI_TBRI', TB2_TBRI_TBRI());  
Observable('TB2_BG', TB2_BG());  
Observable('TB2_TBRI', TB2_TBRI());  
Observable('TB2_TBRII', TB2_TBRII());  
Observable('TB2_TBRII_TBRII', TB2_TBRII_TBRII());  
Observable('TB2_BG_TBRII', TB2_BG_TBRII());  
Observable('TB2_BG_TBRII_TBRI', TB2_BG_TBRII_TBRI());  
Observable('TB2_TBRII_TBRI', TB2_TBRII_TBRI());
```

```

Observable('TB2_TBRII_TBRII_TBRI', TB2_TBRII_TBRII_TBRI());
Observable('TB2_TBRII_TBRI_TBRI', TB2_TBRII_TBRI_TBRI());
Observable('TB2_TBRII_TBRII_TBRI_TBRI', TB2_TBRII_TBRII_TBRI_TBRI());

#Importing functions for data analysis
from matplotlib.pyplot import *
from numpy import linspace, array
from pysb.simulator import ScipyOdeSimulator

# We will integrate from t=0 to t=86400
t = linspace(0, 186400, 186401)
y = ScipyOdeSimulator(model, rtol=1e-4, atol=[1e-8, 1e-14, 1e-6]).run(tspan=t).all

# Gather the observables of interest into a matrix
yobs = array([y[obs] for obs in ('BG', 'TBRII', 'TBRI', 'TB2_BG', 'TB2_TBRI', 'TB2_TBRII',
'TB2_TBRII_TBRII', 'TB2_BG_TBRII', 'TB2_BG_TBRII_TBRI', 'TB2_TBRII_TBRI',
'TB2_TBRII_TBRII_TBRI', 'TB2_TBRII_TBRI_TBRI', 'TB2_TBRII_TBRII_TBRI_TBRI',
'TB2_TBRI_TBRI')]).T

#Recording the concentrations of individual species at 186400 seconds
TetramerShot = ((y['TB2_TBRII_TBRII_TBRI_TBRI'][186400]))
Shot_BG = ((y['BG'][186400]))
ShotTBRII = ((y['TBRII'][186400]))
ShotTBRI = ((y['TBRI'][186400]))
ShotTB2_BG = ((y['TB2_BG'][186400]))
ShotTB2_TBRI = ((y['TB2_TBRI'][186400]))
ShotTB2_TBRII = ((y['TB2_TBRII'][186400]))
ShotTB2_TBRI_TBRI = ((y['TB2_TBRI_TBRI'][186400]))
ShotTB2_TBRII_TBRII = ((y['TB2_TBRII_TBRII'][186400]))
ShotTB2_BG_TBRII = ((y['TB2_BG_TBRII'][186400]))
ShotTB2_BG_TBRII_TBRI = ((y['TB2_BG_TBRII_TBRI'][186400]))
ShotTB2_TBRII_TBRI = ((y['TB2_TBRII_TBRI'][186400]))
ShotTB2_TBRII_TBRII_TBRI = ((y['TB2_TBRII_TBRII_TBRI'][186400]))
ShotTB2_TBRII_TBRI_TBRI = ((y['TB2_TBRII_TBRI_TBRI'][186400]))
ShotTB2_TBRII_TBRII_TBRI_TBRI = ((y['TB2_TBRII_TBRII_TBRI_TBRI'][186400]))

#End of TRR model for TGF-beta2

```

```

#Two-stage Receptor Recruitment (TRR) model for TGF-beta3

#Importing functions for model creation
from __future__ import print_function
from pysb import *
_pysb_doctest_suppress_modelexistswarning = True

#Create model
Model()

Monomer('BG')
Monomer('TBRII')
Monomer('TBRI')
Monomer('TB3_BG')
Monomer('TB3_BG_TBRII')
Monomer('TB3_BG_TBRII_TBRI')
Monomer('TB3_TBRI_TBRI')
Monomer('TB3_TBRII_TBRI')
Monomer('TB3_TBRII_TBRI_TBRI')
Monomer('TB3_TBRII_TBRII_TBRI')
Monomer('TB3_TBRII_TBRII_TBRI_TBRI')
Monomer('TB3_TBRII')
Monomer('TB3_TBRI')
Monomer('TB3_TBRII_TBRII')

#List reactions
#Reaction rates for this system can be found in Supplemental Table 9

#Rxn 13a
Parameter('k13a_on', MF * Z)
Parameter('k13a_off', MR)
#BG + TB3 <-> TB3_BG
Rule('TB3_to_BG', BG() <> TB3_BG(), k13a_on, k13a_off)

#Rxn 14a
Parameter('k14a_on', NF*SEF)
Parameter('k14a_off', NR)
#TB3_BG + TBRII <-> TB3_BG_TBRII
Rule('TB3_BG_to_TB3_BG_TBRII', TB3_BG() + TBRII() <> TB3_BG_TBRII(), k14a_on,
k14a_off)

#Rxn 16
Parameter('k16a_on', QF*SEF)
Parameter('k16a_off', QR)
#TB3_BG_TBRII + TBRI <-> TB3_BG_TBRII_TBRI

```

Rule('TB3_BG_TBRII_to_TB3_BG_TBRII_TBRI', TB3_BG_TBRII() + TBRI() <>
TB3_BG_TBRII_TBRI(), k16a_on, k16a_off)

#Rxn 17a # inverted reaction

Parameter('k17a_on', SF*SEF)

Parameter('k17a_off', SR)

#TB3_BG_TBRII_TBRI <-> TB3_TBRII_TBRI + BG

Rule('TB3_BG_TBRII_TBRI_to_TB3_TBRII_TBRI', TB3_TBRII_TBRI() + BG() <>
TB3_BG_TBRII_TBRI(), k17a_on, k17a_off)

#Rxn 8a

Parameter('k8a_on', HF*SEF)

Parameter('k8a_off', HR)

#TB3_TBRII_TBRI + TBRII <-> TB3_TBRII_TBRII_TBRI

Rule('TB3_TBRII_TBRI_to_TB3_TBRII_TBRII_TBRI', TB3_TBRII_TBRI() + TBRII() <>
TB3_TBRII_TBRII_TBRI(), k8a_on, k8a_off)

#Rxn 9a

Parameter('k9a_on', IF*SEF)

Parameter('k9a_off', IR)

#TB3_TBRII_TBRI + TBRI <-> TB3_TBRII_TBRI_TBRI

Rule('TB3_TBRII_TBRI_to_TB3_TBRII_TBRI_TBRI', TB3_TBRII_TBRI() + TBRI() <>
TB3_TBRII_TBRI_TBRI(), k9a_on, k9a_off)

#Rxn 11a

Parameter('k11a_on', KF*SEF)

Parameter('k11a_off', KR)

#TB3_TBRII_TBRII_TBRI + TBRI <-> TB3_TBRII_TBRII_TBRI_TBRI

Rule('TB3_TBRII_TBRII_TBRI_to_TB3_TBRII_TBRII_TBRI_TBRI',
TB3_TBRII_TBRII_TBRI() + TBRI() <> TB3_TBRII_TBRII_TBRI_TBRI(), k11a_on,
k11a_off)

#Rxn 12a

Parameter('k12a_on', LF*SEF)

Parameter('k12a_off', LR)

#TB3_TBRII_TBRI_TBRI + TBRII <-> TB3_TBRII_TBRII_TBRI_TBRI

Rule('TB3_TBRII_TBRI_TBRI_to_TB3_TBRII_TBRII_TBRI_TBRI',
TB3_TBRII_TBRI_TBRI() + TBRII() <> TB3_TBRII_TBRII_TBRI_TBRI(), k12a_on,
k12a_off)

#Rxn 1

Parameter('k1a_on', AF*Z)

Parameter('k1a_off', AR)

#TB3 + TBRII <-> TB3_TBRII

Rule('TB3_to_TB3_TBRII', TBRII() <> TB3_TBRII(), k1a_on, k1a_off)

```

#Rxn 4
Parameter('k4a_on', DF*SEF)
Parameter('k4a_off', DR)
#TB3_TBRII + TBRI <-> TB3_TBRII_TBRI
Rule('TB3_TBRII_to_TB3_TBRII_TBRI', TB3_TBRII() + TBRI() <> TB3_TBRII_TBRI(),
k4a_on, k4a_off)

#Rxn 3
Parameter('k3a_on', CF*SEF)
Parameter('k3a_off', CR)
#TB3_TBRII + TBRII <-> TB3_TBRII_TBRII
Rule('TB3_TBRII_to_TB3_TBRII_TBRII', TB3_TBRII() + TBRII() <> TB3_TBRII_TBRII(),
k3a_on, k3a_off)

#Rxn 7
Parameter('k7a_on', GF*SEF)
Parameter('k7a_off', GR)
#TB3_TBRII_TBRII + TBRI <> TB3_TBRII_TBRII_TBRI
Rule('TB3_TBRII_TBRII_to_TB3_TBRII_TBRII', TB3_TBRII_TBRII() + TBRI() <>
TB3_TBRII_TBRII_TBRI(), k7a_on, k7a_off)

#Rxn 2
Parameter('k2a_on', BF*Z)
Parameter('k2a_off', BR)
#TB3 + TBRI <-> TB3_TBRI
Rule('TB3_to_TB3_TBRI', TBRI() <> TB3_TBRI(), k2a_on, k2a_off)

#Rxn 5
Parameter('k5a_on', EF*SEF)
Parameter('k5a_off', ER)
#TB3_TBRI + TBRII <-> TB3_TBRI_TBRI
Rule('TB3_TBRI_to_TB3_TBRII_TBRI', TB3_TBRI() + TBRII() <> TB3_TBRII_TBRI(),
k5a_on, k5a_off)

#Rxn 6
Parameter('k6a_on', FF*SEF)
Parameter('k6a_off', FR)
#TB3_TBRI + TBRI <-> TB3_TBRI_TBRI
Rule('TB3_TBRI_to_TB3_TBRI_TBRI', TB3_TBRI() + TBRI() <> TB3_TBRI_TBRI(),
k6a_on, k6a_off)

#Rxn 10
Parameter('k10a_on', JF*SEF)
Parameter('k10a_off', JR)
#TB3_TBRI_TBRI + TBRII <-> TB3_TBRII_TBRI_TBRI

```

```
Rule('TB3_TBRI_TBRI_to_TB3_TBRII_TBRI_TBRI', TB3_TBRI_TBRI() + TBRII() <>
TB3_TBRII_TBRI_TBRI(), k10a_on, k10a_off)
```

```
#Rxn 15
```

```
Parameter('k15a_on', PF*SEF)
```

```
Parameter('k15a_off', PR)
```

```
#TB3_TBRI + TBRI <-> TB3_TBRI_TBRI
```

```
Rule('TB3_TBRII_to_TB3_BG_TBRII', TB3_TBRII() + BG() <> TB3_BG_TBRII(), k15a_on,
k15a_off)
```

```
#Receptor Recycling and Endocytosis in one step
```

```
#Rxn1001
```

```
Parameter('kendo', kendo)
```

```
#TB3_BG -> BG + TB3
```

```
Rule('TB3_BG_Endo1', TB3_BG() >> BG(), kendo)
```

```
#Rxn1002
```

```
#TB3_BG_TBRII -> BG + TBRII + TB3
```

```
Rule('TB3_BG_TBRII_Endo2', TB3_BG_TBRII() >> BG() + TBRII(), kendo)
```

```
#Rxn1003
```

```
#TB3_TBRII -> TB3 + TBRII
```

```
Rule('TB3_TBRII_Endo3', TB3_TBRII() >> TBRII(), kendo)
```

```
#Rxn1004
```

```
#TB3_TBRI -> TBRI + TB3
```

```
Rule('TB3_TBRI_Endo4', TB3_TBRI() >> TBRI(), kendo)
```

```
#Rxn1005
```

```
#TB3_BG_TBRII_TBRI ->
```

```
Rule('TB3_BG_TBRII_TBRI_Endo5', TB3_BG_TBRII_TBRI() >> BG() + TBRII() + TBRI(),
kendo)
```

```
#Rxn1006
```

```
#TB3_TBRII_TBRI -> TBRII + TBRI + TB3
```

```
Rule('TB3_TBRII_TBRI_Endo6', TB3_TBRII_TBRI() >> TBRII() + TBRI(), kendo)
```

```
#Rxn1007
```

```
#TB3_TBRII_TBRII_TBRI -> TBRII(2) + TBRI + TB3
```

```
Rule('TB3_TBRII_TBRII_TBRI_Endo7', TB3_TBRII_TBRII_TBRI() >> TBRII() + TBRII() + TBRI(), kendo)
```

```
#Rxn1008
```

```
#TB3_TBRII_TBRI_TBRI -> TBRII + TBRI + TBRI + TB3  
Rule('TB3_TBRII_TBRI_TBRI_Endo8', TB3_TBRII_TBRI_TBRI() >> TBRII() + TBRI() + TBRI(), kendo)
```

```
#Rxn1009
```

```
#TB3_TBRII_TBRII_TBRI_TBRI -> TBRII + TBRII + TBRI + TBRI + TB3  
Rule('TB3_TBRII_TBRII_TBRI_TBRI_Endo9', TB3_TBRII_TBRII_TBRI_TBRI() >> TBRII() + TBRII() + TBRI() + TBRI(), kendo)
```

```
#Rxn1010
```

```
#TB3_TBRII_TBRII -> TBRII + TBRII + TB3  
Rule('TB3_TBRII_TBRII_Endo10', TB3_TBRII_TBRII() >> TBRII() + TBRII(), kendo)
```

```
#Rxn1011
```

```
Rule('TB3_TBRI_TBRI_Endo11', TB3_TBRI_TBRI() >> TBRI() + TBRI(), kendo)
```

```
#Defining parameters that are not rates
```

```
Parameter('BG_0', Z2)  
Parameter('TBRII_0', RII)  
Parameter('TBRI_0', RI)
```

```
#Initial Values
```

```
#These values would vary depending on screen performed
```

```
Initial(BG(), BG_0)  
Initial(TBRII(), TBRII_0)  
Initial(TBRI(), TBRI_0)
```

```
#Observable Amount of Monomer
```

```
Observable('BG', BG());  
Observable('TBRII', TBRII());  
Observable('TBRI', TBRI());  
Observable('TB3_TBRI_TBRI', TB3_TBRI_TBRI());  
Observable('TB3_BG', TB3_BG());  
Observable('TB3_TBRI', TB3_TBRI());  
Observable('TB3_TBRII', TB3_TBRII());  
Observable('TB3_TBRII_TBRII', TB3_TBRII_TBRII());  
Observable('TB3_BG_TBRII', TB3_BG_TBRII());  
Observable('TB3_BG_TBRII_TBRI', TB3_BG_TBRII_TBRI());  
Observable('TB3_TBRII_TBRI', TB3_TBRII_TBRI());
```

```

Observable('TB3_TBRII_TBRII_TBRI', TB3_TBRII_TBRII_TBRI());
Observable('TB3_TBRII_TBRI_TBRI', TB3_TBRII_TBRI_TBRI());
Observable('TB3_TBRII_TBRII_TBRI_TBRI', TB3_TBRII_TBRII_TBRI_TBRI());

#Importing functions for data analysis
from matplotlib.pyplot import *
from numpy import linspace, array
from pysb.simulator import ScipyOdeSimulator

# We will integrate from t=0 to t=86400
t = linspace(0, 186400, 186401)
y = ScipyOdeSimulator(model, rtol=1e-4, atol=[1e-8, 1e-14, 1e-6]).run(tspan=t).all

# Gather the observables of interest into a matrix
yobs = array([y[obs] for obs in ('BG', 'TBRII', 'TBRI', 'TB3_BG', 'TB3_TBRI', 'TB3_TBRII',
'TB3_TBRII_TBRII', 'TB3_BG_TBRII', 'TB3_BG_TBRII_TBRI', 'TB3_TBRII_TBRI',
'TB3_TBRII_TBRII_TBRI', 'TB3_TBRII_TBRI_TBRI', 'TB3_TBRII_TBRII_TBRI_TBRI',
'TB3_TBRI_TBRI')]).T

#Recording the concentrations of individual species at 186400 seconds
TetramerShot = ((y['TB3_TBRII_TBRII_TBRI_TBRI'][186400]))
Shot_BG = ((y['BG'][186400]))
ShotTBRII = ((y['TBRII'][186400]))
ShotTBRI = ((y['TBRI'][186400]))
ShotTB3_BG = ((y['TB3_BG'][186400]))
ShotTB3_TBRI = ((y['TB3_TBRI'][186400]))
ShotTB3_TBRII = ((y['TB3_TBRII'][186400]))
ShotTB3_TBRI_TBRI = ((y['TB3_TBRI_TBRI'][186400]))
ShotTB3_TBRII_TBRII = ((y['TB3_TBRII_TBRII'][186400]))
ShotTB3_BG_TBRII = ((y['TB3_BG_TBRII'][186400]))
ShotTB3_BG_TBRII_TBRI = ((y['TB3_BG_TBRII_TBRI'][186400]))
ShotTB3_TBRII_TBRI = ((y['TB3_TBRII_TBRI'][186400]))
ShotTB3_TBRII_TBRII_TBRI = ((y['TB3_TBRII_TBRII_TBRI'][186400]))
ShotTB3_TBRII_TBRI_TBRI = ((y['TB3_TBRII_TBRI_TBRI'][186400]))
ShotTB3_TBRII_TBRII_TBRI_TBRI = ((y['TB3_TBRII_TBRII_TBRI_TBRI'][186400]))

#End of TRR model for TGF-beta3

```

REFERENCES

- Abel, J. H., Drawert, B., Hellander, A., & Petzold, L. R. (2016). GillesPy: A Python Package for Stochastic Model Building and Simulation. *IEEE Life Sciences Letters*, 2(3), 35–38. <https://doi.org/10.1109/LLS.2017.2652448>
- Ahmed, F. E., Wiley, J. E., Weidner, D. A., Bonnerup, C., & Mota, H. (2010). Surface Plasmon Resonance (SPR) Spectrometry as a Tool to Analyze Nucleic Acid–Protein Interactions in Crude Cellular Extracts. *Cancer Genomics - Proteomics*, 7(6), 303–309.
- Attisano, L., Wrana, J. L., Montalvo, E., & Massagué, J. (1996). Activation of signalling by the activin receptor complex. *Molecular and Cellular Biology*, 16(3), 1066–1073. <https://doi.org/10.1128/mcb.16.3.1066>
- Bartram, U., Molin, D. G., Wisse, L. J., Mohamad, A., Sanford, L. P., Doetschman, T., ... Gittenberger-de Groot, A. C. (2001). Double-outlet right ventricle and overriding tricuspid valve reflect disturbances of looping, myocardialization, endocardial cushion differentiation, and apoptosis in TGF-beta(2)-knockout mice. *Circulation*, 103(22), 2745–2752. <https://doi.org/10.1161/01.cir.103.22.2745>
- Brown, C. B., Boyer, A. S., Runyan, R. B., & Barnett, J. V. (1999). Requirement of Type III TGF- β Receptor for Endocardial Cell Transformation in the Heart. *Science*, 283(5410), 2080–2082. <https://doi.org/10.1126/science.283.5410.2080>
- Casari, A., Schiavone, M., Facchinello, N., Vettori, A., Meyer, D., Tiso, N., ... Argenton, F. (2014). A Smad3 transgenic reporter reveals TGF-beta control of zebrafish spinal cord development. *Developmental Biology*, 396(1), 81–93. <https://doi.org/10.1016/j.ydbio.2014.09.025>
- Cellière, G., Fengos, G., Hervé, M., & Iber, D. (2011). Plasticity of TGF- β signaling. *BMC Systems Biology*, 5, 184. <https://doi.org/10.1186/1752-0509-5-184>
- Cheifetz, S., & IwataS, K. (1990). *Distinct Transforming Growth Factor- α (TGF- β) Receptor Subsets as Determinants of Cellular Responsiveness to Three TGF- α Isoforms*. 7.
- Chen, H., & Privalsky, M. L. (1995). Cooperative formation of high-order oligomers by retinoid X receptors: An unexpected mode of DNA recognition. *Proceedings of the National Academy of Sciences*, 92(2), 422–426. <https://doi.org/10.1073/pnas.92.2.422>
- Chung, S.-W., Miles, F. L., Sikes, R. A., Cooper, C. R., Farach-Carson, M. C., & Ogunnaike, B. A. (2009). Quantitative modeling and analysis of the transforming growth factor beta signaling pathway. *Biophysical Journal*, 96(5), 1733–1750. <https://doi.org/10.1016/j.bpj.2008.11.050>

De Crescenzo, G., Hinck, C. S., Shu, Z., Zúñiga, J., Yang, J., Tang, Y., ... Hinck, A. P. (2006). Three key residues underlie the differential affinity of the TGFbeta isoforms for the TGFbeta type II receptor. *Journal of Molecular Biology*, 355(1), 47–62. <https://doi.org/10.1016/j.jmb.2005.10.022>

Devalia, J. L., Sapsford, R. J., Wells, C. W., Richman, P., & Davies, R. J. (1990). Culture and comparison of human bronchial and nasal epithelial cells in vitro. *Respiratory Medicine*, 84(4), 303–312.

Di Guglielmo, G. M., Le Roy, C., Goodfellow, A. F., & Wrana, J. L. (2003). Distinct endocytic pathways regulate TGF-beta receptor signalling and turnover. *Nature Cell Biology*, 5(5), 410–421. <https://doi.org/10.1038/ncb975>

Drevon, D., Fursa, S. R., & Malcolm, A. L. (2017). Intercoder Reliability and Validity of WebPlotDigitizer in Extracting Graphed Data. *Behavior Modification*, 41(2), 323–339. <https://doi.org/10.1177/0145445516673998>

Eickelberg, O., Centrella, M., Reiss, M., Kashgarian, M., & Wells, R. G. (2002). Betaglycan Inhibits TGF- β Signaling by Preventing Type I-Type II Receptor Complex Formation
GLYCOSAMINOGLYCAN MODIFICATIONS ALTER BETAGLYCAN FUNCTION. *Journal of Biological Chemistry*, 277(1), 823–829. <https://doi.org/10.1074/jbc.M105110200>

Elowitz, M. B., Levine, A. J., Siggia, E. D., & Swain, P. S. (2002). Stochastic Gene Expression in a Single Cell. *Science*, 297(5584), 1183–1186. <https://doi.org/10.1126/science.1070919>

Fabregat, I., Fernando, J., Mainez, J., & Sancho, P. (2014). TGF-beta signaling in cancer treatment. *Current Pharmaceutical Design*, 20(17), 2934–2947. <https://doi.org/10.2174/13816128113199990591>

Fischer, A. H., Jacobson, K. A., Rose, J., & Zeller, R. (2008). Hematoxylin and Eosin Staining of Tissue and Cell Sections. *Cold Spring Harbor Protocols*, 2008(5), pdb.prot4986. <https://doi.org/10.1101/pdb.prot4986>

Gallenberger, M., Castell, W. zu, Hense, B. A., & Kuttler, C. (2012). Dynamics of glucose and insulin concentration connected to the β -cell cycle: Model development and analysis. *Theoretical Biology & Medical Modelling*, 9, 46. <https://doi.org/10.1186/1742-4682-9-46>

Gardner, T. S., Cantor, C. R., & Collins, J. J. (2000). Construction of a genetic toggle switch in *Escherichia coli*. *Nature*, 403(6767), 339–342. <https://doi.org/10.1038/35002131>

Gilboa, L., Wells, R. G., Lodish, H. F., & Henis, Y. I. (1998). Oligomeric Structure of Type I and Type II Transforming Growth Factor β Receptors: Homodimers Form in the ER and Persist at the Plasma Membrane. *The Journal of Cell Biology*, 140(4), 767–777. <https://doi.org/10.1083/jcb.140.4.767>

Gillespie, D. T. (1976). A general method for numerically simulating the stochastic time evolution of coupled chemical reactions. *Journal of Computational Physics*, 22(4), 403–434. [https://doi.org/10.1016/0021-9991\(76\)90041-3](https://doi.org/10.1016/0021-9991(76)90041-3)

Gillespie, D. T. (2016). Gillespie Algorithm for Biochemical Reaction Simulation. In D. Jaeger & R. Jung (Eds.), *Encyclopedia of Computational Neuroscience* (pp. 1–5).

https://doi.org/10.1007/978-1-4614-7320-6_189-2

Groppe, J., Hinck, C. S., Samavarchi-Tehrani, P., Zubietta, C., Schuermann, J. P., Taylor, A. B., ... Hinck, A. P. (2008). Cooperative Assembly of TGF- β Superfamily Signaling Complexes Is Mediated by Two Disparate Mechanisms and Distinct Modes of Receptor Binding. *Molecular Cell*, 29(2), 157–168. <https://doi.org/10.1016/j.molcel.2007.11.039>

Hahl, S. K., & Kremling, A. (2016). A Comparison of Deterministic and Stochastic Modeling Approaches for Biochemical Reaction Systems: On Fixed Points, Means, and Modes. *Frontiers in Genetics*, 7, 157. <https://doi.org/10.3389/fgene.2016.00157>

Heldin, C.-H., & Moustakas, A. (2016). Signaling Receptors for TGF- β Family Members. *Cold Spring Harbor Perspectives in Biology*, 8(8), a022053.

<https://doi.org/10.1101/cshperspect.a022053>

Hinck, Andrew P. (2012). Structural studies of the TGF- β s and their receptors—Insights into evolution of the TGF- β superfamily. *FEBS Letters*, 586(14), 1860–1870.

<https://doi.org/10.1016/j.febslet.2012.05.028>

Huang, T., David, L., Mendoza, V., Yang, Y., Villarreal, M., De, K., ... Hinck, A. P. (2011). TGF- β signalling is mediated by two autonomously functioning T β RI:T β RII pairs. *The EMBO Journal*, 30(7), 1263–1276. <https://doi.org/10.1038/emboj.2011.54>

Huang, T., Schor, S. L., & Hinck, A. P. (2014). Biological activity differences between TGF- β 1 and TGF- β 3 correlate with differences in the rigidity and arrangement of their component monomers. *Biochemistry*, 53(36), 5737–5749. <https://doi.org/10.1021/bi500647d>

Hyytiäinen, M., Penttinen, C., & Keski-Oja, J. (2004). Latent TGF-beta binding proteins: Extracellular matrix association and roles in TGF-beta activation. *Critical Reviews in Clinical Laboratory Sciences*, 41(3), 233–264. <https://doi.org/10.1080/10408360490460933>

Iino, R., Koyama, I., & Kusumi, A. (2001). Single Molecule Imaging of Green Fluorescent Proteins in Living Cells: E-Cadherin Forms Oligomers on the Free Cell Surface. *Biophysical Journal*, 80(6), 2667–2677. [https://doi.org/10.1016/S0006-3495\(01\)76236-4](https://doi.org/10.1016/S0006-3495(01)76236-4)

Iolascon, A., Giordani, L., Borriello, A., Carbone, R., Izzo, A., Tonini, G. P., ... Ragine, F. D. (2000). Reduced expression of transforming growth factor-beta receptor type III in high stage neuroblastomas. *British Journal of Cancer*, 82(6), 1171–1176.

<https://doi.org/10.1054/bjoc.1999.1058>

Jelinek, D. F., Tschumper, R. C., Stolovitzky, G. A., Iturria, S. J., Tu, Y., Lepre, J., ... Kay, N. E. (2003). Identification of a global gene expression signature of B-chronic lymphocytic leukemia. *Molecular Cancer Research: MCR*, 1(5), 346–361.

- Kaartinen, V., Voncken, J. W., Shuler, C., Warburton, D., Bu, D., Heisterkamp, N., & Groffen, J. (1995). Abnormal lung development and cleft palate in mice lacking TGF-beta 3 indicates defects of epithelial-mesenchymal interaction. *Nature Genetics*, *11*(4), 415–421. <https://doi.org/10.1038/ng1295-415>
- Karim, M. S., Buzzard, G. T., & Umulis, D. M. (2012). Secreted, receptor-associated bone morphogenetic protein regulators reduce stochastic noise intrinsic to many extracellular morphogen distributions. *Journal of The Royal Society Interface*, *9*(70), 1073–1083. <https://doi.org/10.1098/rsif.2011.0547>
- Kim, S. K., Whitley, M. J., Krzysiak, T. C., Hinck, C. S., Taylor, A. B., Zwieb, C., ... Hinck, A. P. (2019). Structural Adaptation in Its Orphan Domain Engenders Betaglycan with an Alternate Mode of Growth Factor Binding Relative to Endoglin. *Structure*, *27*(9), 1427–1442.e4. <https://doi.org/10.1016/j.str.2019.06.010>
- Kingsley, D. M. (1994). The TGF-beta superfamily: New members, new receptors, and new genetic tests of function in different organisms. *Genes & Development*, *8*(2), 133–146. <https://doi.org/10.1101/gad.8.2.133>
- Klein, U., Tu, Y., Stolovitzky, G. A., Mattioli, M., Cattoretti, G., Husson, H., ... Dalla-Favera, R. (2001). Gene expression profiling of B cell chronic lymphocytic leukemia reveals a homogeneous phenotype related to memory B cells. *The Journal of Experimental Medicine*, *194*(11), 1625–1638. <https://doi.org/10.1084/jem.194.11.1625>
- Kremling, A., Bettenbrock, K., & Gilles, E. D. (2007). Analysis of global control of Escherichia coli carbohydrate uptake. *BMC Systems Biology*, *1*(1). <https://doi.org/10.1186/1752-0509-1-42>
- Kulkarni, A. B., Huh, C. G., Becker, D., Geiser, A., Lyght, M., Flanders, K. C., ... Karlsson, S. (1993). Transforming growth factor beta 1 null mutation in mice causes excessive inflammatory response and early death. *Proceedings of the National Academy of Sciences of the United States of America*, *90*(2), 770–774. <https://doi.org/10.1073/pnas.90.2.770>
- Lastres, P., Letamendía, A., Zhang, H., Rius, C., Almendro, N., Raab, U., ... Bernabéu, C. (1996). Endoglin modulates cellular responses to TGF-beta 1. *The Journal of Cell Biology*, *133*(5), 1109–1121. <https://doi.org/10.1083/jcb.133.5.1109>
- Letterio, J. J., & Roberts, A. B. (1998). Regulation of immune responses by TGF-beta. *Annual Review of Immunology*, *16*, 137–161. <https://doi.org/10.1146/annurev.immunol.16.1.137>
- Liu, F., Ventura, F., Doody, J., & Massagué, J. (1995). Human type II receptor for bone morphogenic proteins (BMPs): Extension of the two-kinase receptor model to the BMPs. *Molecular and Cellular Biology*, *15*(7), 3479–3486. <https://doi.org/10.1128/mcb.15.7.3479>
- Lopez, C. F., Muhlich, J. L., Bachman, J. A., & Sorger, P. K. (2013). Programming biological models in Python using PySB. *Molecular Systems Biology*, *9*, 646. <https://doi.org/10.1038/msb.2013.1>

- López-Casillas, F., Cheifetz, S., Doody, J., Andres, J. L., Lane, W. S., & Massagué, J. (1991). Structure and expression of the membrane proteoglycan betaglycan, a component of the TGF-beta receptor system. *Cell*, 67(4), 785–795. [https://doi.org/10.1016/0092-8674\(91\)90073-8](https://doi.org/10.1016/0092-8674(91)90073-8)
- López-Casillas, F., Wrana, J. L., & Massagué, J. (1993). Betaglycan presents ligand to the TGFβ signaling receptor. *Cell*, 73(7), 1435–1444. [https://doi.org/10.1016/0092-8674\(93\)90368-Z](https://doi.org/10.1016/0092-8674(93)90368-Z)
- Martin, J. S., Dickson, M. C., Cousins, F. M., Kulkarni, A. B., Karlsson, S., & Akhurst, R. J. (1995). Analysis of homozygous TGF beta 1 null mouse embryos demonstrates defects in yolk sac vasculogenesis and hematopoiesis. *Annals of the New York Academy of Sciences*, 752, 300–308. <https://doi.org/10.1111/j.1749-6632.1995.tb17439.x>
- Martin-Blanco, N., Blanco, R., Alda-Catalinas, C., Bovolenta, E. R., Oeste, C. L., Palmer, E., ... Alarcon, B. (2018). A window of opportunity for cooperativity in the T Cell Receptor. *Nature Communications*, 9(1), 1–15. <https://doi.org/10.1038/s41467-018-05050-6>
- Mason, A. J., Hayflick, J. S., Ling, N., Esch, F., Ueno, N., Ying, S. Y., ... Seeburg, P. H. (1985). Complementary DNA sequences of ovarian follicular fluid inhibin show precursor structure and homology with transforming growth factor-beta. *Nature*, 318(6047), 659–663. <https://doi.org/10.1038/318659a0>
- Massagué, J. (2000). How cells read TGF-beta signals. *Nature Reviews. Molecular Cell Biology*, 1(3), 169–178. <https://doi.org/10.1038/35043051>
- Massagué, J. (2008). TGFbeta in Cancer. *Cell*, 134(2), 215–230. <https://doi.org/10.1016/j.cell.2008.07.001>
- McAllister, K. A., Grogg, K. M., Johnson, D. W., Gallione, C. J., Baldwin, M. A., Jackson, C. E., ... Marchuk, D. A. (1994). Endoglin, a TGF-β binding protein of endothelial cells, is the gene for hereditary haemorrhagic telangiectasia type 1. *Nature Genetics*, 8(4), 345–351. <https://doi.org/10.1038/ng1294-345>
- Melke, P., Jönsson, H., Pardali, E., ten Dijke, P., & Peterson, C. (2006). A Rate Equation Approach to Elucidate the Kinetics and Robustness of the TGF-β Pathway. *Biophysical Journal*, 91(12), 4368–4380. <https://doi.org/10.1529/biophysj.105.080408>
- Mitra, K., Ubarretxena-Belandia, I., Taguchi, T., Warren, G., & Engelman, D. M. (2004). Modulation of the bilayer thickness of exocytic pathway membranes by membrane proteins rather than cholesterol. *Proceedings of the National Academy of Sciences*, 101(12), 4083–4088. <https://doi.org/10.1073/pnas.0307332101>
- Moses, H. L. (1992). TGF-beta regulation of epithelial cell proliferation. *Molecular Reproduction and Development*, 32(2), 179–184. <https://doi.org/10.1002/mrd.1080320215>
- Motta, S., & Pappalardo, F. (2013). Mathematical modeling of biological systems. *Briefings in Bioinformatics*, 14(4), 411–422. <https://doi.org/10.1093/bib/bbs061>

- Nickel, J., Sebald, W., Groppe, J. C., & Mueller, T. D. (2009). Intricacies of BMP receptor assembly. *Cytokine & Growth Factor Reviews*, 20(5), 367–377. <https://doi.org/10.1016/j.cytogfr.2009.10.022>
- Proetzel, G., Pawlowski, S. A., Wiles, M. V., Yin, M., Boivin, G. P., Howles, P. N., ... Doetschman, T. (1995). Transforming growth factor-beta 3 is required for secondary palate fusion. *Nature Genetics*, 11(4), 409–414. <https://doi.org/10.1038/ng1295-409>
- Radaev, S., Zou, Z., Huang, T., Lafer, E. M., Hinck, A. P., & Sun, P. D. (2010). Ternary Complex of Transforming Growth Factor- β 1 Reveals Isoform-specific Ligand Recognition and Receptor Recruitment in the Superfamily. *The Journal of Biological Chemistry*, 285(19), 14806–14814. <https://doi.org/10.1074/jbc.M109.079921>
- Rallabhandi, P., Nhu, Q. M., Toshchakov, V. Y., Piao, W., Medvedev, A. E., Hollenberg, M. D., ... Vogel, S. N. (2008). Analysis of Proteinase-activated Receptor 2 and TLR4 Signal Transduction A NOVEL PARADIGM FOR RECEPTOR COOPERATIVITY. *Journal of Biological Chemistry*, 283(36), 24314–24325. <https://doi.org/10.1074/jbc.M804800200>
- Roberts, A. B., Anzano, M. A., Lamb, L. C., Smith, J. M., & Sporn, M. B. (1981). New class of transforming growth factors potentiated by epidermal growth factor: Isolation from non-neoplastic tissues. *Proceedings of the National Academy of Sciences of the United States of America*, 78(9), 5339–5343. <https://doi.org/10.1073/pnas.78.9.5339>
- Sanford, L. P., Ormsby, I., Gittenberger-de Groot, A. C., Sariola, H., Friedman, R., Boivin, G. P., ... Doetschman, T. (1997). TGFbeta2 knockout mice have multiple developmental defects that are non-overlapping with other TGFbeta knockout phenotypes. *Development (Cambridge, England)*, 124(13), 2659–2670.
- Schmierer, B., Tournier, A. L., Bates, P. A., & Hill, C. S. (2008). Mathematical modeling identifies Smad nucleocytoplasmic shuttling as a dynamic signal-interpreting system. *Proceedings of the National Academy of Sciences*, 105(18), 6608–6613. <https://doi.org/10.1073/pnas.0710134105>
- Serpe, M., Umulis, D., Ralston, A., Chen, J., Olson, D. J., Avanesov, A., ... Blair, S. S. (2008). The BMP binding protein Crossveinless 2 is a short-range, concentration-dependent, biphasic modulator of BMP signaling in Drosophila. *Developmental Cell*, 14(6), 940–953. <https://doi.org/10.1016/j.devcel.2008.03.023>
- Serra, R., Johnson, M., Filvaroff, E. H., LaBorde, J., Sheehan, D. M., Derynck, R., & Moses, H. L. (1997). Expression of a Truncated, Kinase-Defective TGF- β Type II Receptor in Mouse Skeletal Tissue Promotes Terminal Chondrocyte Differentiation and Osteoarthritis. *The Journal of Cell Biology*, 139(2), 541–552.
- Shinar, G., Milo, R., Martínez, M. R., & Alon, U. (2007). Input–output robustness in simple bacterial signaling systems. *Proceedings of the National Academy of Sciences*, 104(50), 19931–19935. <https://doi.org/10.1073/pnas.0706792104>

- Shull, M. M., Ormsby, I., Kier, A. B., Pawlowski, S., Diebold, R. J., Yin, M., ... Calvin, D. (1992). Targeted disruption of the mouse transforming growth factor-beta 1 gene results in multifocal inflammatory disease. *Nature*, 359(6397), 693–699. <https://doi.org/10.1038/359693a0>
- Siegel, P. M., Shu, W., Cardiff, R. D., Muller, W. J., & Massagué, J. (2003). Transforming growth factor β signaling impairs Neu-induced mammary tumorigenesis while promoting pulmonary metastasis. *Proceedings of the National Academy of Sciences of the United States of America*, 100(14), 8430–8435. <https://doi.org/10.1073/pnas.0932636100>
- Tucker, R. F., Branum, E. L., Shipley, G. D., Ryan, R. J., & Moses, H. L. (1984). Specific binding to cultured cells of 125I-labeled type beta transforming growth factor from human platelets. *Proceedings of the National Academy of Sciences of the United States of America*, 81(21), 6757–6761.
- Tyson, J. J., & Othmer, H. G. (n.d.). Tyson, J.J. and Othmer, H.G. (1978) *The dynamics of feedback cellular control circuits in biochemical pathways*. *Progress in Biophysics, Academic Press, New York*, (5), 1-62. *Progress in Biophysics*.
- Umulis, D. M., Shimmi, O., O'Connor, M. B., & Othmer, H. G. (2010). Organism-scale modeling of early Drosophila patterning via Bone Morphogenetic Proteins. *Developmental Cell*, 18(2), 260–274. <https://doi.org/10.1016/j.devcel.2010.01.006>
- Vilar, J. M. G., Jansen, R., & Sander, C. (2006). Signal processing in the TGF-beta superfamily ligand-receptor network. *PLoS Computational Biology*, 2(1), e3. <https://doi.org/10.1371/journal.pcbi.0020003>
- Villarreal, M. M., Kim, S. K., Barron, L., Kodali, R., Baardsnes, J., Hinck, C. S., ... Hinck, A. P. (2016). Binding Properties of the Transforming Growth Factor- β Coreceptor Betaglycan: Proposed Mechanism for Potentiation of Receptor Complex Assembly and Signaling. *Biochemistry*, 55(49), 6880–6896. <https://doi.org/10.1021/acs.biochem.6b00566>
- Wakefield, L. M., Smith, D. M., Masui, T., Harris, C. C., & Sporn, M. B. (1987). Distribution and modulation of the cellular receptor for transforming growth factor-beta. *The Journal of Cell Biology*, 105(2), 965–975. <https://doi.org/10.1083/jcb.105.2.965>
- Wegner, K., Bachmann, A., Schad, J.-U., Lucarelli, P., Sahle, S., Nickel, P., ... Kummer, U. (2012). Dynamics and feedback loops in the transforming growth factor β signaling pathway. *Biophysical Chemistry*, 162, 22–34. <https://doi.org/10.1016/j.bpc.2011.12.003>
- Wells, R. G., Gilboa, L., Sun, Y., Liu, X., Henis, Y. I., & Lodish, H. F. (1999). Transforming Growth Factor- β Induces Formation of a Dithiothreitol-resistant Type I/Type II Receptor Complex in Live Cells. *Journal of Biological Chemistry*, 274(9), 5716–5722. <https://doi.org/10.1074/jbc.274.9.5716>
- Wiater, E., Harrison, C. A., Lewis, K. A., Gray, P. C., & Vale, W. W. (2006). Identification of Distinct Inhibin and Transforming Growth Factor β -binding Sites on Betaglycan FUNCTIONAL SEPARATION OF BETAGLYCAN CO-RECEPTOR ACTIONS. *Journal of Biological Chemistry*, 281(25), 17011–17022. <https://doi.org/10.1074/jbc.M601459200>

Wilkinson, D. J. (2012). *Stochastic modelling for systems biology* (2nd ed.). Boca Raton: Taylor & Francis.

Yang, L.-T., & Kaartinen, V. (2007). Tgfb1 expressed in the Tgfb3 locus partially rescues the cleft palate phenotype of Tgfb3 null mutants. *Developmental Biology*, 312(1), 384–395. <https://doi.org/10.1016/j.ydbio.2007.09.034>

Zi, Z., Feng, Z., Chapnick, D. A., Dahl, M., Deng, D., Klipp, E., ... Liu, X. (2011). Quantitative analysis of transient and sustained transforming growth factor- β signaling dynamics. *Molecular Systems Biology*, 7, 492. <https://doi.org/10.1038/msb.2011.22>